Nesprin-1 is required to maintain genomic stability and prevent tumorigenesis

Inaugural-Dissertation

zur

Erlangung des Doktorgrades

der Mathematisch-Naturwissenschaftlichen Fakultät

der Universität zu Köln

vorgelegt von

Ilknur Sur

aus Istanbul, Türkei

Köln 2013

Berichterstatter: Prof. Dr. Angelika A. Noegel

Berichterstatter: Prof. Dr. Siegfried Roth

Prüfungsvorsitzender: Prof. Dr. Peter Nürnberg

Tag der mündlichen Prüfung: 22.01.2014

The present research work was carried out from November 2010 to November 2013 at the Centre for Biochemistry, Institute of Biochemistry I, Medical Faculty, University of Cologne, Cologne, Germany, under the supervision of Prof. Dr. Angelika A. Noegel.

Die vorliegende Arbeit wurde in der Zeit von Nov 2010 bis Nov 2013 unter der Anleitung von Prof. Dr. Angelika A.Noegel am Biochemischen Institut I der Medizinischen Fakultät der Universität zu Köln angefertigt.

I am dedicating this thesis to my beloved family for giving me the strength to keep working to make my dreams come true, and especially to my grandmother, Ayşe Sur, who always prays for me. I wish she were here to see her prayer and our dream come true.

.

ACKNOWLEDGEMENTS

Table of contents

Abbreviations

Aa	Amino acid
ABD	Actin-binding domains
cDNA	Complementary DNA
CH	Calponin homology
Co-IP	Co-Immunoprecipitation
Da	Dalton
DAPI	4'-6-diamidino-2-phenylindole
DMEM	Dulbecco`s modified Eagle medium
DMSO	Dimethyl sulfoxide
DNA	Deoxyribonucleic acid
dNTP	Deoxynucleoside triphosphate
DTT	Dithiothreitol
EDTA	Ethylene diamine tetraacetic acid
ECL	Enhanced chemiluminescence
EDMD	Emery Dreifuss Muscular Dystrophy
F-actin	Filamentous actin
FBS	Fetal bovine serum
GAPDH	Glycerinaldehydephosphate dehydrogenase
GFP	Green fluorescent protein
GST	Glutathione S-transferase
HEPES	4-(2-hydroxyethyl)-1-piperazineethanesulfonic acid
HGPS	Hutchinson-Gilford progeria syndrome
IgG	Immunglobulin G
IPTG	Isopropyl-β-Dithiogalactopyranoside

IF	Immunofluorescence
IP	Immunoprecipitation
KASH	Klarsicht, ANC1 and SYNE1 homology
KD	Knock down
KO	Knock out
mRNA	messenger ribonucleic acid
MS	Mass spectrometry
Nesprins	Nuclear envelope spectrin repeat proteins
NPC	Nuclear pore complex
PBS	Phosphate buffered saline
PCR	Polymerase chain reaction
PFA	Paraformaldehyde
pH	negative decadic logarithm of protein concentration
PIC	Proteinase inhibitor cocktail
rpm	Rotation per minute
qRT-PCR	Quantitative real time PCR
SDS-PAGE	Sodium dodecyl sulfate polyacrylamide gel electrophoresis
shRNA	Short hairpin RNA
SR	Spectrin repeats
SUN	Sad1 and UNC-84
TBS	Tris buffered saline
UV	Ultraviolet light
WB	Western blot
WT	Wild type
X-gal	5-bromo-4-chloro-3-indolyl-D-galactopyranosid

Summary

Nuclear envelope (NE) proteins have fundamental roles in maintaining nuclear structure, cell signaling, chromatin organization and gene regulation, and mutations in genes encoding NE components were identified as primary cause of a number of age associated diseases and cancer. Nesprin-1 belongs to a family of multi-isomeric NE proteins that are characterized by spectrin repeats. Our results imply interactions between spectrin repeats and an interaction of Nesprin-1 with Nesprin-2. Furthermore, we analysed NE components in various tumor cell lines and found that Nesprin-1 levels were strongly reduced associated with alterations in further NE components. By reducing the amounts of Nesprin-1 by RNAi mediated knock down we could reproduce those alterations in mouse and human cell lines pointing towards a key role for Nesprin-1 in the maintenance of nucleus morphology, centrosome positioning, nuclear membrane structure, cytoskeleton organization, and cellular senescence. In a search for novel Nesprin-1 binding proteins we identified MSH2, MSH6, and DDB1 proteins of the DNA damage response pathway as interactors. We found alterations in the mismatch repair pathway in cells with lower Nesprin-1 levels. We also noticed an increased number of γH2AX foci in the absence of exogenous DNA damage as was seen in tumor cells. The levels of phosphorylated kinases Chk1 and 2 were altered in a manner resembling tumor cells and the levels of Ku70 were low and the protein was not recruited to the DNA after HU treatment. Our findings indicate a role for Nesprin-1 in the DNA damage response pathway and propose Nesprin-1 as novel regulator of tumorigenesis and genome instability. Loss of Nesprin-1 might play a significant role in cancer progression.

Zusammenfassung

Kernhüllenproteine haben eine wesentliche Rolle bei der Aufrechterhaltung der Kernstruktur, Chromatinorganisation, Genregulation und bei Signaltransduktionsprozessen, und Mutationen in Genen, die für Kernhüllenkomponenten kodieren, wurden als primäre Ursache für eine Reihe von Erkrankungen und Krebs identifiziert. Nesprin-1 gehört zu einer Familie von multi-isomeren Proteinen der Kernhülle, die von Spectrin Wiederholungen gekennzeichnet sind. Unsere Ergebnisse zeigen, dass Nesprin-1 mit Nesprin-2 über Wechselwirkungen ihrer Spectrin Repeats miteinander interagieren. Weiterhin haben wir die Kernhüllenkomponenten in verschiedenen Tumor-Zelllinien analysiert und dabei festgestellt, dass die Nesprin-1-Spiegel stark reduziert und mit Veränderungen in weiteren Kernhüllenproteinen und anderen Kern-assoziierten Prozessen verbunden waren. Durch die Reduzierung der Mengen an Nesprin-1 durch einen RNAi-vermittelten Knockdown konnten wir diese Veränderungen in murinen und humanen Zelllinien reproduzieren. Diese Ergebnisse verweisen auf eine Schlüsselrolle für Nesprin-1 bei der Aufrechterhaltung der Kernmorphologie, Zentrosomenpositionierung, Struktur der Kernmembran, Organisation des Cytoskeletts und der zellulären Seneszenz. Bei der Suche nach neuen Nesprin-1-bindenden Proteinen identifizierten wir MSH2, MSH6 und DDB1 als Interaktionspartner, die Proteine von DNA-Reparaturwegen sind. In Übereinstimmung damit haben wir Veränderungen im Mismatch-Reparaturweg in Zellen mit niedrigen Nesprin-1-Spiegeln beobachtet. Wir haben auch eine erhöhte Anzahl von γH2AX Foci in Abwesenheit von exogenen DNA-Schäden festgestellt, wie es in Tumorzellen gesehen wird. Die Mengen der phosphorylierten Kinasen Chk1 und 2, die an Kontrollpunkten im Zellzyklus auftreten, waren in einer ähnlichen Weise

in Tumorzellen verändert und die Mengen an Ku70 waren niedrig und das Protein wurde nicht an die DNA nach HU Behandlung rekrutiert. Unsere Ergebnisse zeigen eine Rolle für Nesprin-1 im DNA-Reparaturweg und schlagen Nesprin-1 als neuartigen Regulator für Tumorentstehung und Genominstabilität vor. Der Verlust von Nesprin-1 könnte eine wichtige Rolle in der Tumorprogression spielen.

1. Introduction

1.1 Nuclear envelope and LINC complex

The genome is contained within the nucleus in eukaryotic cells and is separated from the cytoplasm by a selective barrier, the nuclear envelope (NE). The proteins of the NE regulate the nucleo-cytoplasmic traffic and connect the nucleoplasm to the cytoplasm (Maraldi *et al.*, 2010; Shimi *et al.*, 2012). The NE consists of an outer (ONM) and inner nuclear membrane (INM) which enclose the perinuclear space (PNS). The ONM is contiguous with the endoplasmic reticulum, the INM contacts the nuclear lamina and chromatin (Figure 1).
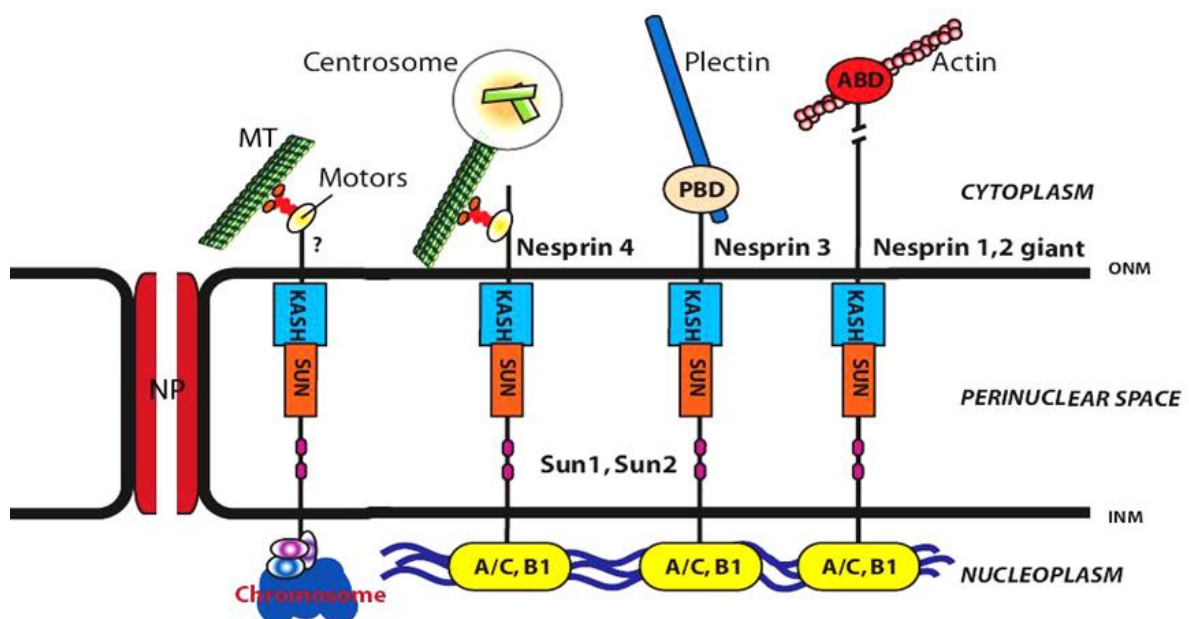
Figure 1: The structure of the nuclear envelope (NE). The NE is a barrier separating the nucleus from the cytoplasm and consists of ONM and INM, nuclear pore complexes (NPC), proteins of the INM, ONM, lamins and other proteins. ABD: Actin-binding domain; PBD: Plectin-binding domain. This model was taken from the lab website of Dr. Didier Hodzic. The question mark points out unknown functions of these connections.

Nuclear pore complexes (NPC) are inserted into the NE and connect the nucleus with the cytoplasm. The protein composition of the NE is complex as more than 100

proteins have been described and differs between the ONM and INM (Schirmer *et al.*, 2003). The NE proteins are involved in a variety of cellular processes including genome organization, gene expression and stability (Therizols *et al.*, 2006; Chow *et al.*, 2012).

An important component of the NE is the LINC (linker of nucleoskeleton and cytoskeleton) complex which connects the nucleus with the cytoskeleton. The LINC complex is present in a wide variety of organisms including amoebae, yeast, worms, flies, vertebrates, and plants (Schneider *et al.*, 2008; Schulz *et al.*, 2009; Graumann and Evans, 2010; Starr and Fridolfsson, 2010). The central components of mammalian LINC complexes are SUN (<u>S</u>ad1p, <u>UN</u>C-84) domain proteins and KASH-domain containing proteins, the Nesprins (<u>N</u>uclear <u>e</u>nvelope <u>spec</u>t<u>rin</u> repeats), which connect to Emerin, Lamins and chromatin at the nucleoplasmic side and to F-actin, microtubules, intermediate filaments and plectin at the cytoplasmic side (Figure 1) (Padmakumar *et al.*, 2005; Crisp *et al.*, 2006).

1.1.1 INM components of LINC complexes, and their functions

Among the first INM components recognized were members of the LEM domain family of proteins, which are named for the founding members, LAP2, Emerin and MAN1 (Figure 2) (Hetzer *et al.*, 2005). The LEM domain is composed of a motif of approximately 40 amino acids that mediates binding to BAF (barrier-to-autointegration factor) which is an abundant chromatin-associated protein (Lin *et al.*, 2000; Laguri *et al.*, 2001; Shumaker *et al.*, 2001). LAP2 (lamina associated polypeptides 2), one of the LEM domain proteins, has several isoforms in mammals (Berger *et al.*, 1996). Specifically, LAP2β is the most ubiquitous LAP2 isoform and interacts with chromatin and Lamin B via a specific region at its C-terminus.

Emerin is a 254 amino acid protein and has an N-terminal LEM-domain. It was the first NE protein which was linked to a human disease, Emery-Dreifuss muscular dystrophy (Bione *et al.*, 1994) and is involved in several protein–protein interactions (Cartegni *et al.*, 1997; Squarzoni *et al.*, 1998; Liu *et al.*, 2003). Emerin plays key roles in signal transduction, chromatin organization and gene expression. Additionally, Emerin links centrosomes to the nuclear envelope via a microtubule association (Holaska *et al.*, 2004; Markiewicz *et al.*, 2006; Salpingidou *et al.*, 2007).
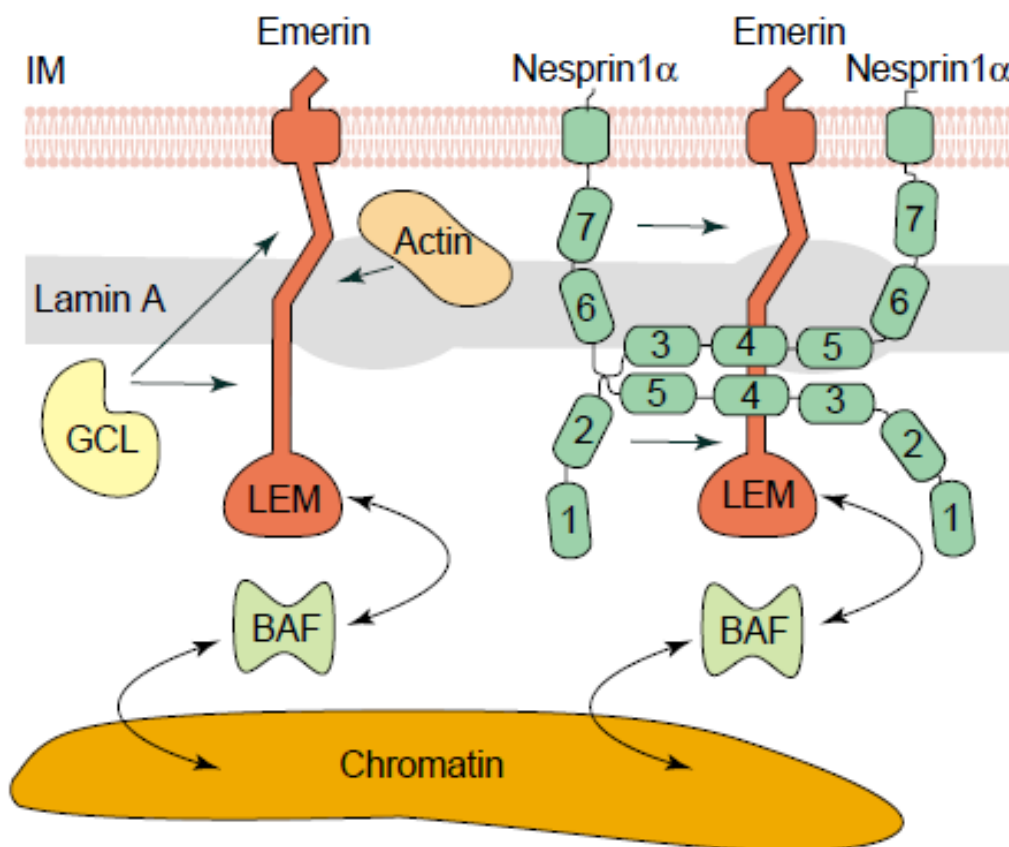
Figure 2: Illustration of LEM interactions. Emerin is anchored at the INM and interacts with lamin A, GCL (germ-cell-less), BAF, actin and a Nesprin-1α dimer. The seven SR domains in Nesprin-1α are numbered 1–7, beginning at the N-terminus. The image is not drawn to scale (Bengtsson and Wilson, 2004).

LEM domain proteins have also been linked to nuclear shape (Lammerding *et al.*, 2005) and transcriptional regulation (Nili *et al.*, 2001) as well as signaling cascades (Pan *et al.*, 2005; Markiewicz *et al.*, 2006).

The nuclear lamina underneath the INM is a network of type V intermediate filaments, and subdivided to A- and B-type lamins (Gerace *et al.*, 1978; McKeon *et al.*, 1986). All A-type Lamins, A, AΔ10, C, and C2 are encoded by the *LMNA* gene (Worman and Bonne, 2007). By contrast, B-type Lamins 1 and 2 are encoded by *LMNB1* and *LMNB2*, respectively (Worman and Bonne, 2007). B-type LaminB3 is a splice variant of the *LMNB2* gene (Furukawa and Hotta, 1993). Several studies suggested that Lamins participate in functions ranging from nuclear shape and stability to replication, transcription and splicing (Moir *et al.*, 2000; Schirmer *et al.*, 2001; Kumaran *et al.*, 2002; Lammerding *et al.*, 2004).

SUN proteins are prototypical type-II transmembrane proteins of the INM components of the LINC complex with their N-terminus facing the nucleoplasm, and a C-terminal conserved SUN domain localizing in the perinuclear space (PNS) between the INM and ONM. At the nuclear side they interact with Lamins (Padmakumar *et al.*, 2005; Crisp *et al.*, 2006; Haque *et al.*, 2006). To date, five SUN proteins have been identified; SUN1 (UNC-84A), SUN2 (UNC-84B), SUN3, SUN4 (SPAG4), and SUN5 (SPAG4L). Remarkably, SUN proteins play important roles in genome stability and nucleus centrosome coupling (Zhang *et al.*, 2009; Lei *et al.*, 2012).

1.1.2 Nesprins, ONM components of LINC complexes and their functions

Nesprins are type II transmembrane proteins, which connect the nucleus with the cytoskeleton. Nesprins localize to both nuclear membranes and have evolutionarily conserved orthologs in lower organisms including *Schizosaccharomyces pombe* (Kms1), *Dictyostelium discoideum* (interaptin), *Caenorhabditis elegans* (ANC-1, ZYG-12 and UNC-83), and *Drosophila melanogaster* (Msp-300). To date, four Nesprins have been described (Nesprin-1, Nesprin-2, Nesprin-3, Nesprin-4). They are

encoded by separate genes (*SYNE1, SYNE2, SYNE3, SYNE4*) that give rise to multiple isoforms (Figure 3.1). Nesprins have a varying number of SR domains, each of which consists of approximately 106 residues that form a triple-helical bundle. SR domains facilitate protein-protein interactions, crosslink actin and microtubules, and function as molecular scaffolds or stabilizers (Rajgor *et al.*, 2012).

The giant isoforms of Nesprin-1 (1 MDa) and Nesprin-2 (800 kDa) are greatly homologous to one another and share an N-terminal actin-binding domain (ABD) made from two calponin homology domains thereby linking the NE to the actin cytoskeleton (Zhen *et al.*, 2002; Padmakumar *et al.*, 2004). On the other hand, Nesprin-1 and Nesprin-2 can bind to microtubule motor proteins, kinesin and dynein, through specific spectrin repeats (Zhang *et al.*, 2009; Schneider *et al.*, 2011b; Yu *et al.*, 2011). Nesprin-3 and Nesprin-4 are much smaller and lack N terminal ABDs. Nesprin-3 interacts with plectin which provides a link to the intermediate filament system, Nesprin-4 can associate with kinesin-1 which establishes a link to microtubules (Wilhelmsen *et al.*, 2005; Roux *et al.*, 2009). In the LINC complex, Nesprins bind through their C-terminal luminal amino acids to the C-terminal SUN domain of SUN proteins. The structure of this complex has been recently solved and the presence of a trimer revealed (Sosa *et al.*, 2012; Wang *et al.*, 2012; Rothballer *et al.*, 2013).
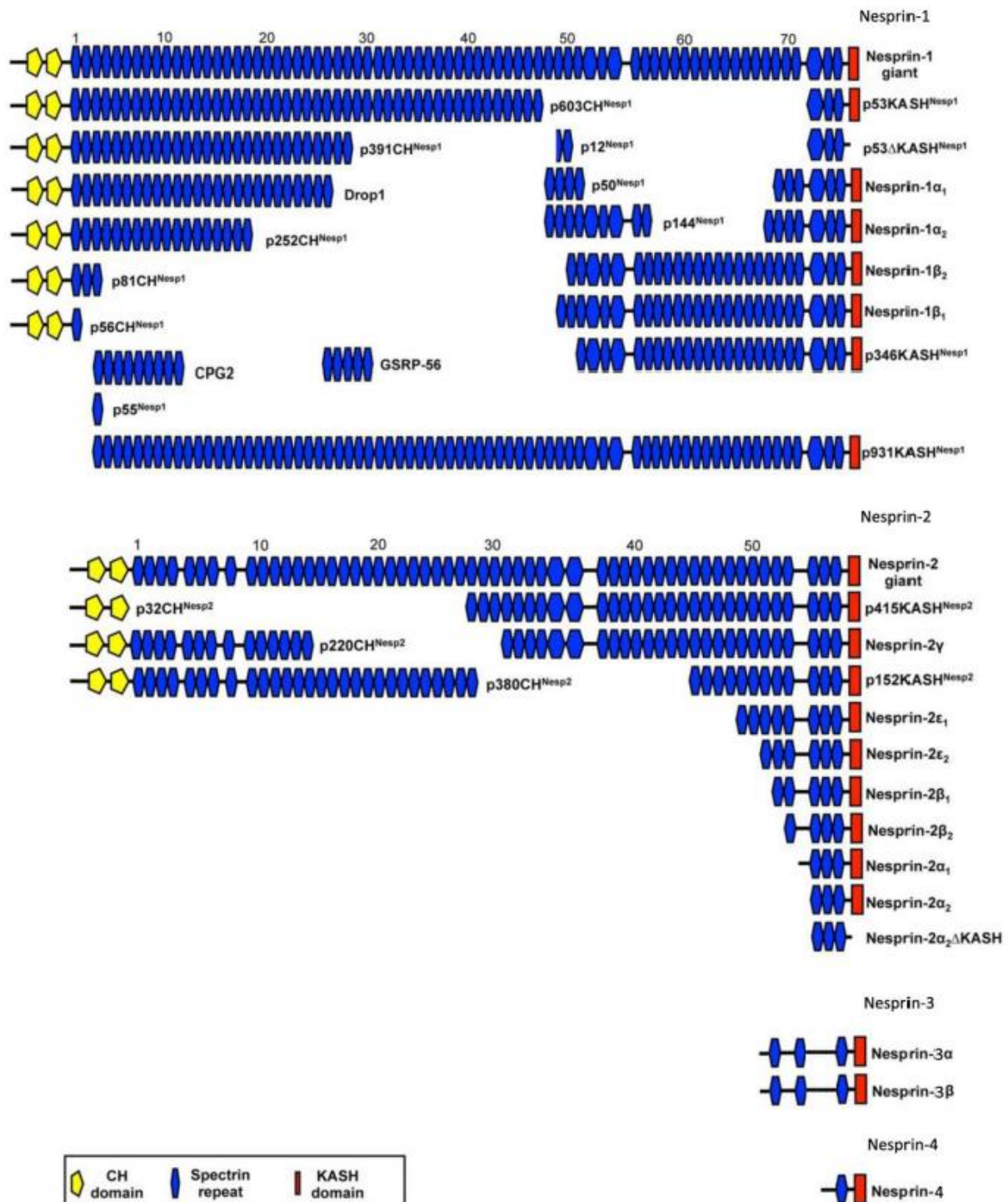
Figure 3.1: Scheme of Nesprin isoforms. Nesprins share common structural features, a N-terminal calponin homology (CH) domain (yellow) and a C-terminal KASH domain (red) and a spectrin repeat containing rod (blue). Each Nesprin is encoded by a single gene that gives rise to many different isoforms. This Figure was taken from (Rajgor *et al.*, 2012) and modified.

On the other hand, Nesprins can form self-interactions via their SRs and the ABD of

Nesprin-1 and Nesprin-2 was shown to interact with N-terminal spectrin repeats of

Nesprin-3 (Mislow *et al.*, 2002a; Lu *et al.*, 2012; Taranum *et al.*, 2012a). Based on these binding abilities, Nesprins enable a more orchestrated protein network along the nuclear envelope (Figure 3.2).
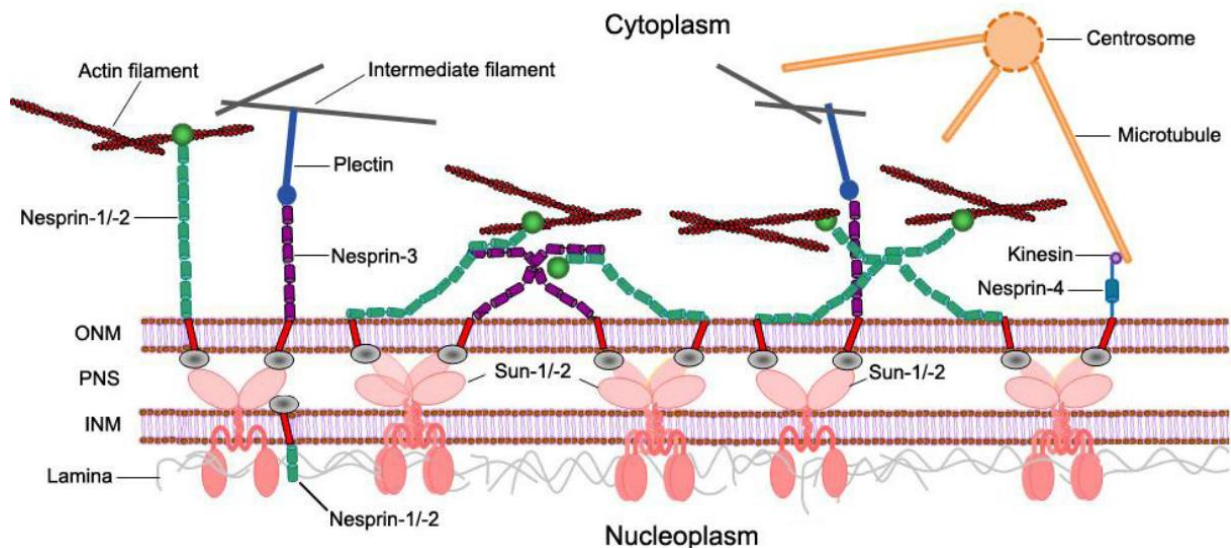
Figure 3.2: Schematic diagram of Nesprin interactions at the outer nuclear membrane surface. Nesprins form self-interactions via their SRs. The ABDs of Nesprin-1/-2 interact with F-actin, N-terminal Nesprin-1 spectrin repeats interact with Nesprin-3 (modified from (Taranum *et al.*, 2012a)).

Due to the establishment of nuclear-cytoskeletal connections, Nesprins play key roles in biologically important functions and this is supported by several studies (Table 1). Especially, Nesprin-1 and Nesprin-2 contribute to nuclear shape and position of the nucleus (Grady *et al.*, 2005; Zhang *et al.*, 2005; Kandert *et al.*, 2007; Luke *et al.*, 2008; Puckelwartz *et al.*, 2009). A recent report also indicated that Nesprin-3 regulates cell morphology and cell migration (Morgan *et al.*, 2011; Khatau *et al.*, 2012). On the other hand, in Nesprin-4 knock out (KO) mice, nuclear position was changed in outer hair cells, thereby leading to hear loss (Horn *et al.*, 2013). More recently, the effects of Nesprin-1, Nesprin-2, and Nesprin-3 on centrosome positioning have been reported (Zhang *et al.*, 2009; Morgan *et al.*, 2011).

Table 1: Interactions of Nesprins with cellular components and functions of these connections. Nesprins have key roles in many aspects of cell functions due to their nuclear-cytoskeletal connections (modified from (Mellad *et al.*, 2011)).

	Connection	Nesprin	Function
Actin	F-actin	Nesprin-1	Nuclear positioning,
		Nesprin-2	Mechanotransduction
	Meckelin	Nesprin-2	Ciliogenesis
IF	Lamin A	Nesprin1/2	Chromatin organization,
			NE architecture
	Plectin	Nesprin-3	NE-IF coupling
Microtubules	Kinesin-1	Nesprin-2/4	Nuclear migration, polarity
	Kinesin-2	Nesprin-1	Vesicular transport
	Dynein	Nesprin-1/2	Nuclear migration, polarity
	Dynactin	Nesprin-1/2	Nuclear migration, polarity

1.1.3 Nesprin-1

The human Nesprin-1 locus (*SYNE1*) at chromosome position 6q25 has 147 exons that encode up to 8,797 residues (Padmakumar *et al.*, 2004). Nesprin-1 is a ~1 MDa protein with 74 predicted spectrin repeats (Figure 3.1). There are several isoforms for Nesprin-1 with many names including Syne-1 (Apel *et al.*, 2000), Drop1 (Marme *et al.*, 2008), GSRP56 (Kobayashi *et al.*, 2006), MSP300 (Rosenberg-Hasson *et al.*, 1996), Myne-1 (Mislow *et al.*, 2002b), Enaptin (Padmakumar *et al.*, 2004), CPG2 (Nedivi *et al.*, 1996), ANC-1 (Starr and Han, 2002). One of the small isoforms, Nesprin-1α, localizes at the nuclear inner membrane and interacts with Emerin and Lamin A (Mislow *et al.*, 2002a). The longest Nesprin-1 isoforms contain the ABD motif at their N-terminus, which colocalizes with F-actin in vivo (Starr and Han, 2002;

Padmakumar *et al.*, 2004) and a highly conserved KASH domain at their C-terminus (Zhang *et al.*, 2002). Nesprin-1-165 harbors the ABD and the first 11 spectrin repeats, CPG2 contains spectrin repeats 3 to 11.

In several cell lines, Nesprin-1 isoforms are localized to the nucleolus, to microtubules, stress-fibres, focal adhesions, and RNA processing bodies. It is important to note that the localization of individual Nesprin-1 isoforms can vary depending on which cell types express them, suggesting that any single Nesprin-1 isoform may have different functions in different cell lines. Beyond that, Nesprin-1 isoforms anchor to the Golgi apparatus and to mitochondria and overexpression of the Golgi-binding domain of Nesprin-1 causes the Golgi to collapse into a condensed structure near the centrosome (Gough *et al.*, 2003). Moreover, Nesprin-1 has been reported to localize to the Golgi apparatus and over-expression of dominant-negative Nesprin-1 fragments composed of SRs within the central rod domain disrupt Golgi organization and function (Gough *et al.*, 2003; Gough and Beck, 2004; Kobayashi *et al.*, 2006). The candidate plasticity gene 2 (*cpg2*), brain-specific Nesprin-1 isoform, encompasses solely SRs and localizes to the neuronal postsynaptic endocytic zone surrounding dendritic spines where it regulates clathrin-mediated uptake and recycling of chemokine receptors (Nedivi *et al.*, 1996; Cottrell *et al.*, 2004).

Analysis of Nesprin-1 KO mice strongly indicate the importance of Nesprin-1 for nuclear morphology, NE organization, actin organization and cell motility (Grady *et al.*, 2005; Zhang *et al.*, 2007; Chancellor *et al.*, 2010; Zhang *et al.*, 2010), and in vitro studies demonstrated that knock down of Nesprin-1 led to nuclear defects and mislocalization of Emerin and SUN2 in U20S and fibroblast cells (Zhang *et al.*, 2007).

1.2 The LINC complex in human diseases and its cancer connections

Disruption of the nuclear-cytoskeletal connection has severe consequences: The stability, size and shape of the nucleus are altered, its position in the cell is disturbed, cell migration is affected, the mechanical properties of the cell and mechanotransduction from the extracellular space to the nucleus are impaired as well as signaling processes. The importance of the LINC complex is further underlined by the large group of diseases in which components of the LINC complex are mutated generating a variety of degenerative diseases affecting striated muscle and peripheral nerves, skeletal and fat development, and premature aging syndromes (Zaremba-Czogalla *et al.*, 2011).

Disruption of the LINC complex via mutations in the genes encoding Nesprin-1 and Nesprin-2 or their binding partners such as Emerin and Lamin A/C gives rise to Emery-Dreifuss Muscular Dystrophy (EDMD) (Table 2). Other mutations in *LMNA* cause Hutchinson Gilford progeria syndrome (HGPS) or Charcot-Marie-Tooth (CMT) disorder and many other syndromes (Zaremba-Czogalla *et al.*, 2011). Mutations in *SYNE1* in addition to being responsible for some forms of Emery-Dreifuss muscular dystrophy cause cerebellar ataxia and arthrogryposis (Gros-Louis *et al.*, 2007; Zhang *et al.*, 2007; Attali *et al.*, 2009). To date, more than 300 mutations in ten genes encoding proteins of the NE have been linked with laminopathies (Mejat and Misteli, 2010).

Table 2: Diseases caused by gene mutations in NE proteins. This table summarizes mutated genes and the resulting diseases. *LMNA* (A-type lamins), *LMNB1* (lamin B1), *LMNB2* (lamin B2), *EDMD* (emerin), *SYNE1* (Nesprin-1), *SYNE2* (Nesprin-2), *TMEM43* (transmembrane protein 43), *TMPO* (thymopoietin), *ZMPSTE24* (zinc metallopeptidase STE24), *BANF1* (barrier to autointegration factor 1), *LEMD3* (MAN1), *LBR* (lamin B receptor) (taken from (Schreiber and Kennedy, 2013)).

	Gene Mutated
Striated Muscle Diseases	
Emery-Dreifuss muscular dystrophy	*LMNA, EDMD, SYNE1, SYNE2, TMEM43, TMPO*
Limb-girdle muscular dystrophy	*LMNA*
Dilated cardiomyopathy	*LMNA, EDMD, SYNE1, SYNE2, TMEM43, TMPO*
Congenital muscular dystrophy	*LMNA*
Heart-hand syndrome	*LMNA*
Lipodystrophy Syndromes	
Dunnigan-type familial partial lipodystrophy	*LMNA*
Mandibuloacral dysplasia	*LMNA, ZMPSTE24*
Lipoatrophy	*LMNA*
Partial lipodystrophy	*LMNB2*
Accelerated Aging Disorders	
Atypical Werner syndrome	*LMNA*
Hutchinson-Gilford progeria syndrome	*LMNA*
Restrictive dermopathy	*LMNA, ZMPSTE24*
Atypical progeria syndrome	*BANF1*
Peripheral Nerve Disorders	
Charcot-Marie-Tooth disease	*LMNA*
Adult-onset leukodystrophy	*LMNB1*
Spinocerebellar ataxia type 8	*SYNE1*
Bone Diseases	
Buschke-Ollendorff syndrome	*LEMD3*
Melorheostosis	*LEMD3*
Osteopoikilosis	*LEMD3*
Greenberg skeletal dysplasia	*LBR*
Other	
Pelger-Huet anomaly	*LBR*
Arthrogryposis	*SYNE2*

During tumor formation several cellular activities are deregulated. This includes cell motility, adhesion, proliferation, metabolism and DNA damage response. Many of these features depend on the integrity and organization of NE and morphological changes of the NE and LINC complex are a hallmark of cancer. Although much of the emphasis has been on deciphering the aetiology of these specific and often devastating diseases, recent studies also shed new light on how cancer associated alterations of LINC complex protein expression levels may affect tumorigenesis and provide an informative parameter in tumor detection and characterization.

Several components of the LINC complex, Lamins (Broers *et al.*, 1993; Moss *et al.*, 1999), LAP2 (Somech *et al.*, 2007), and Emerin (Capo-chichi *et al.*, 2009) were discovered as biomarkers in a wide range of cancer types (Table 3). Interestingly, not only was mRNA encoding lamin B1 found in the blood circulation (Sun *et al.*, 2010), and its detection in plasma indicate early stage hepatocellular carcinoma, but lamin B1 was also in a proteomic approach found to be upregulated in hepatocellular tumors (Lim *et al.*, 2002). On the other hand, the nucleoporin NUP88 has been assessed as a cancer biomarker (Martinez *et al.*, 1999) and was found in several studies to be overexpressed in malignant tissues (Gould *et al.*, 2002; Agudo *et al.*, 2004; Knoess *et al.*, 2006; Brustmann and Hager, 2009; Schneider *et al.*, 2010).

Down regulation of Drop1, an N-terminal isoform of Nesprin-1, has been observed in early tumor stages in a wide range of human carcinomas and may play a role in chromatin organization (Raffaele Di Barletta *et al.*, 2000; Dou *et al.*, 2005; Marme *et al.*, 2008). Furthermore, mutations in *SYNE1* were observed in ovarian and colorectal cancers (Sjoblom *et al.*, 2006; Doherty *et al.*, 2010). Additionally, the *SYNE1* gene was frequently methylated in lung cancer cell lines, lung adenocarcinoma (Tessema *et al.*, 2008) and colorectal cancer (Schuebel *et al.*, 2007). By bioinformatic analysis of data from a collection of cancer genome samples Mascia and Karchin identified

SYNE1 as one of the genes that participated in glioblastoma progression (Masica and Karchin, 2011). They observed that mutations in *SYNE1* were associated with a large number of differentially expressed genes.

Table 3: Nuclear envelope components and tumorigenesis. The table summarizes cancer-associated alterations in the nuclear envelope components (modified from (Chow *et al.*, 2012)).

Protein	Phenotype and clinical correlate (if applicable)	Tumour type
Emerin	Reduced expression	Ovarian cancer
Lamin A and lamin C	Reduced expression or mislocalized	Numerous cancer types
	Low expression of lamin A correlates with high proliferation (as determined by Ki67 staining)	Basal cell carcinoma
	Low expression of lamin C correlates with low proliferation (as determined by Ki67 staining)	Basal cell carcinoma
	Increased expression correlates with poor prognosis or advanced stage	Colorectal, ovarian and prostate cancer
	Low expression correlates with increased relapse	Colon cancer stage II and stage III
	High expression in basal cell layer of epidermis overlying carcinoma	Basal cell carcinoma and squamous cell carcinoma
	Decreased expression correlates with poorer overall survival	Diffuse large B cell lymphoma and gastric cancer
Lamin B	Changes in level or localization	Numerous cancer types
	Elevated expression correlates with indicators of poor prognosis	Hepatocellular carcinoma and prostate cancer
	Detection of mRNA in plasma indicates the presence of carcinoma	Hepatocellular carcinoma
LAP2	Increased expression correlates with high proliferation	Malignant lymphocytes
Nesprin 1	Polymorphism correlates with increased risk	Invasive ovarian cancer
	Proposed to be a candidate cancer gene (mutated in cancer)	Colorectal cancer
Nesprin 2	Proposed to be a candidate cancer gene (mutated in cancer)	Breast cancer
NUP88	Increased expression	Ovarian cancer
	Increased expression correlates with high-grade malignancies	Numerous cancer types
	Increased expression correlates with poor differentiation	Hepatocellular carcinoma and colorectal cancer
	Increased expression corresponds with tumour invasiveness, high proliferation and/or metastasis	Breast, colorectal and endometrial cancer
	Increased serum level correlates with tumour invasion and advanced stage	Colorectal cancer
NUP98	Involved in oncogenic chromosomal translocations	Haematopoietic malignancies
NUP133	Increased expression	Breast cancer
	Proposed to be a candidate cancer gene (mutated in cancer)	Breast cancer
NUP214	Involved in oncogenic chromosomal translocations	Haematopoietic malignancies
	Increased expression	Breast cancer
	Proposed to be a candidate cancer gene (mutated in cancer)	Breast cancer

1.3 DNA repair pathways and mechanisms

Biologically, nuclear DNA is the most important component in the cell since it has all the genetic information required for proper cell functions. It is well known that mutagenic compounds, ionizing radiation, oxidative stress, and also normal DNA metabolic activities like replication and recombination can cause alterations in the DNA. It is therefore not surprising that any damage that leads to a break in the DNA double helix triggers a quick cellular reaction.

To maintain genetic stability and relay genetic information from one cell to another, mechanisms are required to protect the DNA against the accumulation of DNA damage. These mechanisms have been defined as DNA repair pathways. The major DNA repair pathways are non-homologous end-joining (NHEJ), nucleotide excision repair (NER), mismatch repair (MMR), homologous recombination (HR), and base excision repair (BER) (Figure 4).
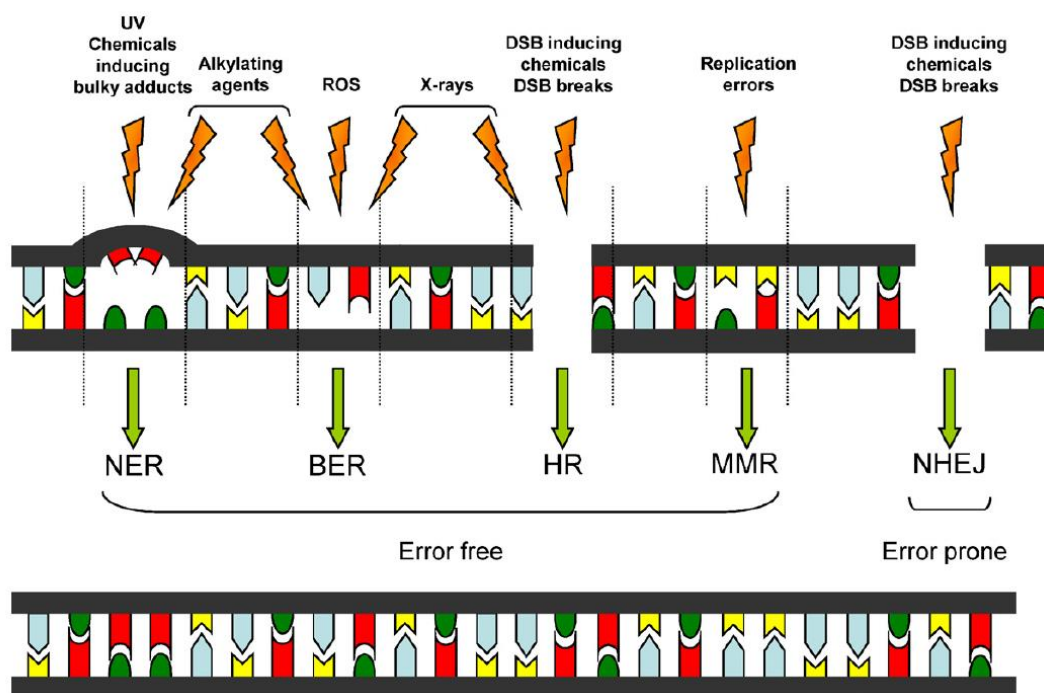
Figure 4: DNA repair pathways. Non-homologous end-joining (NHEJ), nucleotide excision repair (NER), mismatch repair (MMR), homologous recombination (HR), and base excision repair (BER) are the major DNA repair pathways (Melis *et al.*, 2011).

14

More importantly, defects in DNA repair pathways lead to genome instability, tumorigenesis, and aging owing to accumulative DNA damage (de Boer and Hoeijmakers, 2000).

1.3.1 Non-homologous end-joining (NHEJ) pathway

One of the most dangerous forms of DNA damage is the DNA double-strand breaks (DSBs), which can result in genome instability if not repaired successfully (Hartlerode and Scully, 2009). DSBs initiate signalling cascades that trigger cell cycle checkpoints and change gene transcription to maintain genome stability (Valerie and Povirk, 2003; Cann and Hicks, 2007).

There are two main signalling networks in eukaryotic cells to repair DSBs: homologous recombination (HR) and nonhomologous end-joining (NHEJ) (Figure 5). A recent report indicated that HR uses a homologous chromosome or sister chromatid as template to repair the broken DNA and NHEJ re-ligates the two broken DNA ends together (Cann and Hicks, 2007). Based on this the NHEJ is an error-prone repair mechanism that might cause insertion and deletion of DNA sequences.

The DDR pathway is initiated by a phosphorylation cascade that triggers chromatin modifications which improve accessibility of the broken DNA to repair complexes and promotes the subsequent accumulation of DDR complexes into lesions at the site of damage (Riches *et al.*, 2008). Ataxia telangiectasia mutated (ATM)-mediated phosphorylation of the histone variant H2AX is the initial step to create a platform to which other DDR complexes are able to bind (Marti *et al.*, 2006). ATM triggers signaling cascades that activate cell cycle checkpoints leading to cell cycle arrest through phosphorylation of several proteins including CHK1, CHK2, p53, MDC1, and BRCA1 (Lavin and Kozlov, 2007).
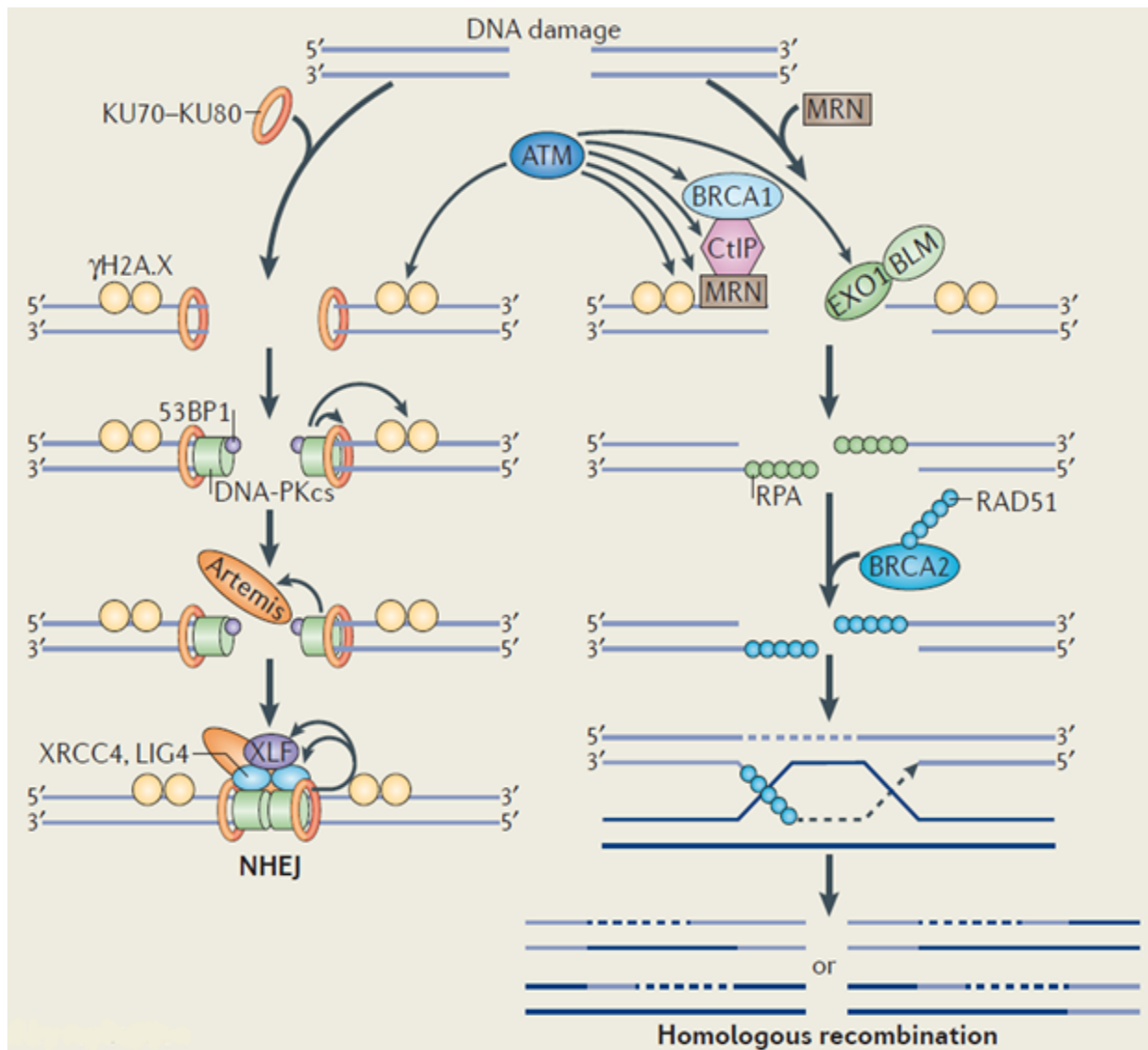
Figure 5: Overview of DNA DSBs repair pathways. DSBs in the DNA are induced by damaging agents. Phosphorylation of histone H2AX (γH2AX) is the initial step of these pathways. In the NHEJ pathway, the two broken ends are bound by the DNA-end-binding protein Ku, which recruits the DNA-dependent protein kinase catalytic subunit (DNA-PKcs) to the free DNA ends. Homologous recombination requires BRCA1, RAD51 (which forms filaments along the unwound DNA strand to facilitate strand invasions) and RAD52 (a DNA-end-binding protein) (modified from (Chowdhury *et al.*, 2013)).

Ku is the DNA-binding component of the NHEJ repair machinery. Ku recruits DNA-PKcs to form the active protein kinase complex DNA-PK upon recognition and binding to the broken DNA end (Mahaney *et al.*, 2009). Following this process, Ku appears to protect broken DNA from nuclease binding or activity (Downs and Jackson, 2004). In addition, Ku has also been shown to bind to telomeres and to

function in telomere maintenance, remarkably by anchoring telomeres to the nuclear periphery, thus contributing to telomeric silencing and preventing telomere shortening (Riha *et al.*, 2006).

Sharpless et al. carried out a study which indicated that NHEJ-deficiency predisposes to cancer (Sharpless *et al.*, 2001). Moreover, mice lacking p53, DNA-PKcs or Ku80 succumb in early postnatal life to progenitor B cell lymphomas (Guidos *et al.*, 1996; Nacht *et al.*, 1996; Difilippantonio *et al.*, 2000; Lim *et al.*, 2000).

1.3.2 Nucleotide excision repair

The nucleotide excision repair (NER) pathway is characterized by the removal of bulky DNA helix-distorting injuries of both exogenous and endogenous origin. These helix-distorting DNA lesions recruit the proteins of this pathway to the damaged DNA sites (Figure 6).

GG-NER (global genomic repair) and TC-NER (transcription-coupled repair) are two subpathways of NER (Bohr *et al.*, 1985; Mellon *et al.*, 1987). GG-NER is independent of transcription and is constantly screening the genome for the identification of distorting lesions in the DNA helix, whereas TC-NER is recruited to the transcribed DNA strand of active genes to repair transcription blocking lesions (Yasuda *et al.*, 2007). About 30 proteins participate in the NER pathway, most function in GG-NER as well as in TC-NER (Christmann *et al.*, 2003). However, they have different types of damage recognition and therefore contain different proteins that recognize the damage.
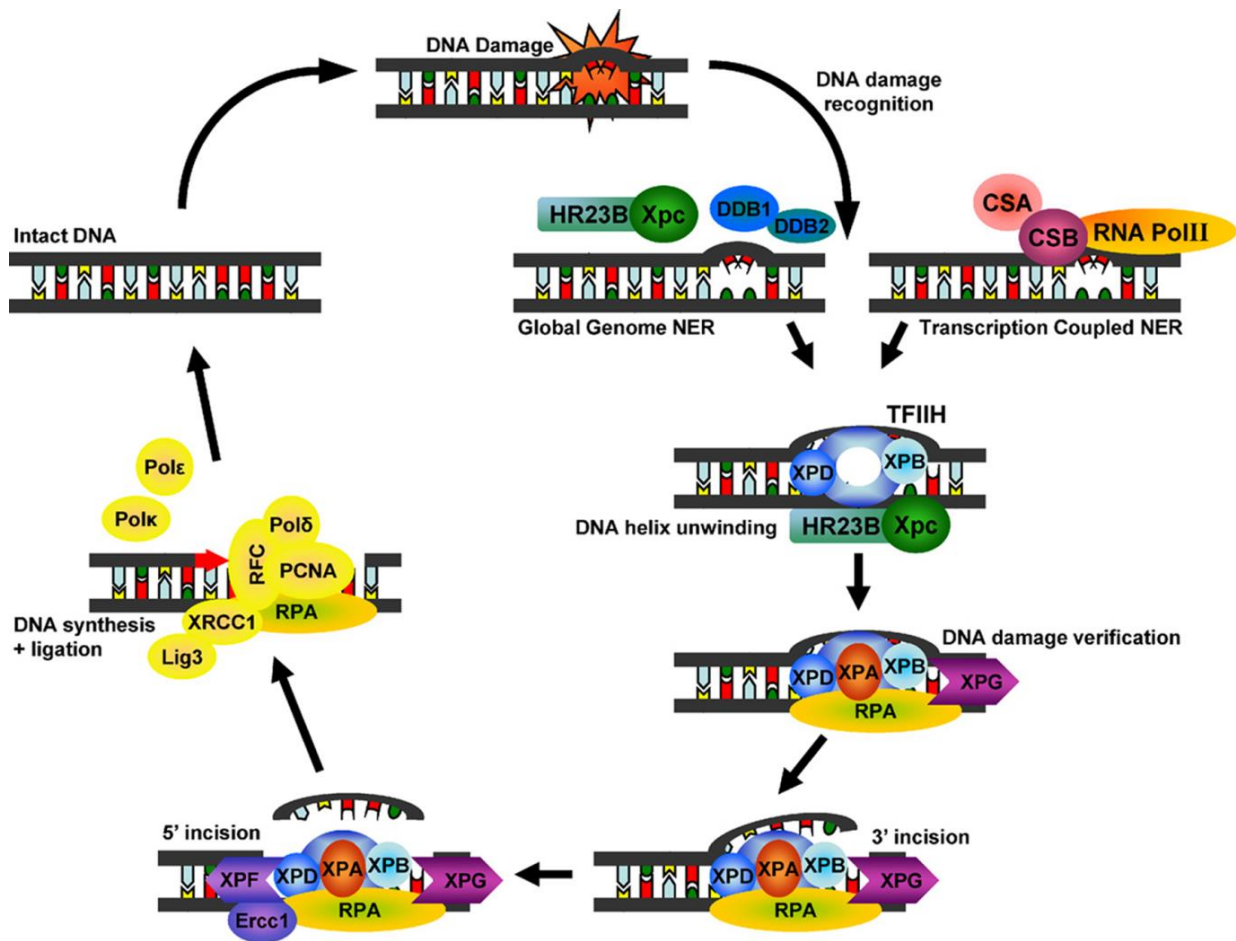
Figure 6: NER repairs UV-induced pyrimidine dimers, protein-DNA and intra-strand crosslinks, and a wide range of bulky chemical adducts. Global GG-NER and TC-NER differ in their damage recognition. In GG-NER, damage recognition is accomplished by the XPC-HR23B protein complex whereas CSA and CSB proteins are responsible for the initial detection of damaged DNA in TC-NER (Melis *et al.*, 2011).

GG-NER uses the XPC-HR23B protein complex as the primary recognition factor (Volker *et al.*, 2001; Hanawalt, 2002). Recently, it has been reported that, for certain types of lesions, different proteins are responsible for the initial recognition. Additionally, DDB2 (or XPE) bound to DDB1 can recognise CPD lesions. The XPE-DDB1 complex recruits the XPC-HR23B complex to the lesion, where it gets exchanged by the XPC-HR23B complex and repair takes place (Kulaksiz *et al.*, 2005). In TC-NER, DNA damage is recognized by CSA and CSB proteins. After recognition, these proteins bind to the DNA lesion thereby distorting the DNA and

recruiting other factors of this repair system to reproduce the correct DNA sequence (Gillet and Scharer, 2006; Trego and Turchi, 2006).

Although somatic alterations in some of the NER factors lead to skin cancer, defects in the NER pathway associate with genetic disorders such as the Xeroderma pigmentosum (XP) syndrome (Yasuda *et al.*, 2007).

1.3.3 Mismatch repair network

The mismatch repair (MMR) is a conserved biological pathway from bacteria to man that plays a critical role in maintaining genome stability. Its function is in correcting DNA mismatches occurred during DNA replication to prevent mutations in dividing cells. MMR is also required for damage-induced cell cycle checkpoint response. Deficiency of MMR activity causes replication-associated errors leading to point and frameshift mutations and tumorigenesis (Jacob and Praz, 2002).

The initial step in MMR is identification of the mispaired region (Figure 8). Two separate heterodimers known as MutSα (Msh2/Msh6 in eukaryotes) (Iaccarino *et al.*, 1996), and MutSβ (Msh2/Msh3) participate in this process (Habraken *et al.*, 1996; Palombo *et al.*, 1996). MutS is a DNA-binding protein, contains an ATPase domain and a protein-protein interaction domain that allows two MutS molecules to interact in order to form dimers (Lamers *et al.*, 2000; Obmolova *et al.*, 2000). While MutSα binds primarily to single-base pair mismatches and small insertion/deletion loops, MutSβ binds to larger insertion/deletion loops (Acharya *et al.*, 1996; Marsischky *et al.*, 1996). After mismatch recognition, MutL homologs are responsible to repair mismatches. At least 4 human MutL homologs, hMLH1, hMLH3, hPMS1, and hPMS2 have been identified (Bronner *et al.*, 1994; Nicolaides *et al.*, 1994; Papadopoulos *et al.*, 1994; Lipkin *et al.*, 2000).
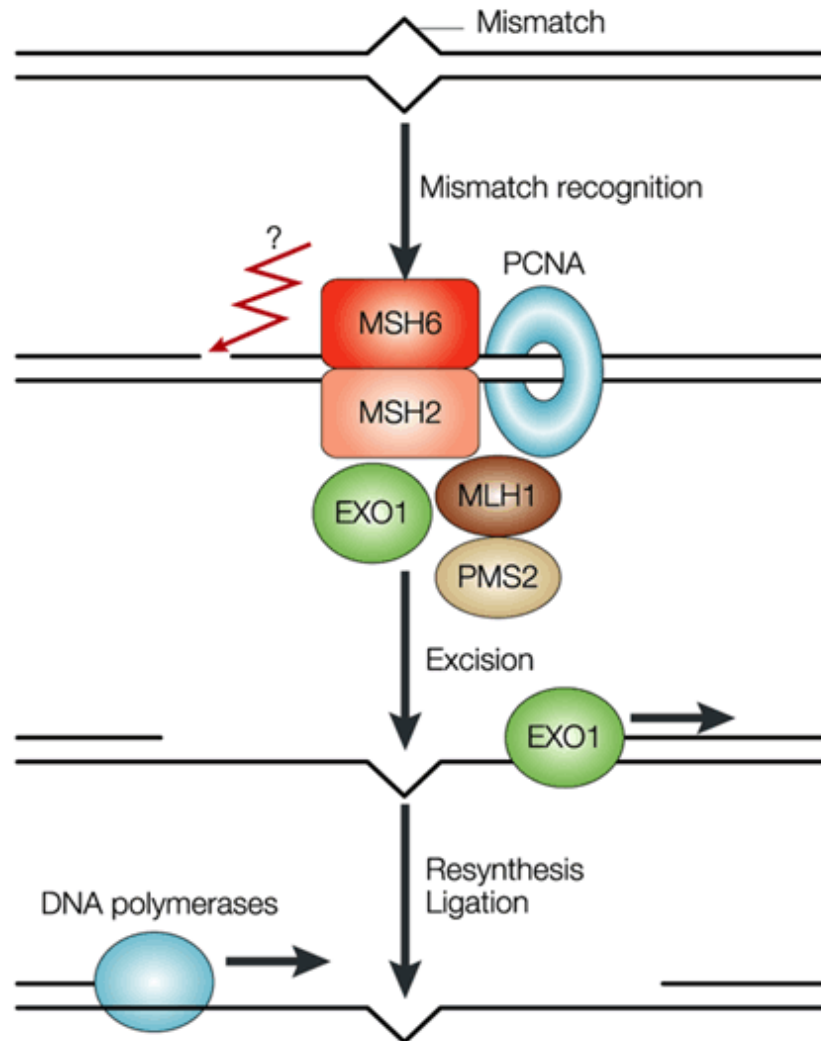
Figure 7: Mismatch repair. MSH2–MSH6 and PMSH2-MLH1 heterodimers bind to single base pair mismatches in an ATP-dependent manner. The lesion is digested by EXO1, and then filled in by DNA polymerases. Question mark points out the unknown homologue of prokaryote MutH in eukaryotes (Martin and Scharff, 2002).

hMLH1 heterodimerizes with hPMS2, hPMS1, or hMLH3 to form hMutLα, hMutLβ, or hMutLγ, respectively (Kunkel and Erie, 2005). MutLα heterodimer (Mlh1/Pms1) initiates subsequent repair events (Prolla *et al.*, 1994; Pang *et al.*, 1997). hMutLα is required for MMR and hMutLγ plays a role in meiosis, but no specific biological role has been identified for hMutLβ (Kunkel and Erie, 2005). hMutLα possesses an ATPase activity and defects in this activity inactivate MMR in human cells. Defects in the MMR pathway have been associated with a number of different malignancies (Gazzoli *et al.*, 2002).

1.4 Aim of the project

Goal of this study is to provide a picture of the interactions and roles of Nesprin-1. This will allow defining its roles in health and disease more precisely and will provide mechanisms underlying these roles. We will specifically try

1. to understand the role of Nesprin-1 in tumorigenesis and genome stability

2. to identify possible interaction partners of Nesprin-1

3. to detect consequences of Nesprin-1 loss

4. to elucidate the role of Nesprin-1 in DDR and DNA repair pathways.

2. Results

2.1 Nesprin-1 interactions

2.1.1 Interactions of N-terminal Nesprin-1 spectrin repeats

Earlier studies have demonstrated that the C-terminal isoform Nesprin-1α can self-associate through its third and fifth spectrin repeat to form an antiparallel dimer (Mislow *et al.*, 2002a; Zhong *et al.*, 2010). Whether other spectrin repeats of Nesprin-1, in particular the N-terminal spectrin repeats, possess similar oligomerization properties is not known. When we compared Nesprin-1's N-terminal spectrin repeats to the spectrin repeats of mouse α-actinin 2, SR1, 2, and 4 showed homology with SR2 from α-actinin, and SR10 and 11 resembled SR1 and SR4, respectively. The remaining SRs exhibited less homology with the ones of α-actinin. From earlier reports it is known that spectrin repeats of the α-actinin type can dimerize as in α-actinin or in spectrin determining the protein structure (Noegel *et al.*, 1987; Djinovic-Carugo *et al.*, 2002).

To understand whether N-terminal sequences of Nesprin-1 can interact with themselves, bacterially produced GST-fusion proteins encompassing several spectrin repeats of Nesprin-1-165 (aa 573-858, 859-1144 and 1145-1431; Figure 8A) was used to pull down the corresponding GFP-tagged proteins from COS7 cells.

While all fusion proteins pulled down their GFP-tagged counterpart, GST alone did not interact with anyone of the GFP fusion proteins (Figure 8B). Furthermore, Nesprin-1-165-GFP was transfected in COS7 cells and the GST-fusion proteins used in pull down experiments. Interestingly, Nesprin-1-165-GFP was precipitated with GST-573-858 and GST-1145-1431, but not with GST-859-1144. The polypeptide encompassing aa 859-1144 encodes part of SR6, SR7, 8 and part of 9 which in the comparison showed a lower resemblance to the ones of α-actinin. GST alone also

did not bind to Nesprin-1-165-GFP (Figure 8C, D). Our results imply that Nesprin-1

oligomerizes through N-terminal spectrin repeats.
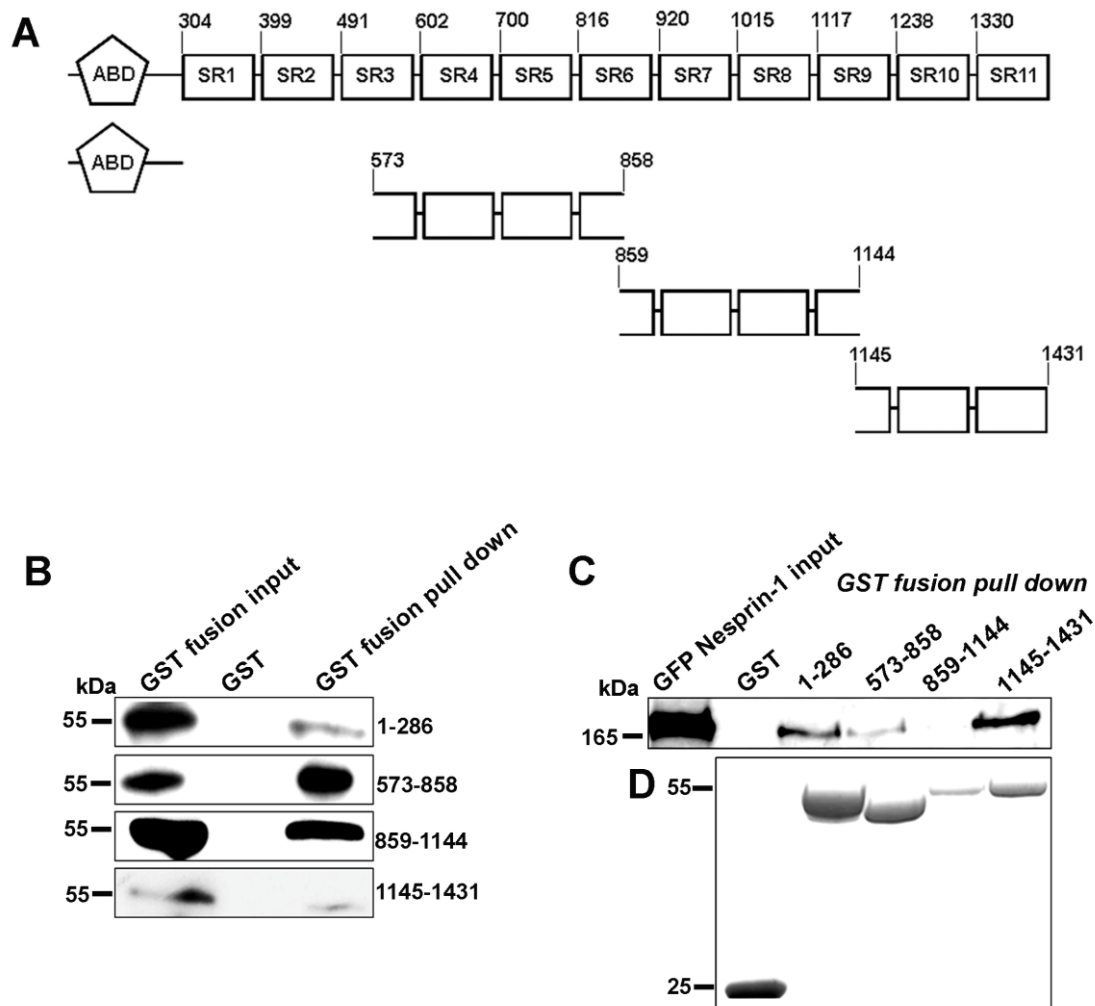
Figure 8: N-terminal spectrin repeats of Nesprin-1 can self-associate through its amino terminal sequences. (A) Overview of Nesprin-1-165 and constructs used as GST and GFP fusion proteins. Numbers indicate the location of amino acids. (B, C) GFP-tagged ABD (aa 1–286), and spectrin repeats of Nesprin-1-165 (aa 573–858, 859–1144, and 1145–1431) and full-length Nesprin-1-165 (C) were expressed in COS-7 cells. (B) The cell lysates were incubated with either immobilized GST-fused aa 1–286, 573–858, 859–1144, and 1145–1431 or GST alone for control. The precipitated proteins resolved in 10% acrylamide gels by SDS-PAGE. The membranes were probed with GFP antibody mAb K3-184-2. (C) Interaction of N-terminal spectrin repeats with GFP Nesprin-1-165. (D) The GST-fusion proteins used for the pull down are shown by Coomassie Blue staining (bottom panel).

2.1.2 The C-terminus of Nesprin-1 interacts with Nesprin-2

By immunoprecipitation experiments we next asked whether the possibility of an association between Nesprin-1 and Nesprin-2 exists. Human fibroblasts (HF) were transfected with plasmids encoding GFP-tagged Nesprin-1 polypeptides that were differently composed and possessed or lacked the KASH domain (aa 8034-8749; 7938-8644) (Figure 9A, B).
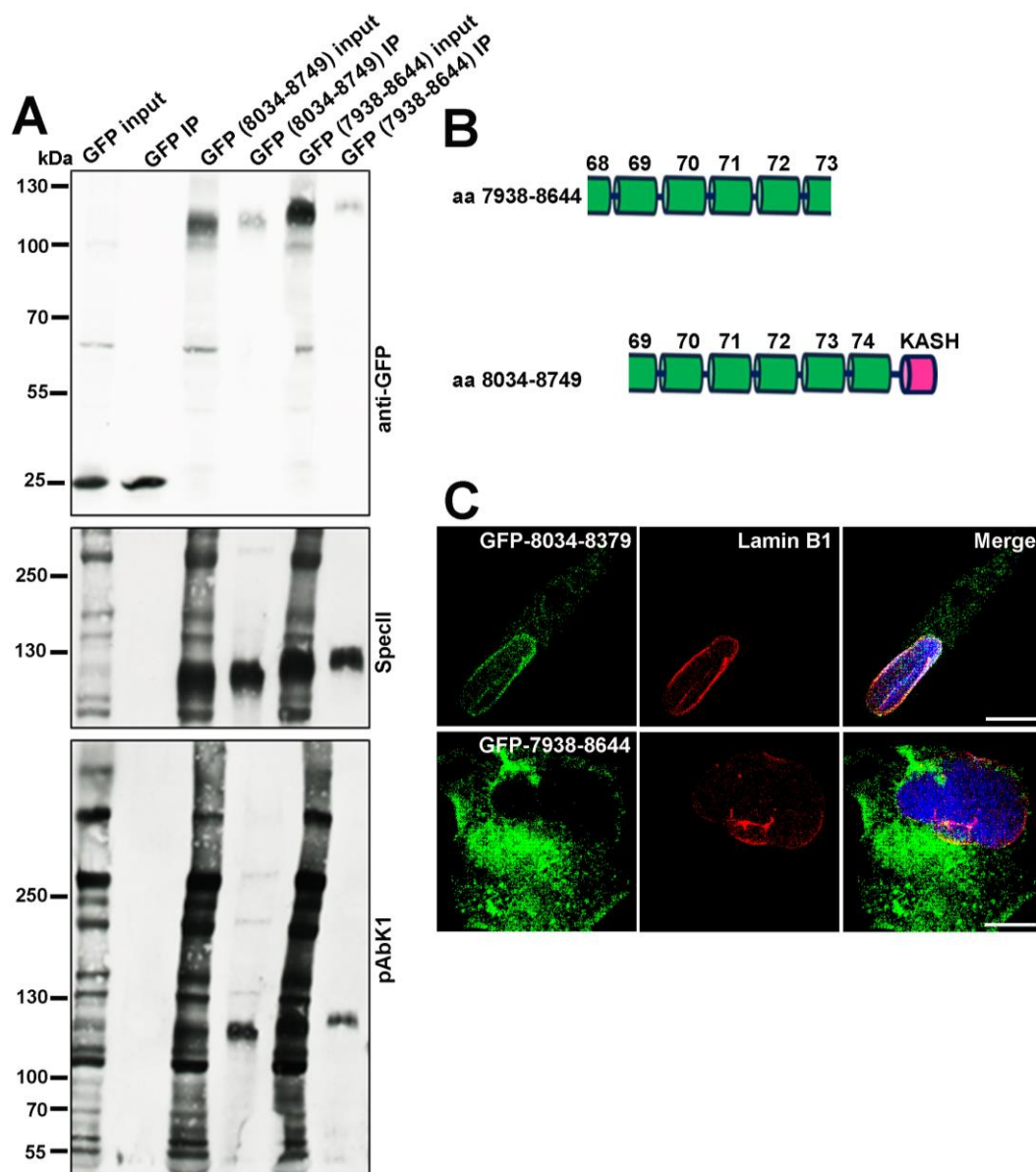
Figure 9: Nesprin-1 interacts with Nesprin-2. (A) GFP-tagged Nesprin-1 (aa 8034-8749; 7938-8644) were expressed in HF cells. Numbers indicate the location of amino acids and used for immunoprecipitation experiments. Immunoprecipitation was carried out with GFP-TRAP beads. Detection of precipitated proteins was with mAb

K3-184-2. The blot was further probed with pAbK1 and SpecII antibodies specific for Nesprin-2 and Nesprin-1, respectively. (B) Schematic of the Nesprin-1 constructs. (C) HF cells were transfected with plasmids allowing GFP-Nesprin-1-8034-8379, and GFP-Nesprin-1-7938-8644 expression (green) and stained with Lamin B1 (red), and DAPI (blue). Scale bar, 10 µm.

GFP transfected cells served as negative control for Nesprin-1 and Nesprin-2 interaction. The proteins were immunoprecipitated using GFP-TRAP beads and the resulting blot probed with pAbK1 specific for Nesprin-2 and SpecII specific for Nesprin-1.

We found that Nesprin-2 proteins detected by pAbK1 which is directed against C-terminal Nesprin-2 sequences precipitated with GFP-Nesprin-1-8034-8749, but not with GFP-Nesprin-1-7938-8644. The interacting domain is therefore located within the C-terminal sequences of Nesprin-1. GFP alone did not bind to Nesprin-2 (Figure 9A). Furthermore, we studied the subcellular localization of GFP-Nesprin-1-8034-8749 and GFP-Nesprin-1-7938-8644. GFP-Nesprin-1-8034-8749 localized mostly to the NE as revealed by Lamin B1 colocalization. GFP-Nesprin-1-7938-8644, which lacks the KASH domain containing the transmembrane region, was also present at the NE but was most prominent in the cytoplasm (Figure 9C).

2.1.3 Nesprin-3 is able to recruit vimentin to the nucleus

Our group had previously reported that N-terminal sequences of Nesprin-1 can associate with N-terminal spectrin repeats of Nesprin-3 (Taranum *et al.*, 2012a). Nesprin-3 binds to plectin, a huge protein which associates with intermediate filaments.

Earlier reports indicate that Nesprin-1 and -2 through their association with F-actin can assemble an F-actin cage around the nucleus (Khatau *et al.*, 2009). In analogy we asked whether Nesprin-3 is able to recruit an intermediate filament network to the

nucleus. Since Nesprin-3 is not normally expressed in COS7 cells (Wilhelmsen *et al.*, 2005), HA-Nesprin-3 was expressed in these cells to study vimentin localization. In untransfected cells, vimentin staining was not particularly enriched around the nucleus. However, vimentin colocalized with Nesprin-3 in HA-Nesprin-3 expressing cells (Figure 10) extending recent report findings from zebrafish to mammalian cells (Postel *et al.*, 2011). By contrast, GFP-tagged Nesprin-1 ABD was recruited to the nuclear envelope but it did not affect vimentin localization (Figure 10).
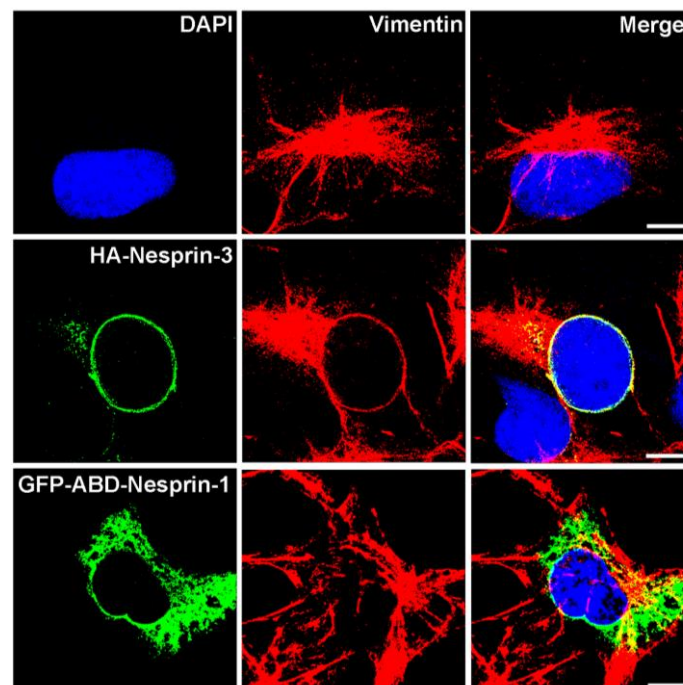
Figure 10: Nesprin-3 recruits intermediate filaments to the nuclear envelope in COS7 cells. COS7 cells stained for vimentin reveal the typical cytoskeletal staining. In HA-Nesprin-3 transfected COS7 cells vimentin was recruited to the NE and co-localized with HA-Nesprin-3. GFP-fused ABD-Nesprin-1 was recruited to the nuclear envelope but it did not affect vimentin localization. Confocal images are shown in (Taranum *et al.*, 2012a). Size bars, 10 µm.

2.2 Nesprin-1 role in tumorigenesis

2.2.1 Nesprin-1 isoform expression in cancer cell lines

As mutations in *SYNE1* have been identified in different types of human cancers and Nesprin-1 transcripts were down regulated at early tumor stages in a wide range of human carcinomas ((Marme *et al.*, 2008); www.oncomine.org), we probed several human and murine cancer cell lines with Nesprin-1 specific antibodies by immunoblotting and immunofluorescence analysis. Monoclonal antibody K43-322-2 generated against spectrin repeats 9, 10 and 11 (Figure 11A) recognized proteins of ~600, 400, 300, 250, 150, 55 and 50 kDa in CH310T1/2 cells. The proteins correspond in their molecular weights to Nesprin-1 isoforms described in a recent detailed analysis (Rajgor et al., 2012).

The ~600 and 400 kDa proteins were absent from all cancer cell lines and only the ~150 kDa protein was present with the exception of WIDR, where ~300, 250, 150 and 60 kDa proteins were detected. In the CT26 and Huh7 cell lysates the signal was rather faint, even after prolonged exposure (Figure 11B). Furthermore, a protein of high molecular weight which presumably corresponds to Nesprin-1 Giant (Taranum *et al.*, 2012a) was detected in C2F3, HaCaT, and HeLa and Hep3B cell lysates. Based on the low expression levels of the N terminal Nesprin-1 isoforms in Hep3B and Huh7 liver cancer cells compared to colon, cervic, and skin cancer cells, we focused our studies on these cell lines. Furthermore, recent data also suggested that Nesprin-1 expression levels are significantly reduced in liver cancer samples compared with matched normal tissue (www.oncomine.org).
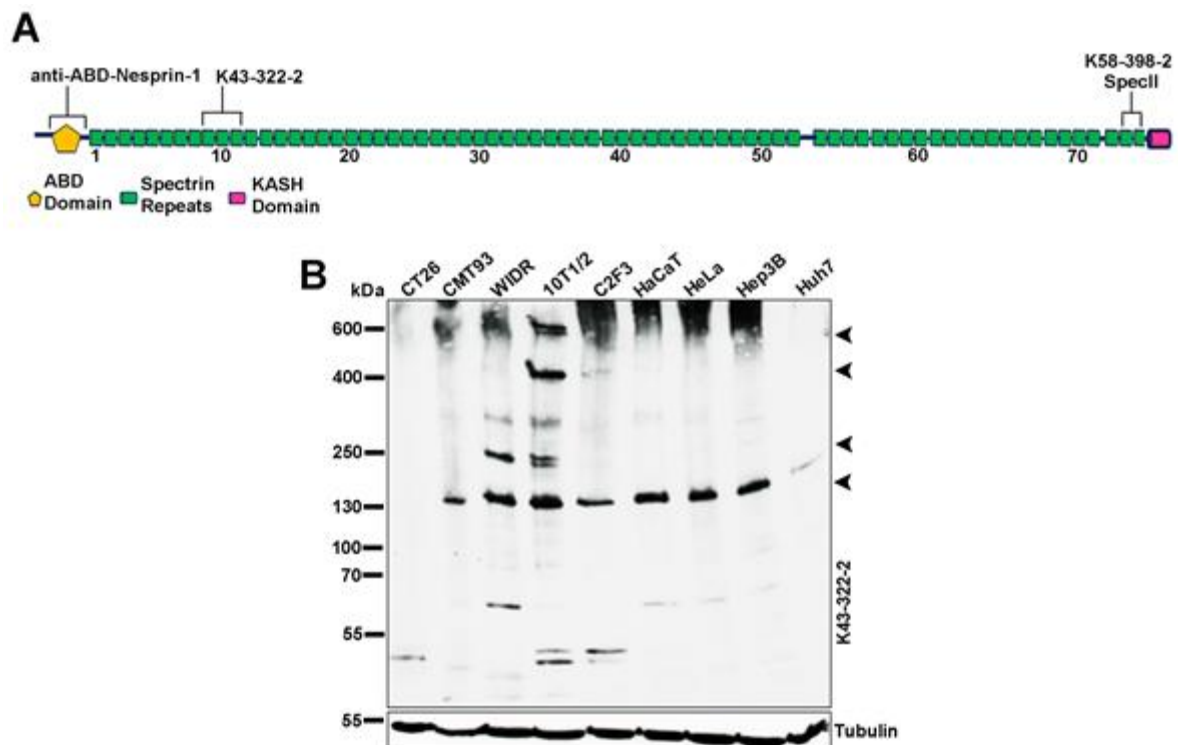
Figure 11: Nesprin-1 isoforms in various cell lines. (A) Location of the binding sites of Nesprin-1 antibodies. The largest isoform Nesprin-1 giant is depicted. ABD, actin binding domain. (B) Lysates were separated on a 3-15% SDS-PA gradient gel and probed with mAb K43-322-2 to detect N terminal isoforms. Arrow heads point to proteins discussed in the main text. Tubulin amounts were checked on a separate gel.

Nesprin-1 C-terminal isoforms were identified in Hep3B and Huh7 cell lysates with polyclonal SpecII antibodies directed against the C-terminus of Nesprin-1(Taranum *et al.*, 2012b). In fibroblasts we detected a 400 kDa protein which was absent from Hep3B and Huh7. Instead, they harbored low levels of 100 kDa and in case of Hep3B of 250 kDa proteins (Figure 12A). When probing for Nesprin-2, we detected several isoforms of Nesprin-2 with polyclonal antibodies pAbK1 directed against the C-terminus of Nesprin-2. The amounts were significantly higher in Hep3B and Huh7 cells as compared to fibroblasts (Figure 12B).
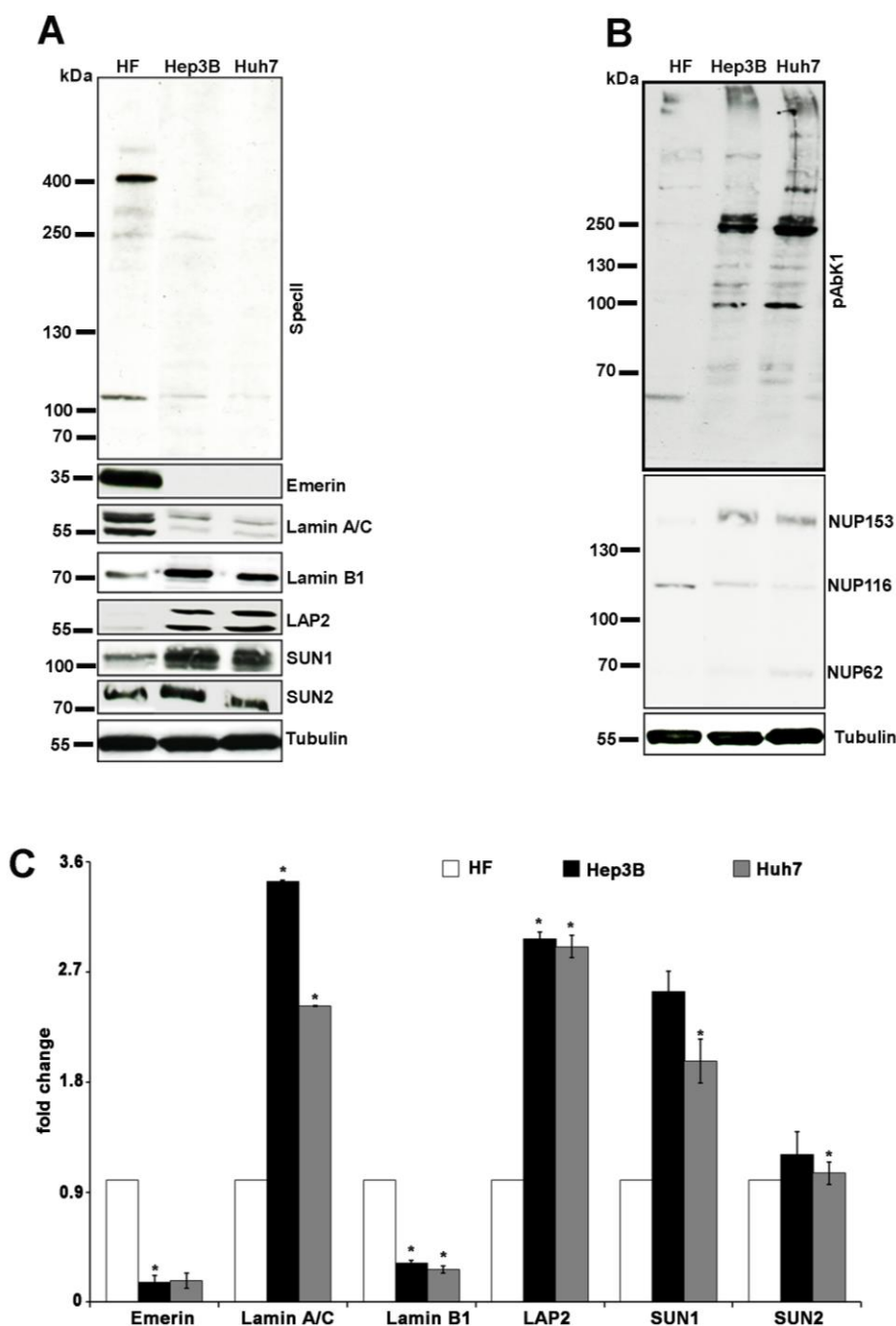
Figure 12: Cancer cells have alterations in nuclear envelope components. (A) Nesprin-1 expression in human fibroblasts (HF), Hep3B and Huh7 cells using SpecII antibodies. The blots were probed with Emerin, Lamin A/C, Lamin B1, LAP2, SUN1 and SUN2 antibodies. Tubulin was used to assess equal loading. (B) Presence of Nesprin-2 as detected with pAbK1 directed against the C-terminus. NPC proteins were detected with mAb414. (C) Changes at the protein level in HF, Hep3B and Huh7 cell lines as determined by western blotting. Fold change of Emerin, Lamin A/C, Lamin B1, LAP2, SUN1, SUN2 in HF, Hep3B and Huh7 cells. Band intensities were normalized relative to the loading control (tubulin). Histogram representing fold changes in band intensity. The results are the average from 3 independent experiments (*p<0.05, **p<0.001).

In further studies we compared Nesprin-1 expression in lysates from normal mammary tissue (N1, N2, N3) and tumor tissue (T1, T2, T3) of different patients. The SpecII antibodies recognized primarily a ~55 kDa protein which was strongly reduced in the tumor tissue (Figure 13A, B).
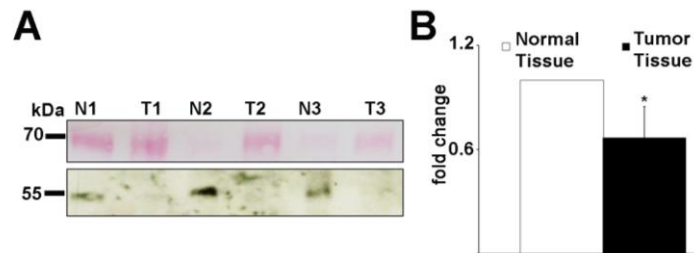
Figure 13: Nesprin-1 is reduced in human tumor tissues. (A) Nesprin-1 expression in normal (N1, N2, N3) and tumor (T1, T2, T3) mammary tissues using SpecII for detection. Upper panel, PonceauS staining of the nitrocellulose membrane. (B) Histogram representing fold change in band intensity of Nesprin-1 for normal and tumor tissues (*$p < 0.05$).

2.2.2 Hep3B and Huh7 have nuclear shape defects and alterations in components of the nuclear envelope

The nuclei of Hep3B and Huh7 cells were enlarged and often displayed a deformed morphology in contrast to the oval shape in HFs which we used for control. We further noted folds, lobulations, protrusions, blebs and micronuclei (Figure 14A, B).

In Hep3B, 37% of the cells had misshapen nuclei, in Huh7 26% and in control 7%. Micronuclei were observed in 11% of the Hep3B cells, in 8% in case of Huh7 and 1% of HF cells (Figure 14B). SpecII antibodies labeled the NE in fibroblasts and gave some cytoplasmic staining in the vicinity of the nucleus whereas the Nesprin-1 presence at the NE was strongly reduced in the cancer cells (Figure 14A).
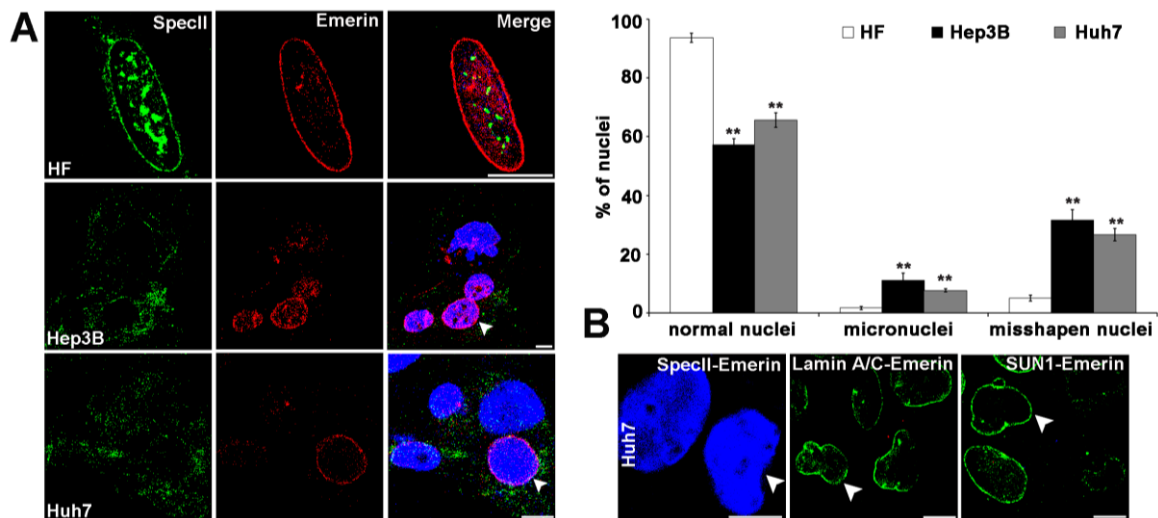
Figure 14: Hep3B and Huh7 have nuclear shape defects and alterations in components of the LINC complex. (A) Staining was with SpecII (green) to detect Nesprin-1 and a mAb specific for Emerin (red). DAPI staining of DNA is in blue. Arrow heads indicate nuclei with regular shape and staining for SpecII and Emerin. Scale bar, 10 µm. (B) Huh7 cells have nuclear shape defects and alterations in components of the nuclear envelope. Staining was with polyclonal SpecII antibodies against Nesprin-1 (green), Lamin B1 (green), SUN1 (green) and mAb Emerin (red) antibodies. DAPI staining of DNA is in blue. Scale bar, 10 µm. Upper panel, statistical analysis of nuclear aberrations. 300 nuclei each for HF (passage 7), Hep3B and Huh7 were evaluated (**$p < 0.001$).

Remarkably, Emerin was nearly absent from the NE in the cancer cells (Figure 14A, B). The absence of Emerin was also confirmed in western blots (Figure 12A, C).

Lamin A/C specific antibodies showed a rim like staining pattern in HFs. In Hep3B and Huh7 cells a discontinuous, patchy Lamin A/C distribution at the NE was observed. Lamin B1 staining of the NE was homogenous in HFs, in Hep3B and Huh7 cells the distribution was patchy (Figure 15A).

LAP2, a member of a group of NE proteins involved in tethering chromatin to the nuclear envelope and affecting gene expression, showed an unaltered localization at the NE in Hep3B and Huh7 cells. The expression level appeared to be significantly higher than in fibroblasts which expressed low amounts of LAP2 (Figure 15A).

NPC proteins regulate nuclear transport, are connected to chromatin and participate in the regulation of transcription. Increased expression of individual NPC components

has been noticed in several tumor types. Hep3B and Huh7 cells exhibited NE staining with mAb 414, which recognizes several NPC proteins based on the presence of FXFG-repeats, however staining was reduced in nearly 45% of the cells (Figure 15B, C).
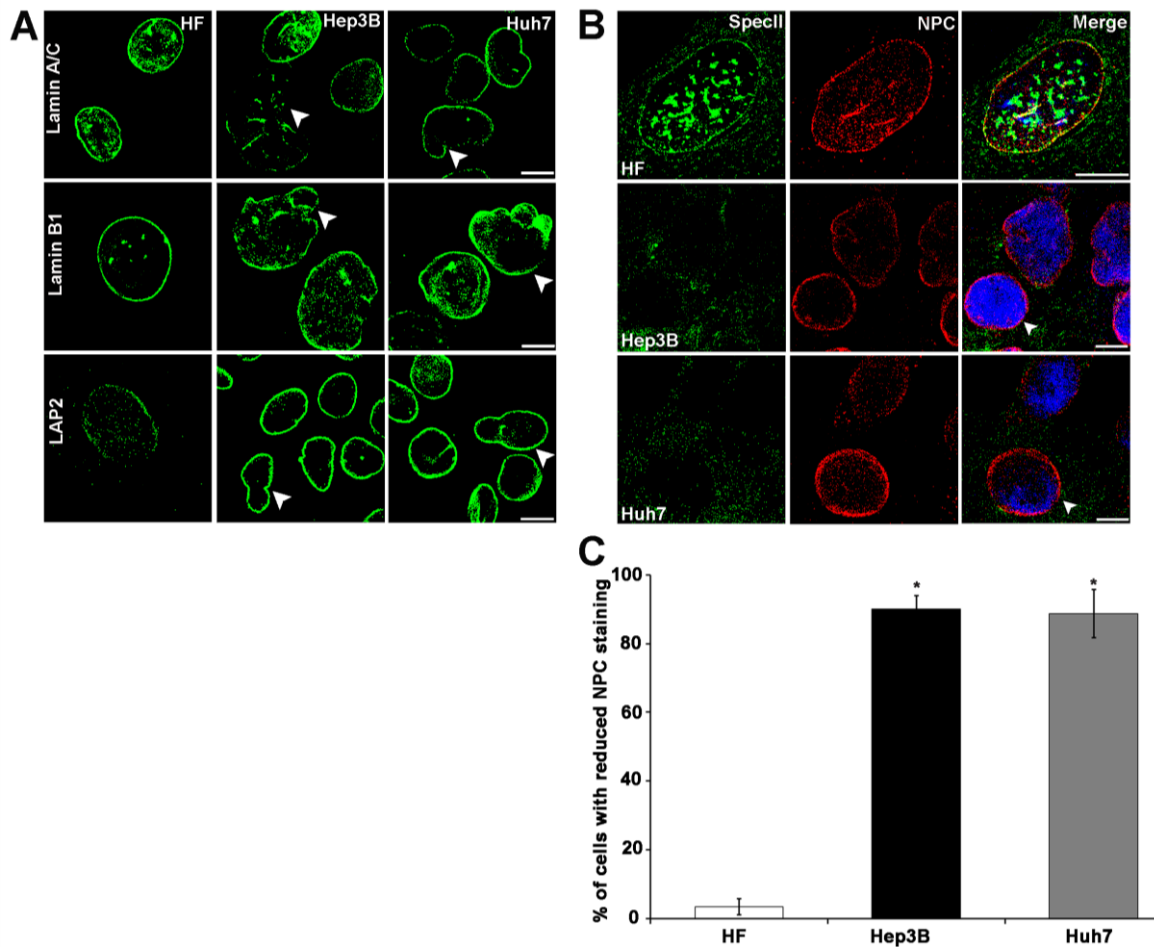
Figure 15: Nuclear envelope components are altered in Hep3B and Huh7 cells. (A) Distribution of Lamin A/C, Lamin B1, and LAP2 in HF, Hep3B and Huh7 cells. Arrow heads indicate the observed defects. Scale bar, 10 μm. (B) HF, Hep3B and Huh7 cells were stained with anti-Nesprin-1 SpecII (green), mAb NPC (red), DAPI (blue). Arrow heads point to normal shaped nuclei stained with SpecII and NPC. Scale bar, 10 μm. (C) Statistical analysis of NPC staining. 200 cells per strain were analysed (*p<0.0001).

Analysing individual proteins by western blotting, we found that NUP153 levels were higher in Hep3B and Huh7 cells compared to the HF control and NUP116 levels were

decreased (Figure 12B). In colon cancer cell lines, localization of Nesprin-1 and other

nuclear envelope components was unperturbed (Figure 16).
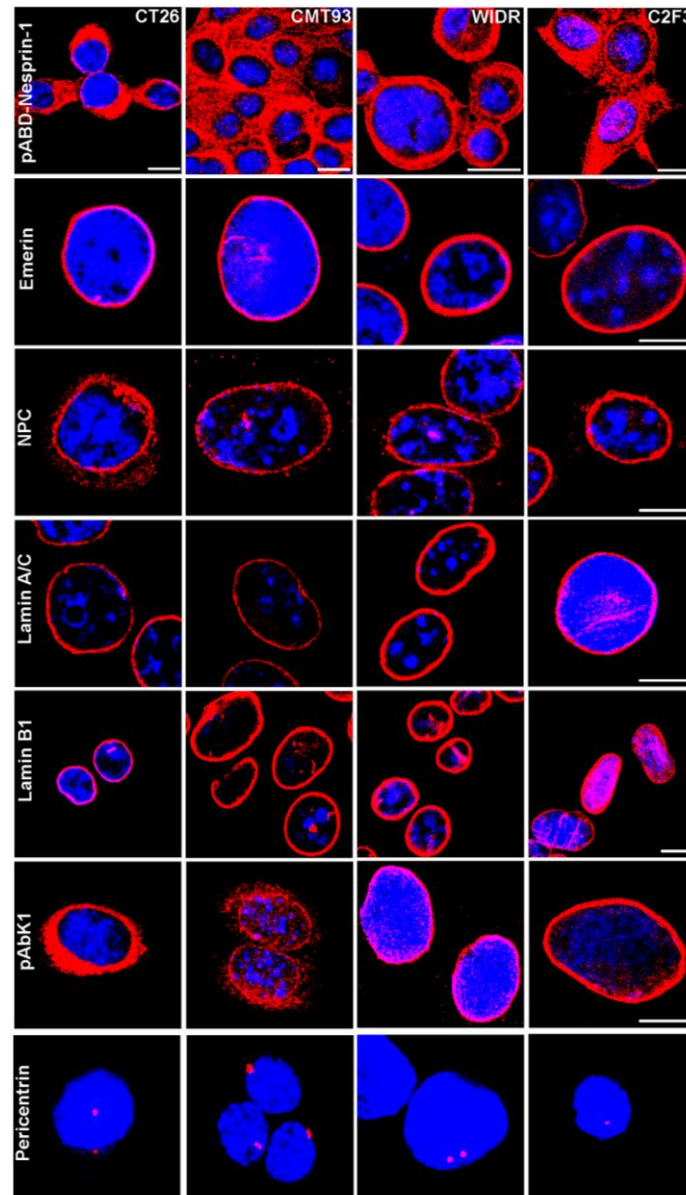
Figure 16: Nuclear envelope components in colon cancer cells. Distribution of Nesprin-1 detected by anti-ABD-Nesprin-1, Emerin, NPC, Lamin A/C, Lamin B1, Nesprin-2 as detected by pAbK1 in CT26, CMT93, WIDR, C2F3 cells. DAPI staining of DNA is in blue. Scale bar, 10 μm.

Immunofluorescence analysis for SUN proteins revealed a rim like staining for SUN1

in Hep3B and Huh7 cells. Some cells exhibited a brighter SUN1 staining which was

associated with misshapen and enlarged nuclei (Figure 17, arrows). When we

examined the amounts of SUN1 and SUN2 in western blots, we found that particularly the SUN1 levels were higher in Hep3B and Huh7 as compared to HFs (Figure 12A, C). Quantification of the mRNA levels by qRT-PCR showed that SUN1 and SUN2 mRNA were significantly increased in Hep3B and slightly increased in Huh7 cells (Figure 17B).
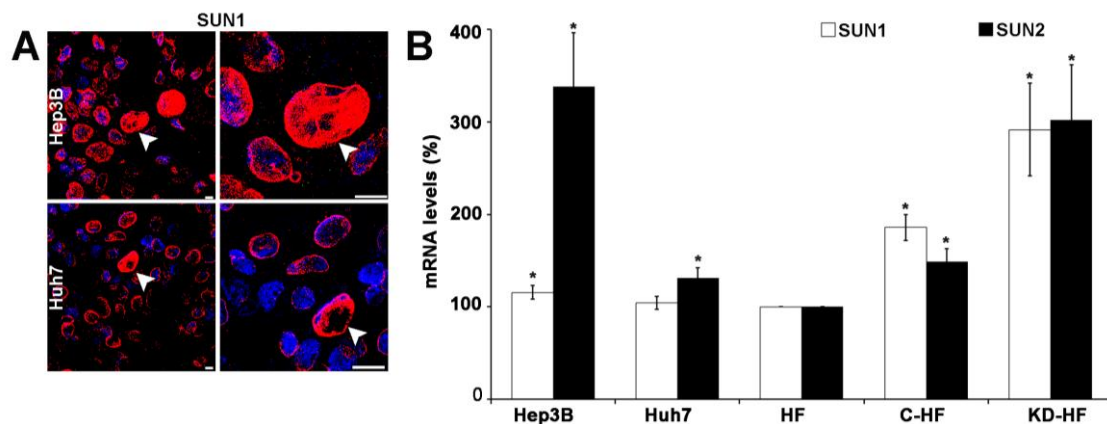
Figure 17: Cells with misshapen and enlarged nuclei exhibited a brighter SUN1 staining. (A) SUN1 (red) staining in Hep3B and Huh7 cells, DAPI, blue. Arrow heads point to cells with high SUN1 expression and misshapen and enlarged nuclei. Scale bar, 10 µm. (B) SUN1 and SUN2 transcript levels in control, Hep3B and Huh7 cells as determined by qRT-PCR. Significant up-regulation of SUN1 and SUN2 was detected in Hep3B, Huh7, and KD-HF cells compared to HF cells (*p<0.05, **p<0.001). The SUN1 and SUN2 mRNA level in HF at passage 7 was taken for reference. For normalization, GAPDH was used.

2.2.3 The centrosome-nucleus distance is increased in Hep3B and Huh7 cells

Centrosomal aberrations are frequently observed in cancer cells. Normal cells in the G1 phase of the cell cycle have a single centrosome which is attached to the nucleus. In HFs, centrosomes were positioned near the nucleus at a mean distance of 0.33±0.25 µm. In Hep3B and Huh7 cells the distance between the centrosome and the nucleus was highly variable and cells with normal shaped as well as deformed nuclei displayed an increased centrosome-nucleus distance. In Hep3B and Huh7

cells we observed an increase to 6.29±4.24 µm and 3.56±3.0 µm, respectively (Figure 18A, B). The number of centrosomes also differed. 15% of Hep3B and 14.3% of Huh7 cells had more than two centrosomes (Figure 18C). The centrosome number was not necessarily associated with nuclear shape changes.
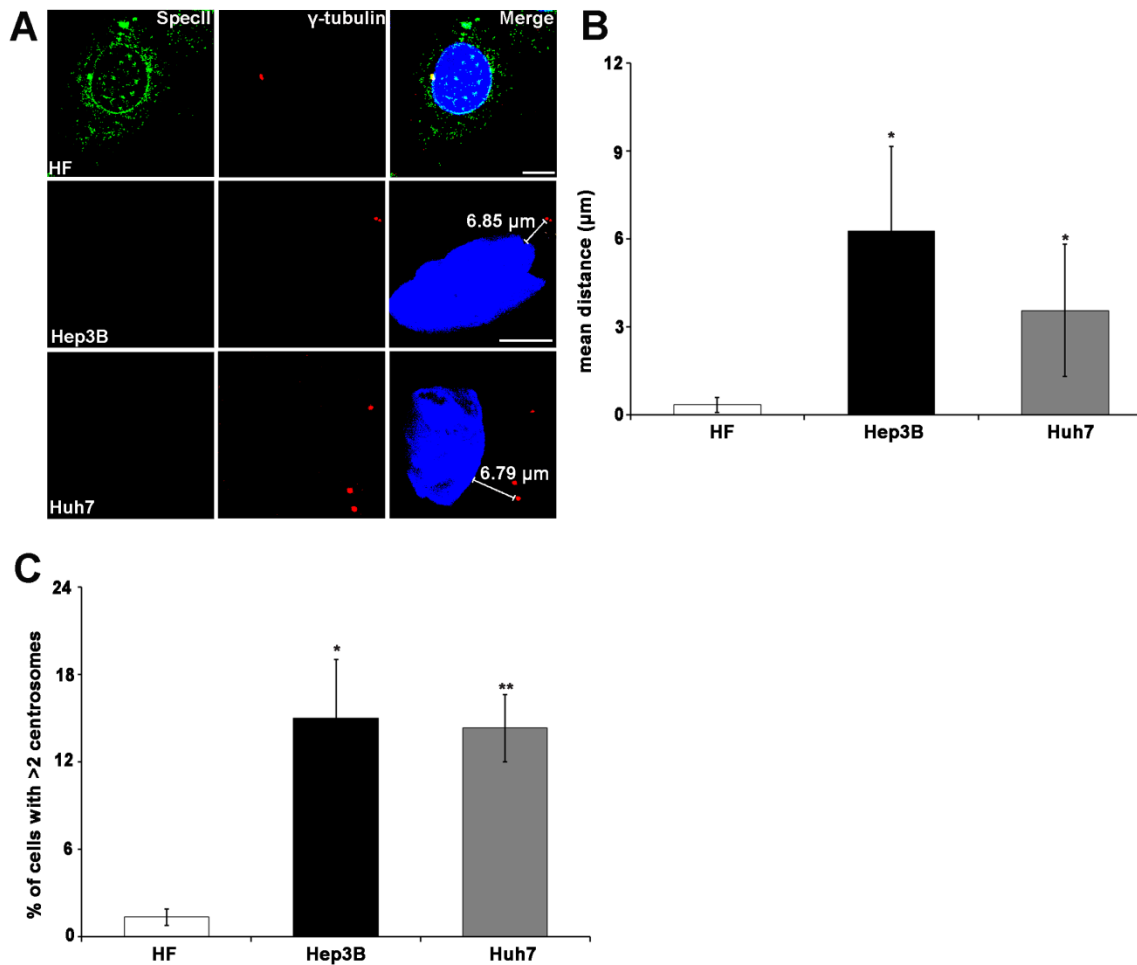
Figure 18: Centrosome-nucleus-distance is altered in Hep3B and Huh7 cells. (A) Centrosome-nucleus-distance is altered in Hep3B and Huh7 cells. γ-Tubulin (red) specific antibodies were used to label the centrosome. DAPI (blue), nuclear staining. Scale bar, 10 µm. (B) Statistical evaluation of the centrosome-nucleus distance. (C) Statistical evaluation of cells with >2 centrosomes. Error bars indicate standard deviations (*p<0.001, **p<0.0001).

2.3 Loss of Nesprin-1

2.3.1 Knock down of Nesprin-1 elicits changes that are observed in cancer cell lines

To test whether a loss of Nesprin-1 can cause the changes observed in the cancer cells, we reduced the amounts of Nesprin-1 by shRNA mediated knock down in C3H10T1/2 (KD-CH310T1/2) and in human fibroblasts (KD-HF) using knock down vectors targeting N-terminal and C-terminal sequences of human or mouse Nesprin-1 (see Materials and Methods) and analyzed the consequences.

For control we used untransfected cells (HF, CH310T1/2) and cells transfected with the empty pSHAG-1 vector used for cloning (C-HF, C-CH310T1/2). Western blot analysis with mAb K43-322-2 and SpecII labeling confirmed the knock down (KD) (Figure 19A, B). Labeling with mAb K43-322-2 showed that in Nesprin-1 KD cells particularly the 250 kDa and larger proteins of 400 and 600 kDa were significantly reduced in amounts (Figure 19A, arrow heads). The 130 kDa protein and smaller proteins were also less prominent. The expression level of the smallest ones were not altered (Figure 19A).

Reduction of Nesprin-1 was associated with a down regulation of Emerin, Lamin B1, NPC proteins and LAP2. By contrast, SUN1 and SUN2 protein amounts were increased (Figure 19A, C). This was also observed for SUN1 in CH310T1/2 in which the levels of endogenous SUN1 were quite low (Figure 19A). An increase was also seen at the transcript level as revealed by qRT PCR (Figure 17B).
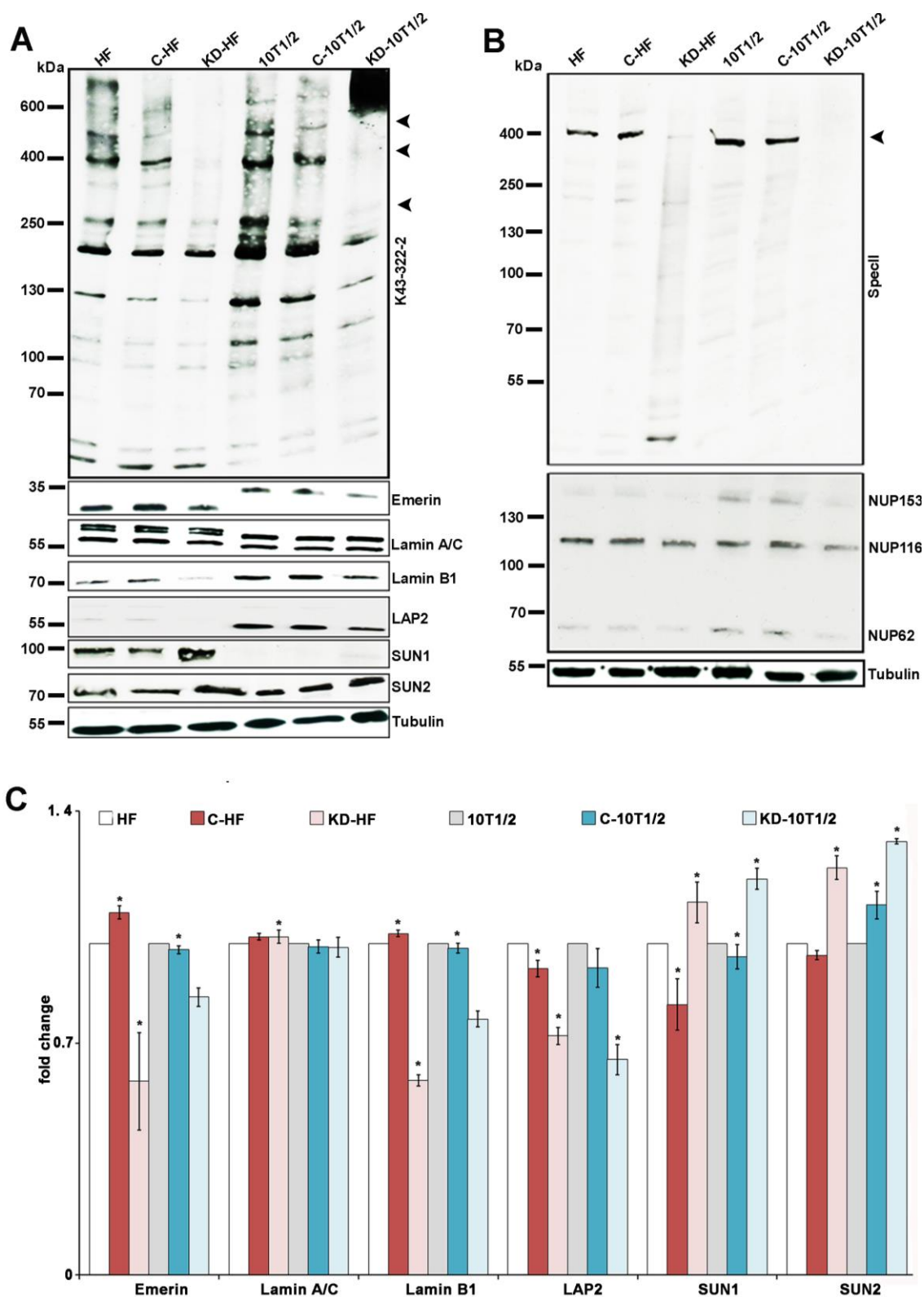
Figure 19: Loss of Nesprin-1 elicits changes that are observed in cancer cell lines. (A) Immunoblot analysis of Nesprin-1 Giant knock down HF and CH310T1/2 cells. Detection was with mAb K43-322-2 and pAb SpecII. Tubulin served as control. Emerin, Lamin A/C, Lamin B1, LAP2, SUN1 and SUN2 specific antibodies were used for analysis. Human and murine Emerin differ in their primary sequence explaining the observed difference in molecular weight. (B) The blot in (A) was reprobed with SpecII antibodies and mAb414 to detect NPC proteins. (C) Changes of NE

components at the protein level after knock down of Nesprin-1. Knock down was carried out using plasmids targeting the N and C terminal regions of Nesprin-1. Histogram representing fold changes in band intensities of Emerin, Lamin B1, LAP2, SUN1 for HF, C-HF, KD-HF, CH310T1/2, C-CH310T1/2, KD-CH310T1/2 cells (*p<0.05).

For Nesprin-1, alterations in transcript levels were assessed by qRT-PCR. KD-HF and Huh7 cells showed significant reductions (Figure 20).
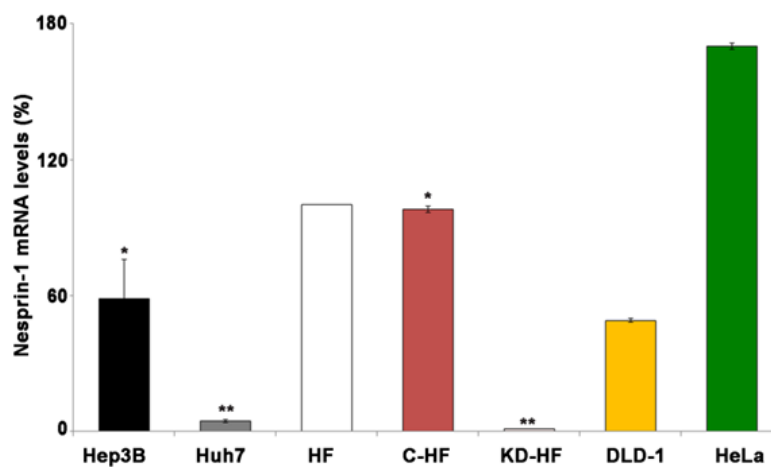
Figure 20: The transcript levels of Nesprin-1 vary significantly in Hep3B, Huh7, HF, C-HF, and KD-HF cells as determined by qRT-PCR. Significant down-regulation of Nesprin-1 was detected in Hep3B, Huh7, and KD-HF cells compared to HF cells (*p<0.05, **p<0.0001). The primers used for amplification were located in the N terminus of Nesprin-1. For normalization GAPDH was used.

In immunofluorescence analysis the clear NE staining by SpecII and Emerin antibodies was lost and some residual punctate staining in the cytosol of KD-HF and KD-CH310T1/2 cells was seen (Figure 21A). The NPC antibodies labeled the nuclear envelope in control fibroblasts and in CH310T1/2, whereas in the knock down cells NPC staining is strongly reduced (Figure 21B).
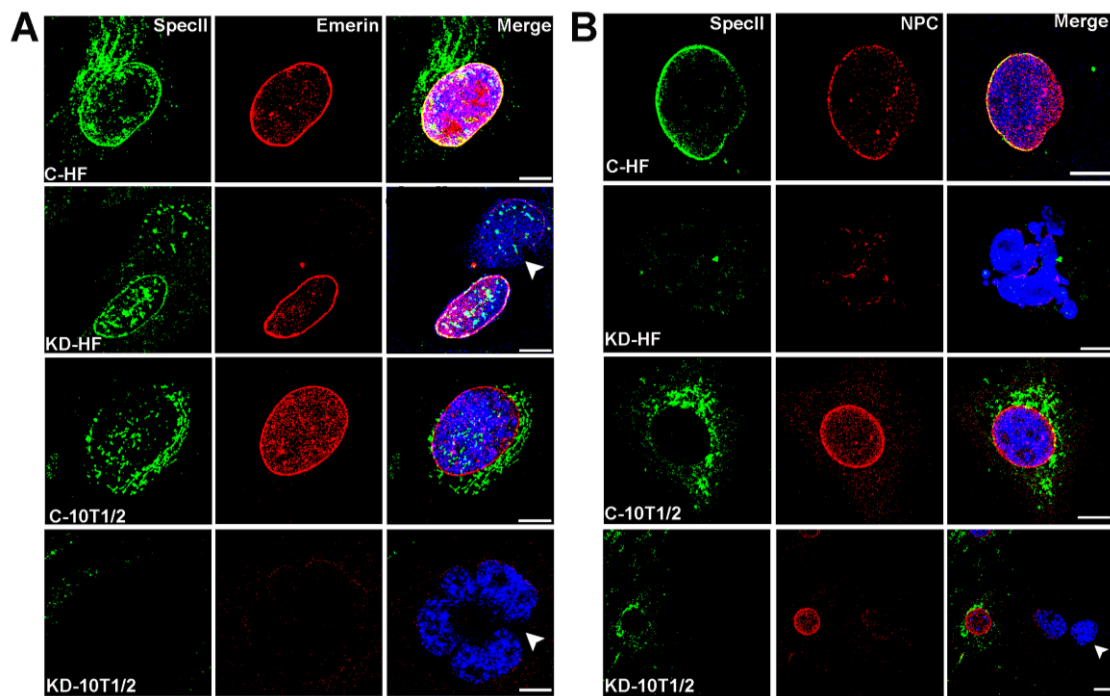
Figure 21: Effect of Nesprin-1 knock down on NE components. (A, B) Cells were stained for Nesprin-1 with pAb SpecII (green), Emerin (red), mAb NPC (red) and DAPI (blue). Knock down was carried out with vectors targeting N and C terminal sequences of Nesprin-1. Arrow heads indicate the NE phenotypes described. Scale bars, 10 µm.

Nearly all cells that had an altered staining pattern exhibited nuclear shape defects. SUN1 antibodies strongly stained the NE in KD-HF. Cells with particularly strong SUN1 staining exhibited a variety of nuclear shape defects including folds, lobulations, blebs and micronuclei (Figure 22).
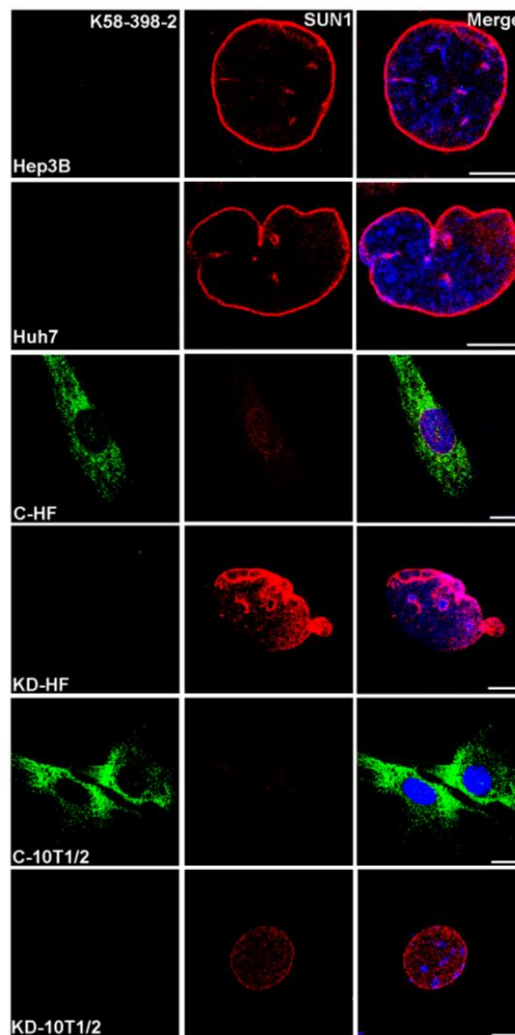
Figure 22: SUN1 staining revealed a variety of nuclear shape defects including folds, lobulations, blebs and micronuclei. SUN1 (red) staining in Hep3B, Huh7, C-HF, KD-HF, C-CH310T1/2, KD-CH310T1/2 cells. Nesprin-1 was detected with mAb K58-398-2 (green). Nuclei are stained by DAPI (blue). Scale bars, 10 µm.

Heat treatment is often used to probe the stability of the nuclear envelope (Vigouroux *et al.*, 2001). To understand the link between Nesprin-1 loss and heat resistance, the cells were stained with LAP2 to evaluate nuclear shape changes after heat shock. When we incubated cells for 30 min at 45°C, Nesprin-1 knock down fibroblasts, Hep3B and Huh7 cells exhibited increased nuclear deformations with folds and pleats after heat treatment (Figure 23A, B). Many nuclei also displayed notches, tears and herniations (Figure 23A, arrow heads). Knock down with plasmids targeting N-terminal or C-terminal sequences showed similar results as knock down experiments

where we used vectors targeting N-terminal and C-terminal sequences together (data

not shown).
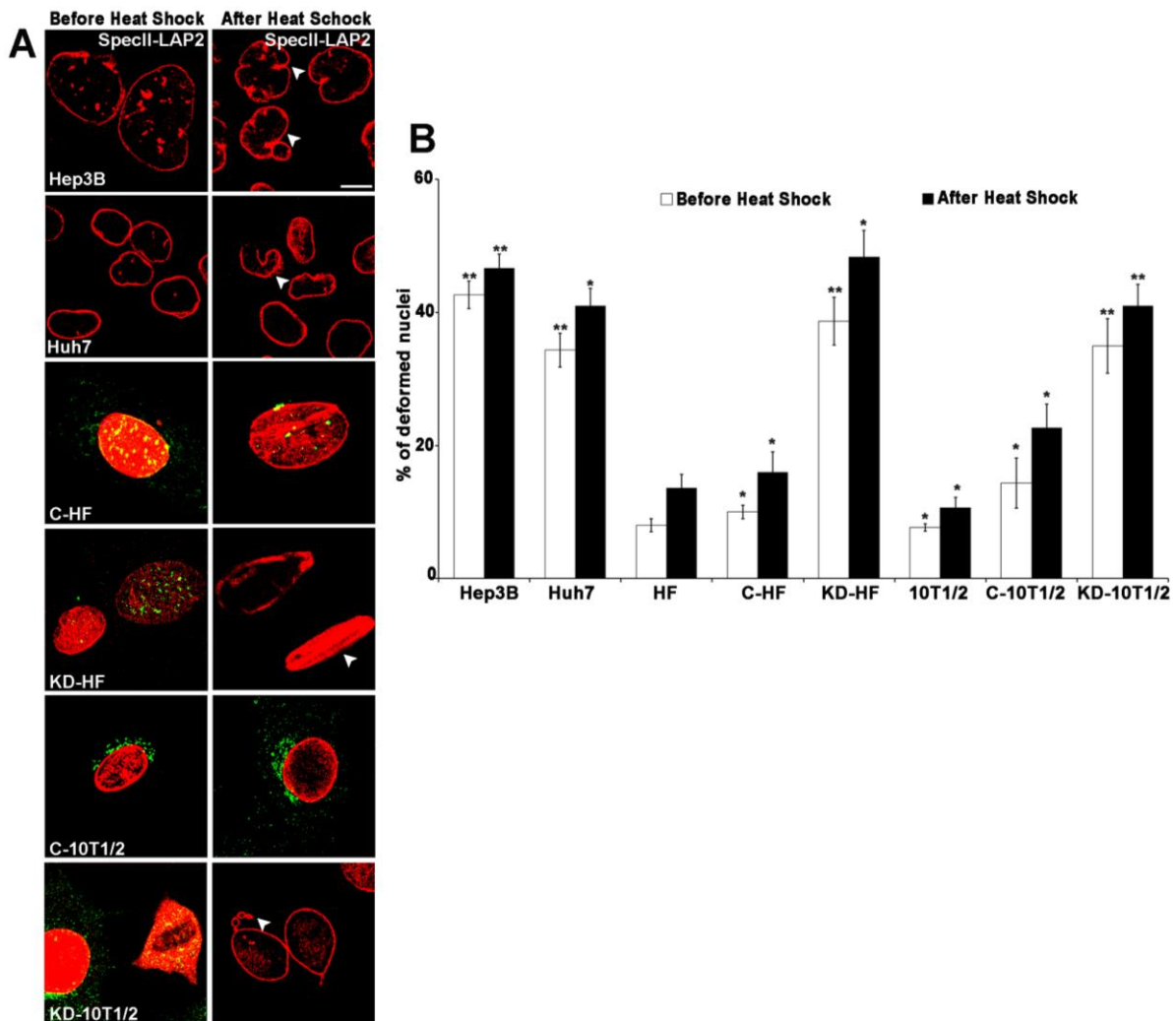
Figure 23: Loss of Nesprin-1 leads to hypersensitivity towards heat shock. (A) Cells were immunostained with SpecII (green) and LAP2 (red) antibodies to detect the nuclei deformations after heat shock at 45°C for 30 min. Arrow heads point to nuclear deformations. Scale bar, 10 µm. (B) Histograms representing the percentage of deformed nuclei of cells before (white bars) or after heat shock (black bars). Data are the mean ±SD from three samples per group of three independent experiments. Statistically significant differences were determined between before and after heat shock groups (*p<0.05, **p<0.0001).

When we quantified the defects for each cell type, we found that Hep3B and Huh7

had more abnormal nuclei in general. This number increased only slightly upon heat

treatment. Compared with unheated Hep3B (42%) and Huh7 (34%) cells, deformed nuclei after heat shock was 46% for Hep3B and 41% for Huh7 cells. Stronger increases in the number of deformed nuclei were observed for the KD-HF cells (35%±4.09 before and 41%±3.22 after heat shock). Moreover, no significant changes were observed among C-CH310T1/2 cells before (7% misshapen nuclei) or after (10%) heat shock. The extent of nuclear deformations caused in KD-CH310T1/2 (29.5%±4.37 before and 40.83%±2.86 after heat shock) was similar to heat shock experiments performed in KD-HF cells (Figure 23B). These results suggest that heat treatment leads to more deformed nuclei in Nesprin-1 KD, Hep3B and Huh7 cells.

2.3.2 The centrosome-nucleus distance is increased in Nesprin-1 KD cells

The LINC complex proteins play essential roles in centrosome biology (Salpingidou *et al.*, 2007; Schneider *et al.*, 2008; Zhang *et al.*, 2009). Moreover, recent studies revealed that centrosome defects, including alterations in centrosome shape, size, number, position, composition lead to tumorigenesis (Lingle and Salisbury, 2001; Fukasawa, 2005; Salisbury, 2005; Nigg, 2006; Hassold *et al.*, 2007). To further address whether the Nesprin-1 is associated with centrosome position and number, the cells were stained with ɣ-tubulin. We investigated the centrosome-nucleus distance and centrosome number upon loss of Nesprin-1 and found that centrosomes were positioned 0.35±0.29 and 3.20±2.34 µm away from the NE in C-HF and Nesprin-1 KD-HF cells, respectively. Similarly, in Nesprin-1 KD-CH310T1/2 cells the mean centrosome-nucleus distance increased from 0.44±0.27 µm in C-CH310T1/2 cells to 2.40±1.49 µm in Nesprin-1 KD-CH310T1/2 cells (Figure 24A, B).
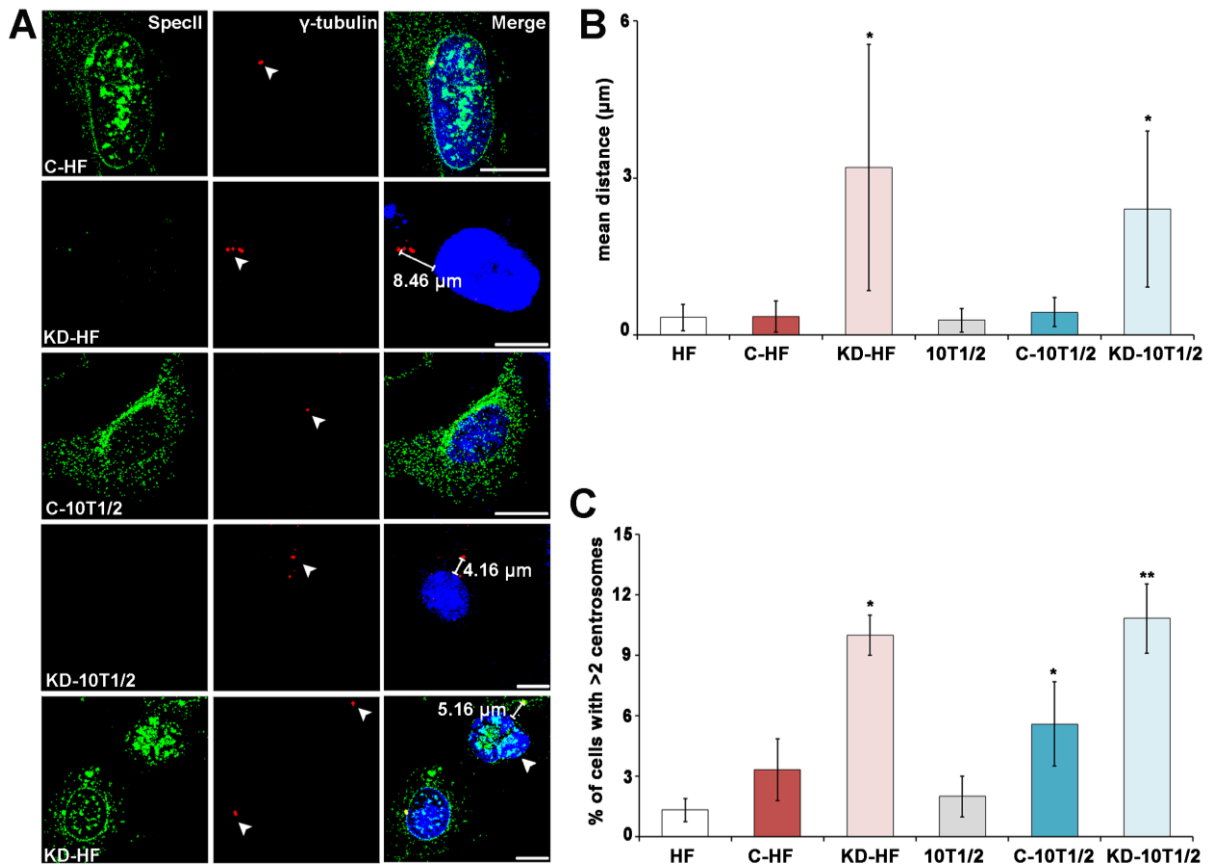
Figure 24: The centrosome-nucleus distance and centrosome number are increased in Nesprin-1 KD cells. (A) Centrosome position in C-HF, KD-HF, C-10T1/2, and KD-10T1/2 cells. Centrosomes were visualized with a γ-tubulin antibody (red), Nesprin-1 with SpecII (green). The nucleus was stained with DAPI (blue). Scale bars, 10 µm. (B) Statistical evaluation of the centrosome-nucleus distance. 100 cells for each cell line were evaluated (*p<0.0001). (C) Statistical analysis of the percentage of cells with >2 centrosomes was calculated from three independent experiments (100 cells were counted per experiment, *p<0.05, **p<0.0001).

Nesprin-1 loss was also accompanied by alterations of the centrosome number. More than two centrosomes were seen in 3.3% C-HF, for Nesprin-1 KD-HF this number increased to 10% and for CH310T1/2 it increased from 6% in the C-CH310T1/2 to 11% after knock down (Figure 24C).

2.3.3 Loss of Nesprin-1 leads to cytoskeletal alterations

To gain insight into the role of Nesprin-1 in cytoskeleton organization, cells were stained with TRITC-phalloidin to visualize the actin cytoskeleton and mAb YL1/2 to stain the microtubule network. In C-HF and C-CH310T1/2 cells F-actin was abundant and distributed throughout the cells. Nesprin-1 KD fibroblast, Hep3B, and Huh7 cells had fewer stress fibers and displayed irregular F-actin staining in particular over and around the nucleus where filaments were nearly absent (Figure 25A). Hep3B and Huh7 cells had fewer microtubules and the network appeared disorganized. The microtubule organization was also altered in KD-HF and KD-CH310T1/2 cells and a circular arrangement of microtubules in the cell periphery was noted (Figure 25B).

Cell migration requires precisely orchestrated changes in the actin and tubulin organization. In particular, migration of tumor cells has been extensively studied due to its importance in the process of cancer metastasis (Yamaguchi *et al.*, 2006; Sahai *et al.*, 2007). As loss of Nesprin-1 led to distinct changes in the F-actin and microtubule system, we analyzed the migration behavior of Nesprin-1 KD fibroblast, Hep3B and Huh7 cells after scratch wounding. C-KD exhibited a mean speed of migration of 11±1.2 (C-HF) and 13.1±1.8 (C-CH310T1/2) µm/hour whereas Nesprin-1 KD cells migrated with a cell velocity of 15.6±1.09 (KD-HF) and 20.8±1.0 (KD-CH310T1/2) µm/hour. In Hep3B and Huh7 cells, cell migration speed was markedly enhanced and the cell velocities were measured as 19.2±0.80 and 16.1±2.6 µm/hour, respectively (Figure 25C).

These findings could indicate that Nesprin-1 has an inhibitory role for the reorganization of the actin and microtubule cytoskeleton and for cell migration and its loss leads to enhanced migration as it is required for tumor metastasis and invasion.
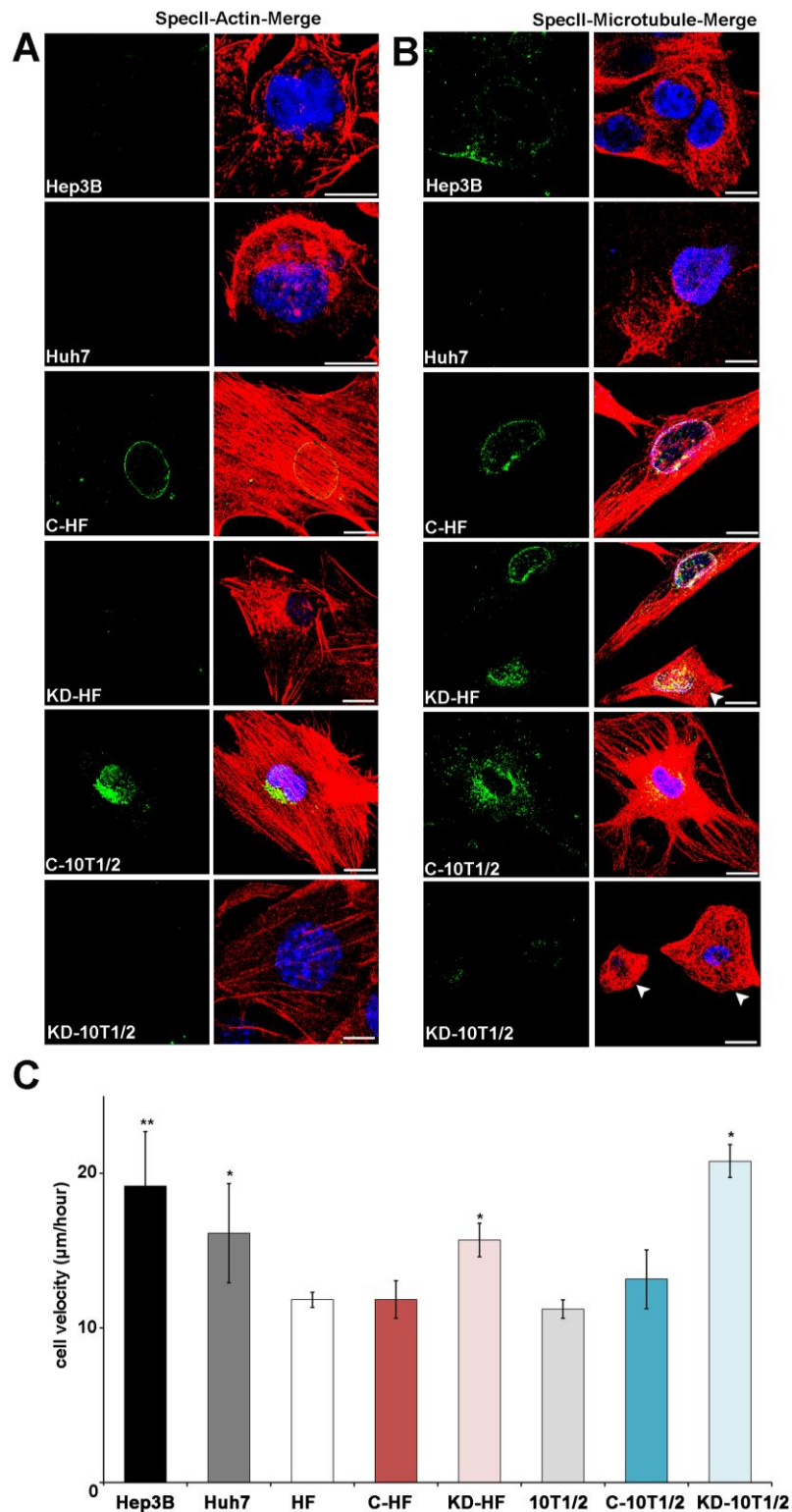
Figure 25: Alterations in the cytoskeletal networks upon loss of Nesprin-1. (A) Detection of the actin cytoskeleton in Hep3B, Huh7, Nesprin-1 KD-HF and KD-CH310T1/2 cells. Cells were fixed with PFA and stained for Nesprin-1 with pAb SpecII (green), F-actin with TRITC-Phalloidin (red), and DAPI (blue). Scale bar, 10 µm. (B) Detection of the microtubule network in Hep3B, Huh7, Nesprin-1 KD-HF, KD-CH310T1/2 cells. Arrow heads indicate cells with a disorganized microtubule network. Cells were stained with YL1/2 for tubulin (red), pAb SpecII (green) and DAPI (blue). Scale bars, 10 µm. (C) Histogram representing the cell velocity (µm/h). The

cell velocity was calculated using Image J. The values represent the mean ± SD of three separate experiments. Student's t-test was used for the evaluation (*p<0.001, **p<0.0001).

2.3.4 Senescence is increased in Nesprin-1 knock down fibroblasts

Cellular aging or senescence is formally described by Hayflick as a limited proliferation of cells during in vitro propagation (Hayflick, 1965). In vivo senescent cells stimulate biological processes that are associated with aging and tumorigenesis (Rodier and Campisi, 2011). A recent study indicated that cancer cells can undergo senescence due to several mechanisms such as telomere shortening, DNA-damage and oxidative stress (Di Micco *et al.*, 2006). Furthermore, cells harboring defects in components of the NE are reported to display an increased senescence (Le Dour *et al.*, 2011; Taranum *et al.*, 2012b).

To investigate whether Nesprin-1 loss leads to cellular aging, cells were plated and used for an assay in which the number of β-galactosidase positive cells (senescence-associated β-galactosidase, SA-β-gal) was determined. Notably, HF (6%) and CH310T1/2 (4.6%) cells displayed low percentage of blue staining. The extent of cellular senescence was similar between C-HF and C-CH310T1/2 cells (9%); in Hep3B and Huh7 cells, high levels of senescence were observed (51% and 92%, respectively). In KD-HF cells more than 80% were β-galactosidase positive. 9% of the C-CH310T1/2 cells were positive and after Nesprin-1 KD this number increased to 40% (Figure 26).
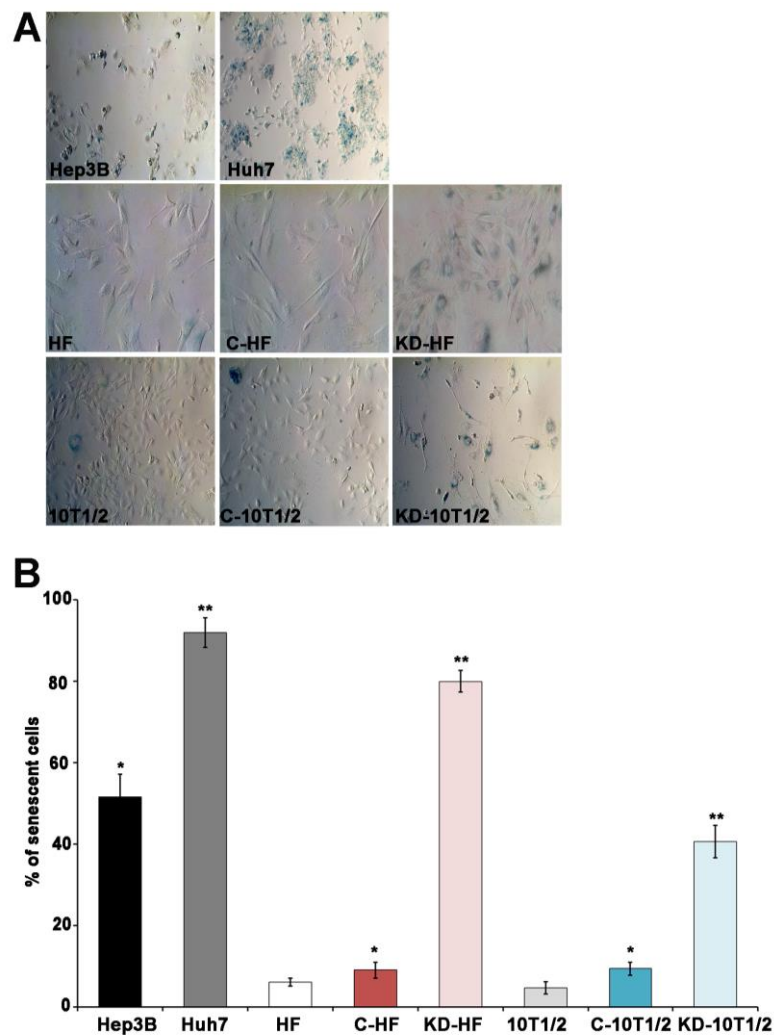
Figure 26: Loss of Nesprin-1 leads to cellular senescence and alterations in the cytoskeleton. (A) Staining for senescence associated β-galactosidase. Cells were imaged using bright field microscopy at 40x magnification. (B) Quantification of SA-β-gal-positive cells. Standard deviations are from three independent experiments counting 100 to 500 cells in each experiment (*$p<0.001$, **$p<0.0001$).

2.4 Nesprin-1 and DNA damage response (DDR) network

2.4.1 ABD of Nesprin-1 interact with DNA mismatch repair proteins MSH2 and MSH6

In a search for Nesprin-1 interaction partners we performed pull-down experiments with GST-Nesprin-1-286 and C2F3 cell lysates. Among the identified proteins, the

DNA mismatch repair protein (MSH2) and DNA damage binding protein-1 (DDB1) were chosen for further experiments (Table 4).

Table 4. The possible interaction partners of Nesprin-1. Pull-down assay was performed using GST-Nesprin-1-286 and C2F3 cell lysates.

Protein	Sequence coverage (%)	Score	MW (kDa)	No. of unique Peptides
Plectin	32.6	6056.1	533.9	138,00
Filamin-C	6.0	644.3	290.9	12,00
60S ribosomal protein L7	11.5	176.8	31.4	3,00
Filamin-A	2.3	158.7	281.0	4,00
Cytoplasmic dynein 1 heavy chain 1	1.0	146.1	531.7	4,00
Histone H1.4	5.5	50.4	22.0	1,00
60S ribosomal protein L6	3.0	48.5	33.5	1,00
Keratin, type II cytoskeletal 1	1.9	37.9	65.6	1,00
Myosin-9	39.6	3835.4	226.2	82,00
Myosin-Va	4.3	211.5	215.5	6,00
Ribosome-binding protein 1	3.2	113.6	172.8	3,00
Nischarin	0.8	54.8	174.9	1,00
Cytoskeleton-associated protein 5	0.6	48.6	225.5	1,00
Zinc transporter 1	2.8	37.8	54.7	1,00
Importin-7	9.0	363.2	119.4	7,00
Caprin-1	5.9	245.0	78.1	4,00
DNA damage-binding protein 1	8.7	221.7	126.8	7,00
Aspartyl/asparaginyl beta-hydroxylase	7.2	133.1	83.0	4
Probable ATP-dependent RNA helicase	1.4	49.4	113.8	1

Importin-9	1.1	48.0	116.0	1
Zinc transporter 1	2.8	44.8	54.7	1
Dynein heavy chain 17, axonemal	0.2	41.4	511.3	1
Nucleolin	39.9	1397.1	76.7	35,00
AP-2 complex subunit alpha-2	14.3	408.2	104.0	11,00
AP-2 complex subunit beta-1	11.2	363.3	104.5	10,00
Coatomer subunit beta	8.2	238.4	107.0	6,00
AP-2 complex subunit alpha-1	7.1	233.9	107.6	6,00
Transcription intermediary factor 1-beta	11.9	199.8	199.8	5,00
Endoplasmin	6.6	195.2	92.4	4,00
DNA mismatch repair protein Msh2	4.4	136.5	104.1	3,00
DNA replication licensing factor MCM3	3.4	90.4	91.5	2,00
Rho guanine nucleotide exchange factor 2	1.9	63.6	111.9	1,00
Kinesin-like protein KIF2A	1.6	57.5	79.7	1,00
Alpha-actinin-1	1.3	48.1	103.0	1,00
Apoptosis-inducing factor 1, mitochondrial	5,20	127.7	66.7	3,00
ATP-dependent RNA helicase DDX3X	5,60	113.0	73.1	3,00
Eukaryotic translation initiation factor 3 subunit D	4,70	99.5	63.9	2,00
ADP-ribosylation factor GTPase-activating protein 3	3,30	73.8	57.4	1,00
RNA-binding protein 39	2,80	38.2	59.5	1,00
DNA polymerase delta subunit 3	3.0	34.4	50.8	1,00
Hypermethylated in cancer 2 protein	1,50	44.5	72.6	1,00

To verify the interaction we repeated the experiment with HeLa cell lysates and probed the precipitate directly for the presence of MSH2 with antibodies. In addition to MSH2 we also found MSH6 and DDB1 in the precipitate (Figure 27A). MSH2 forms a complex with MSH6 which binds to DNA mismatches and functions in the repair of DNA double strand breaks (Warren *et al.*, 2007). GST alone as control did not precipitate MSH2, MSH6, and DDB1. To pursue the interaction of Nesprin-1 with MSH2, MSH6 and DDB1 in vivo, we transiently expressed GFP-Nesprin-1-286 in COS7 cells. GFP-Nesprin-1-286 colocalized with MSH2 and MSH6 at the nuclear envelope and also inside the nucleus (Figure 27B).
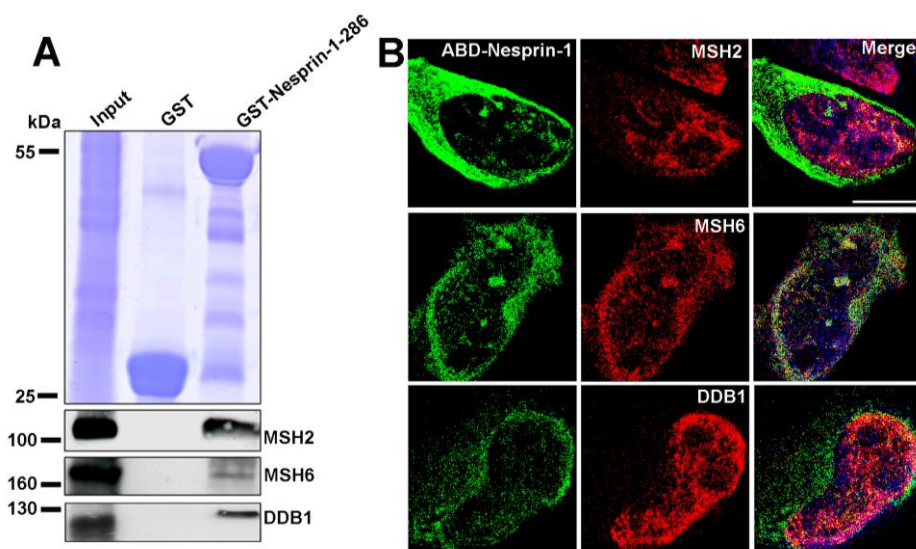
Figure 27: Nesprin-1 interacts with DNA repair proteins. (A) Interaction of Nesprin-1 with MSH2, MSH6, and DDB1. HeLa cells were incubated with GST-Nesprin-1-286 and GST for control. Detection of the 105 kDa MSH2, 163 kDa MSH6 and 127 kDa DDB1 in the pull down was with MSH2, MSH6, and DDB1 specific antibodies, respectively (lower panels). Upper panel, Coomassie Blue staining of the gel. (B) COS-7 cells were transfected with GFP-Nesprin-1-286 (green) and stained for MSH2 (red) and MSH6 (red), DAPI (blue). Scale bar, 10 µm.

We then carried out immunoprecipitation experiments and included also UV-treated cells. GFP-Nesprin-1-286 was immunoprecipitated from nuclear extracts using GFP beads and the precipitates probed for the presence of MSH2, MSH6, and DDB1. We

found that MSH2, MSH6, and DDB1 coprecipitated with GFP-Nesprin-1-286 from untreated and UV-treated nuclear extracts showing the relevance of the interaction also in the situation of DNA damage (Figure 28).
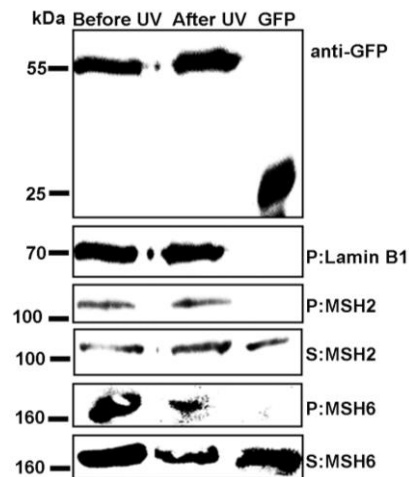
Figure 28: Nesprin-1 interacts with DNA repair proteins in vivo. HF cells were transfected with plasmids coding for GFP-ABD-Nesprin-1 and GFP and nuclei isolated and used for immunoprecipitations using GFP specific antibodies. MSH2, MSH6 and DDB1 coimmunoprecipitate with Nesprin-1 from nuclear extracts. MSH2; MSH6 and DDB1 also coimmunoprecipitated from nuclear extract upon UV-C treatment (20 J/m^2). GFP-ABD-Nesprin-1 and GFP were detected with mAb K3-184-2 (upper panel). Subcellular fractionation was confirmed by probing with Lamin B1 antibodies.

Next we tested whether MSH2 and MSH6 levels were affected by Nesprin-1 levels. In immunoblot analysis we found that Huh7 and KD-HF cells expressed lower levels of MHS2 and nearly no MSH6 was detected whereas their levels were considerably higher in Hep3B and C-HF cells (Figure 29A, B). The amounts of Nesprin-1 detected with anti-ABD-Nesprin-1 were reduced compared to C-HF cells as were the transcript levels (Figure 20). We also included the human colorectal cell line DLD-1 which is deficient in DNA mismatch repair (MMR) in order to test whether MMR deficiency is correlated with the Nesprin-1 levels. In western blots we found low levels of MSH2 and nearly no MSH6 and with Nesprin-1-ABD antibodies we detected strongly

reduced amounts of the ~100 kDa and 250 kDa proteins that were also present in the

cancer cell lines (Figure 29A, B).
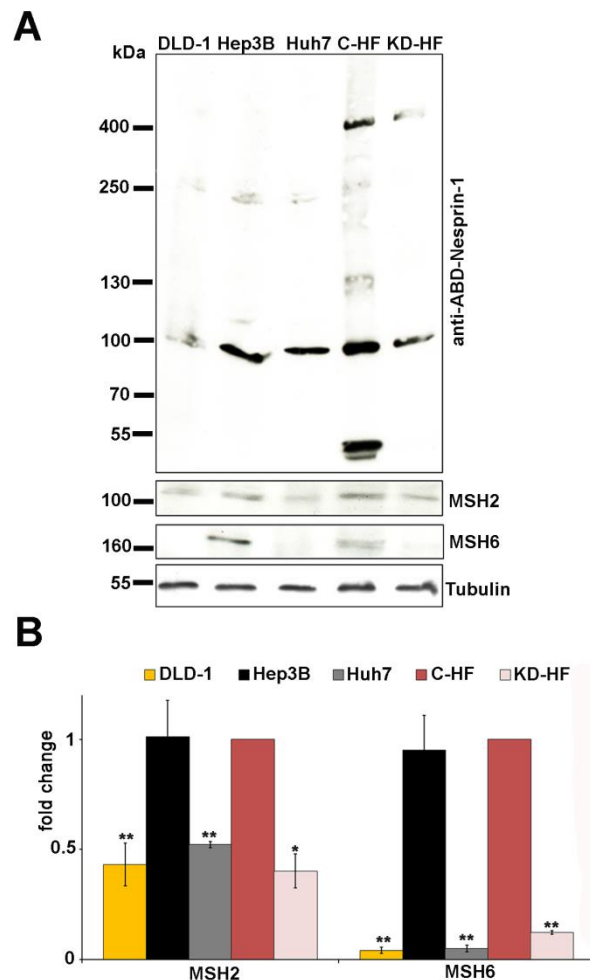
Figure 29: Loss of Nesprin-1 affects the MMR network. (A) Immunoblot analysis of DLD-1, Hep3B, Huh7, HF and KD-HF cells. Detection was with anti-ABD-Nesprin-1 and MSH2 and MHS6 antibodies. Tubulin served as control. (B) Histograms representing fold changes of band intensities of MSH2 and MSH6. Band intensities were normalized relative to the loading control (tubulin). Data are the mean ±SD from three samples per group of three independent experiments (*p<0.001, **p<0.0001).

Furthermore, we observed reduced expression of MSH2 and fewer MSH6 foci in KD-

HF cells compared to C-HF cells (Figure 30A, B). Quantification of the MSH2 and

MSH6 mRNA levels by qRT-PCR showed that they were significantly reduced in

Nesprin-1 KD-HF cells. Similar results were obtained with KD-HeLa cells (Figure

30C).
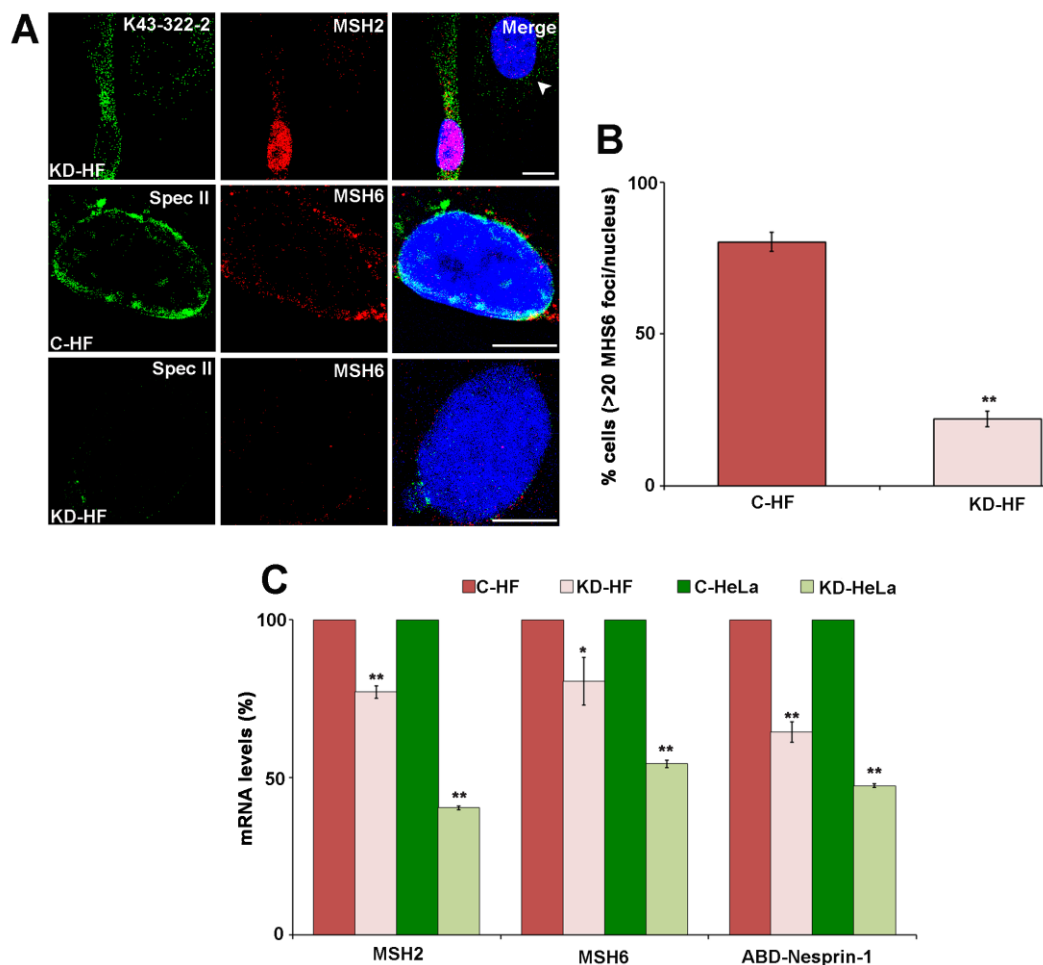
Figure 30: Nesprin-1 loss and MMR proteins. (A) Effect of Nesprin-1 knock down on MSH2 (red) and MSH6 (red). Nesprin-1 was detected with K43-322-2 (green) or pAb SpecII (green). Nuclei were stained with DAPI (blue). Arrow head indicates the KD-HF cell. Scale bars, 10 µm. (B) Quantification of the percentage of cells presenting >20 MSH6 foci for C-HF (red bar) or KD-HF (pink bar). Error bars represent standard deviations (**p<0.0001). (C) MSH2, MSH6 and Nesprin-1 transcript levels in C-HF, KD-HF, C-HeLa, and KD-HeLa as determined by qRT-PCR. Significant down-regulation of MSH2 and MSH6 was detected in KD-HF and KD-HeLa cells compared to C-HF and C-HeLa cells (*p<0.05, **p<0.0001). For normalization, GAPDH was used.

We also studied the NE characteristics of DLD-1 cells and found abnormal nuclear morphology, centrosomal aberrations, altered expression of NE components as were observed in Nesprin-1 KD cells (Figure 31). In this context it is interesting to note that *SYNE1* is a candidate gene for colorectal cancer, but the molecular mechanism is not clear (Sjoblom *et al.*, 2006).
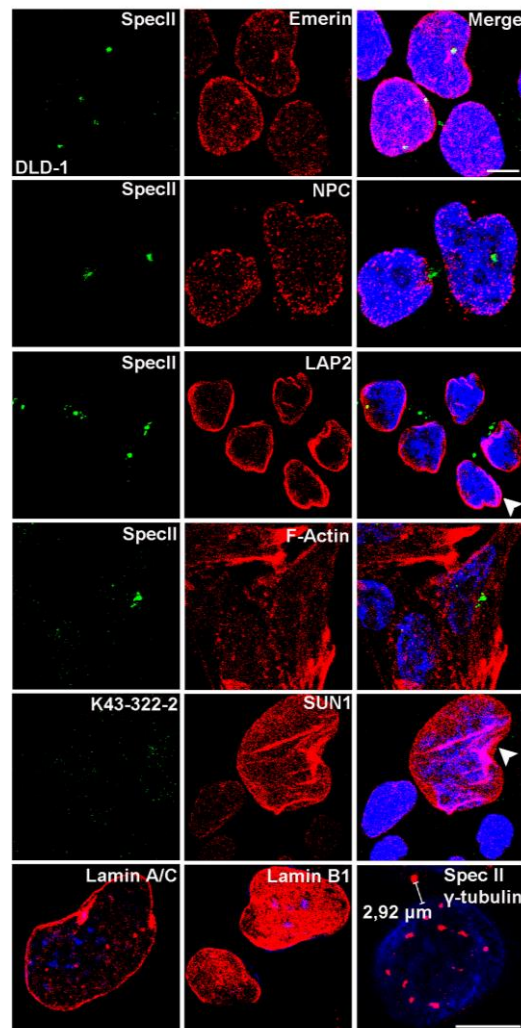
Figure 31: DLD-1 cells resemble Nesprin-1 KD cells with respect to the NE.
Distribution of Emerin (red), NPC (red), LAP2 (red), Actin (red), SUN1 (red), Lamin
A/C (red), Lamin B1 (red), γ-Tubulin (red), Spec2 (green), K43-322-2 (green) in DLD-
1 cells. Arrow heads indicate the observed defects. Scale bar, 10 µm.

In order to determine possible effects of Nesprin-1 on the MSH2-MSH6 heterodimer
(MutSα) during DNA replication or the repair process, C-HF and KD-HF cells were
synchronized at G1, S or G2/M phase and the chromatin association of the proteins
tested. The cell cycle status was confirmed by flow cytometry (FACS). MSH2 was
present in all phases and strongly accumulated in the nucleus during S and G2/M
phase (Figure 32A). MSH6 was primarily observed in S phase where it was present
in the nucleus and showed some colocalization with Nesprin-1 (Figure 32B).
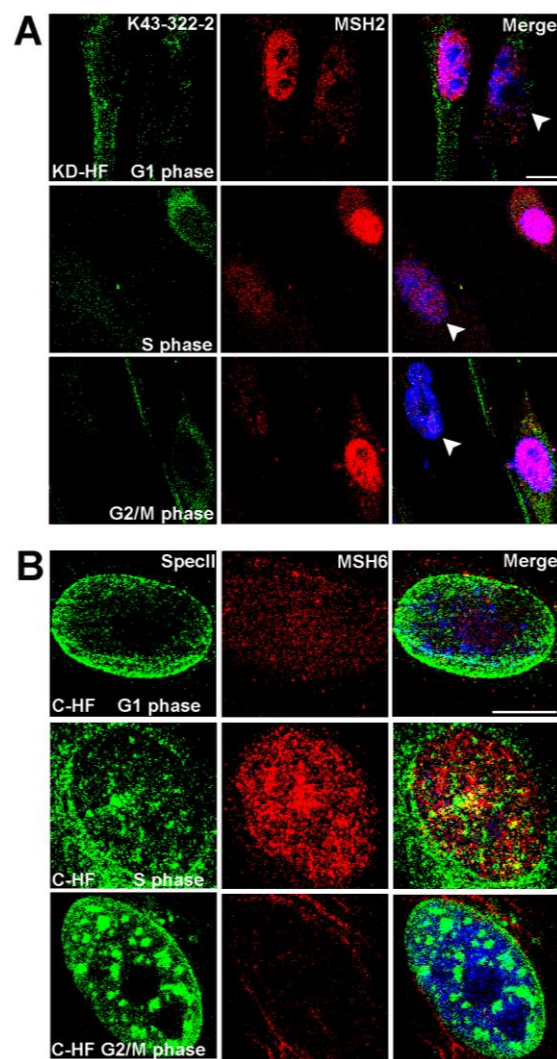
Figure 32: MSH2 and MSH6 during mitosis in Nesprin-1 KD cells. (A) KD-HF cells were arrested at G1, S, G2/M as indicated. Immunofluorescence was performed to determine nuclear distribution of K43-322-2 (green) and its colocalization with MSH2 (red). (B) Immunofluorescence analysis showing colocalization of MSH6 with Nesprin-1 in C-HF cells. Nesprin-1 (Spec II) and MSH6 localization for C-HF cells in G1, S or G2/M phase. The colocalization is increased in S phase. Scale bar, 10 μm.

Nesprin-1 deficient HF cells had strongly reduced levels of MSH2 and MSH6 was undetectable (Figure 32A; data not shown). In HeLa cells the expression levels of MSH2 and MSH6 appeared to be higher. The results in C-HeLa and KD-HeLa cells resembled those for HF cells (Figure 33A, B). We conclude that localization of MSH2-MSH6 to the nucleus and to chromatin is facilitated by Nesprin-1 leading to successful DNA repair.
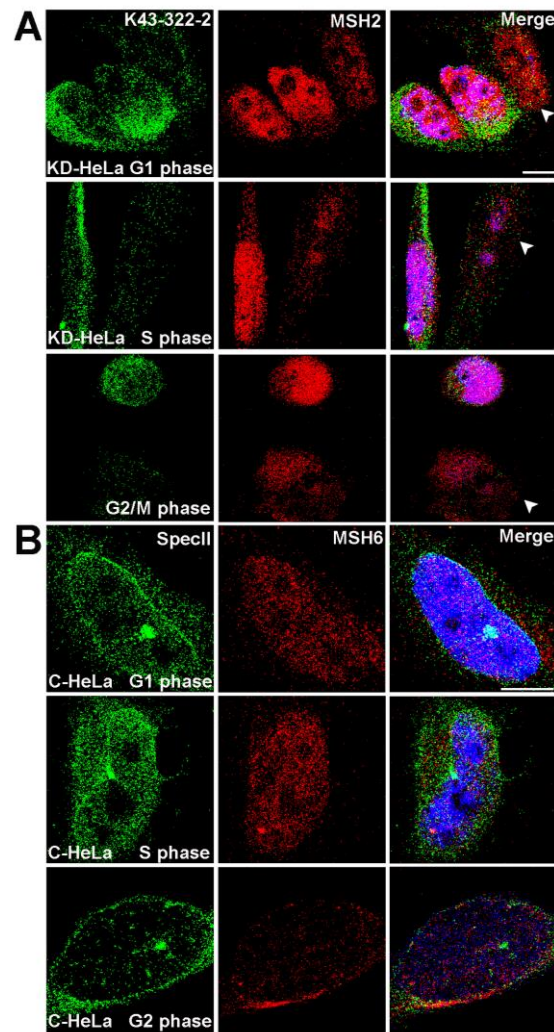
Figure 33: MMR in KD-HeLa cells. (A) KD-HeLa cells were arrested at G1, S, G2/M as indicated. Immunofluorescence was performed to determine the distribution of Nesprin-1 with K43-322-2 (green) and MSH2 (red). Arrow heads point to KD-HeLa cells. (B) Immunofluorescence analysis showing localization of MSH6 in C-HeLa cells in G1, S, and G2/M phase. Nesprin-1 (Spec II, green) and MSH6 (red). Scale bar, 10 μm.

Recent work by Li and coworkers showed that H3K36me3 has a role in MMR and is required to recruit hMSH2-hMSH6 to chromatin (Li *et al.*, 2013). Their results indicated that a maximum abundance of H3K36me3 occurred in early S phase which could increase the efficiency of MMR in actively replicating chromatin.

We therefore tested for H3K36me3 presence in early S phase and found that KD-HF cells behaved like Nesprin-1 positive cells and showed H3K36me3 positive spots (Figure 34). This shows that the MSH2-MSH6 recruitment to chromatin is affected in

Nesprin-1 KD whereas accumulation of H3K36me3 still takes place in Nesprin-1 KD cells. The results imply that MSH2-MSH6 recruitment to chromatin depends not only on H3K36me3 but also on Nesprin-1.
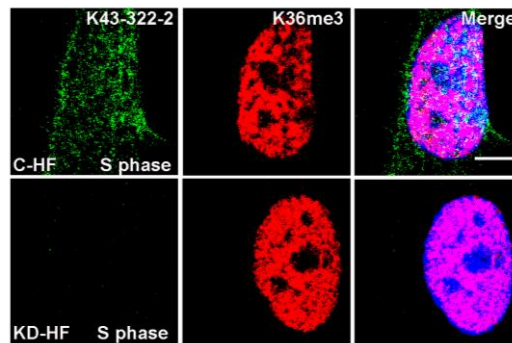
Figure 34: H3K36me3 in C-HF and KD-HF cells. K43-322-2 (green) and H3K36me3 (red) staining for C-HF and KD-HF cells in early S phase. Scale bar, 10 µm.

Nesprin-1 may play an important role for the function of MSH2 and MSH6 in the DNA mismatch repair, and a defect in this connection may also lead to alterations in earlier DDR events. Therefore, it is possible that the Nesprin-1 interaction with the MutSα complex is a constitutive cellular event required for proper DNA repair, and the interaction is not required for just the NE localization of MutSα complex.

2.4.2 Loss of Nesprin-1 affects the DDR network

The DDR pathway is associated with cancer development. MMR and NHEJ are two interlinked processes, and loss of MSH2 and MSH6 has been correlated with altered response to double strand breaks (DSBs) as well (Villemure *et al.*, 2003; Shahi *et al.*, 2011). To gain insight into specific steps during DDR, we monitored the cellular levels of key components, namely histone H2AX, checkpoint kinases Chk1 and Chk2, and Ku70/Ku80 heterodimer in Hep3B, Huh7, C-HF and Nesprin-1 KD-HF.

Phosphorylation of H2AX and Chk1 and Chk2 is among the initial events that occur in response to DNA damage (Kastan and Lim, 2000; Liu *et al.*, 2000; Marti *et al.*, 2006). Ku70/Ku80 binds to DNA double-strand breaks during NHEJ and recruits the DNA repair kinase DNA-dependent protein kinase catalytic subunit to the lesion. Following this process, the Ku70/Ku80 heterodimer is required to inhibit nuclease binding or activity at broken DNA ends thereby effectively functioning to maintain genome stability and successful repair (Liang and Jasin, 1996; Downs and Jackson, 2004; Sun *et al.*, 2012).

In C-HF nearly no γH2AX foci marking broken DNA were observed. Upon HU treatment γH2AX positive spots formed (Figure 35 A).
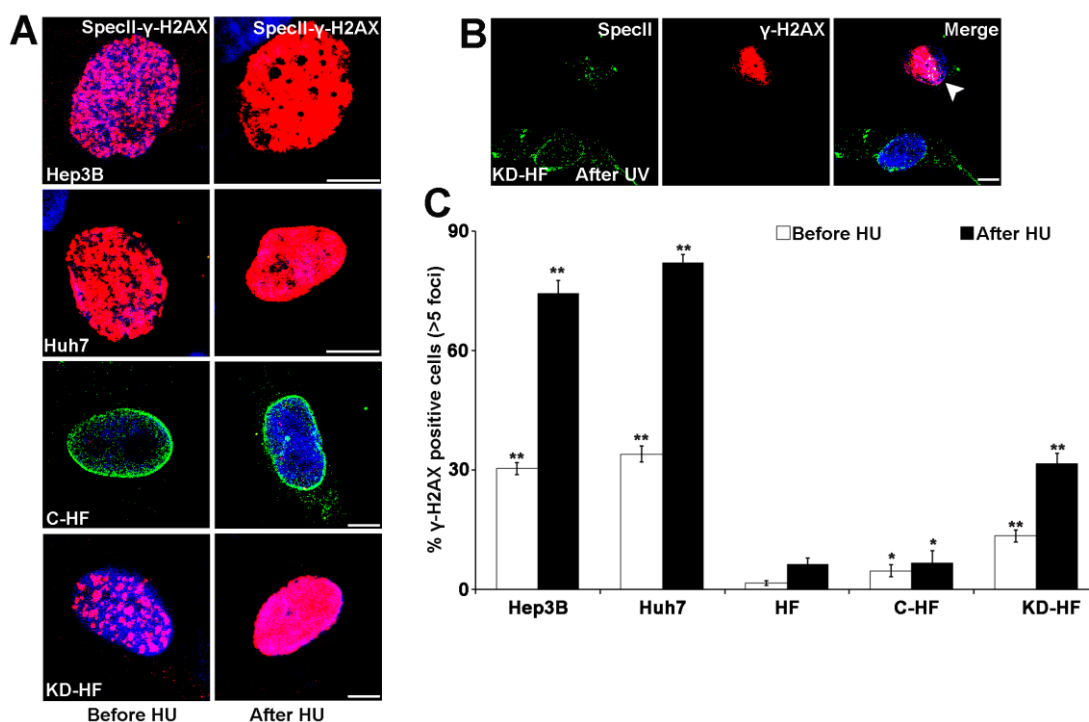
Figure 35: Nesprin-1 and the DDR network. (A) Nesprin-1 (pAb SpecII, green) and γH2AX (red) staining of Hep3B, Huh7, HF, Nesprin-1 KD-HF cells before (left) and after treatment (right) with hydroxyurea (HU). Loss of Nesprin-1 leads to increased γH2AX staining. (B) SpecII (green) and γH2AX (red) staining of Nesprin-1 KD-HF cells after UV treatment (arrow indicates KD-HF cells). Scale bars, 10 μm. (C) Quantification of the percentage of cells presenting >5 γH2AX-labelled foci before (white bar) or after (black bar) HU treatment. Graphs show results from at least three independent experiments. Error bars represent standard deviations (*$p<0.001$, **$p<0.0001$).

After knock down of Nesprin-1 a strong increase in the number of γH2AX foci was observed that exceeded the one of C-HF cells after HU or UV treatment and was indicative of an elevated DNA damage upon loss of Nesprin-1 (Figure 35B). Untreated Hep3B and Huh7 cells had a similar high number of γH2AX foci. This number was further enhanced following HU treatment both in Nesprin-1 KD-HF and the tumor cells (Figure 35C).

Ku70 was present in untreated C-HF cells whereas Nesprin-1 KD-HF cells had low levels of Ku70. After HU treatment Ku70 levels decreased in all cell lines with the exception of C-HF cells where an elevated expression was noted. After HU or UV treatment Ku70 levels decreased in KD-HF cells (Figure 36A, B). Similar reduction of Ku70 expression was also observed in Hep3B and Huh7 cells after HU treatment. The decrease was also detected at the protein level (Figure 37A).
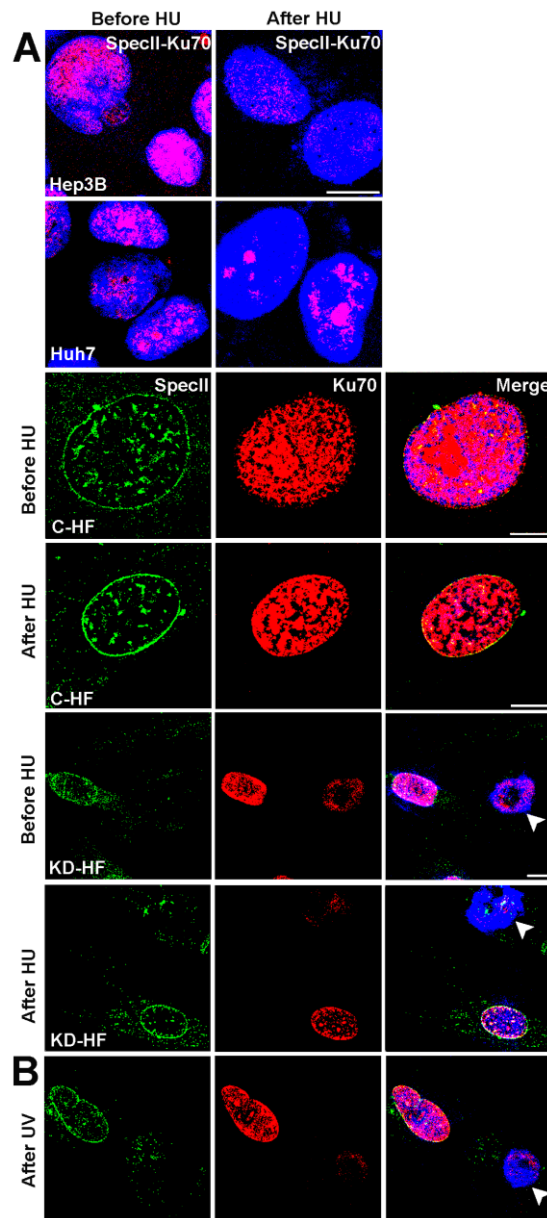
Figure 36: Loss of Nesprin-1 leads to defective recruitment of DNA repair proteins to DSBs. (A) Immunofluorescence analysis of Ku70 in Hep3B, Huh7, C-HF and KD-HF cells before and after HU treatment. pAb SpecII (green), Ku70 (red), DAPI (blue). Arrow heads point to Nesprin-1 KD-HF cells. Scale bars, 10 μm. (B) SpecII (green), Ku70 (red) staining in Nesprin-1 KD cells after UV treatment. Scale bar, 10 μm.

Nesprin-1 reduction also had an effect on the presence of phosphorylated H2AX, Chk1 and Chk2 (Figure 37A-C). In all untreated cell lines no phosphorylated Chk1 and Chk2 was detected. Upon HU treatment their levels strongly increased as

detected with antibodies recognizing specific phosphorylated forms in all cell lines except for C-HF where the increase was hardly noticeable (Figure 37D-F).
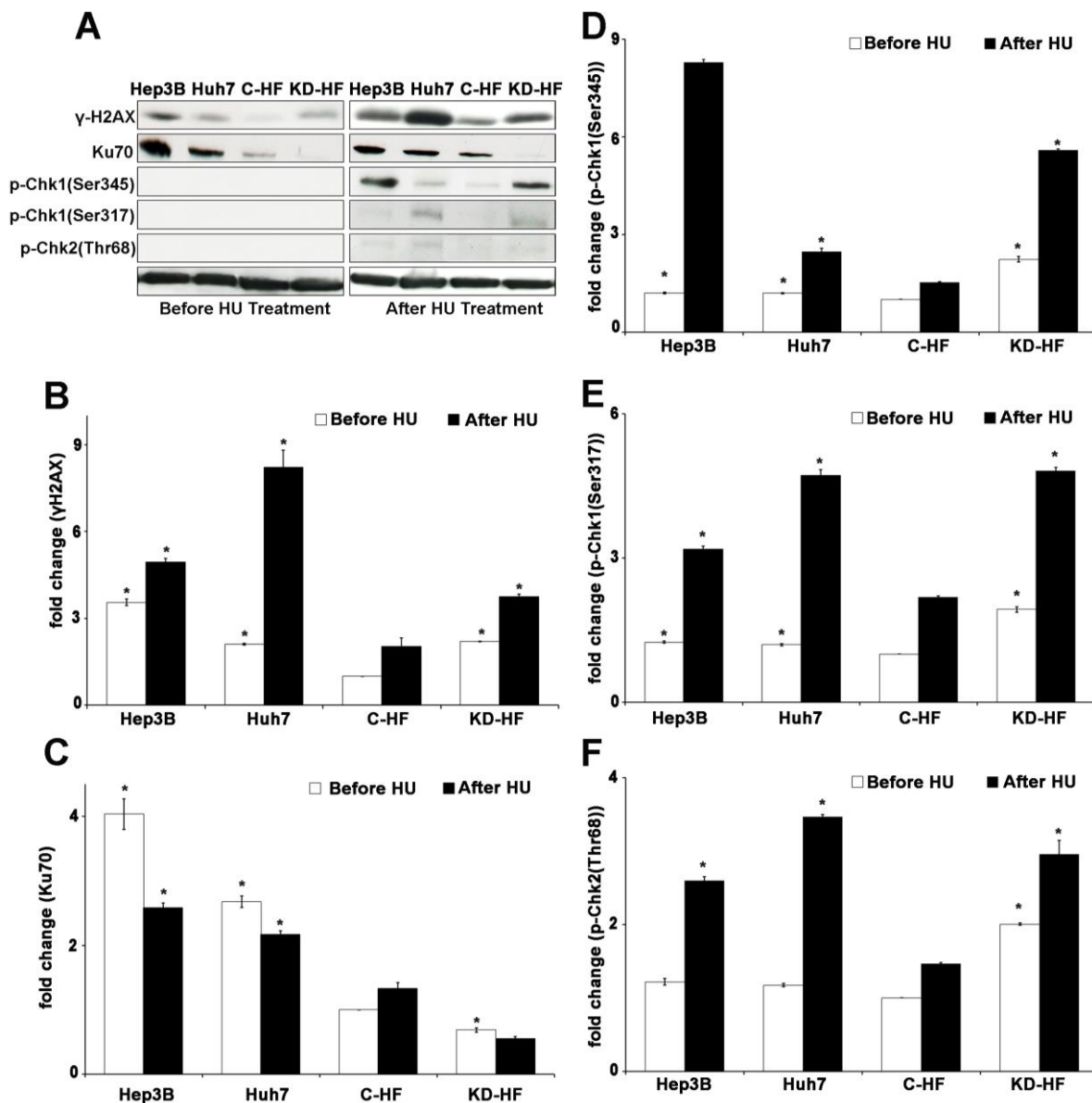
Figure 37: Nesprin-1 is involved in DNA damage response. (A) Western blot analysis for determination of levels of H2AX (Ser319), CHK1 (Ser345), and CHK1 (Ser317), CHK2 (Thr68), and Ku70 before and after HU treatment. Tubulin was used for loading control. (B-F) Histograms representing fold changes of band intensities of H2AX (Ser319), CHK1 (Ser345), and CHK1 (Ser317), CHK2 (Thr68), and Ku70 before (white bar) or after (black bar) HU treatment. Data are the mean ±SD from three samples per group of three independent experiments (*p<0.0001).

The elevated levels of these proteins indicate greater DNA damage in KD-HF compared to C-HF cells (Figure 37). Ku70 was present in untreated Hep3B, Huh7 and C-HF cells, whereas Nesprin-1 KD-HF cells had very low levels. Upon HU-treatment the levels decreased in Hep3B, Huh7 and Nesprin-1 KD-HF. By contrast, an increase was seen in Nesprin-1 C-HF (Figure 37A, C). These results indicate a defective response in the tumor cell lines and in Nesprin-1 deficient cells and a defective recruitment of Ku70 to sites of DNA damage resulting in a failure to protect the broken DNA ends from unwanted and excessive nuclease activity which leads to misrepair and loss of genetic information.

3. Discussion

The LINC complex is conserved from yeast to mammals and formed by interactions between Nesprins and SUN proteins (Libotte *et al.*, 2005; Crisp *et al.*, 2006). Nesprins are giant proteins of the LINC complex with a length of 300 nm-500 nm and situated in the nuclear envelope. Due to alternative splicing generating proteins with differing spectrin repeat copy numbers, there is a great variation in the length of Nesprins. Nesprin-1 is one of four Nesprins displaying a pair of connections in a molecular chain bridging the nucleus and the cytoskeleton. More specifically, Nesprin-1 also contains specific domains to facilitate the integration of the ONM with several cytoskeletal structures (Starr and Fridolfsson, 2010; Schneider *et al.*, 2011a).

Earlier reports indicated that Nesprin-1 C-terminal spectrin repeats interact with Lamin and Emerin. On the other hand, these spectrin repeats self-associate to form an antiparallel dimer (Mislow *et al.*, 2002a; Zhong *et al.*, 2010). According to our findings, N terminal Nesprin-1 spectrin repeats can also self-associate. Moreover, our data demonstrate that, presumably with the exception of aa 859-1144, which encode spectrin repeats with lower resemblance to the ones of α-actinin, the N-terminal spectrin repeats interact with full length Nesprin-1-165. The KASH domain containing Nesprin-1 (aa 8034-8749) interact with Nesprin-2, but not with KASH domain lacking Nesprin-1 (aa 7938-8644). Notably, these interactions, self-association and interaction among the N-terminal spectrin repeats of Nesprin-1 make them ideal candidates for maintaining the nuclear architecture. Furthermore, our findings suggest that Nesprin-3 mediates recruitment of vimentin to the NE in transfected cells.

Studies with KO mice highlight the biological and functional importance of Nesprin-1.

Importantly, mice with C-terminal deletion of *SYNE1* including the KASH domain die after birth owing to respiratory failure (Puckelwartz *et al.*, 2009). Overall, Nesprin-1 mutant mice display reduced survival rates, kyphoscoliosis, growth retardation, neurogenesis defects, and skeletal and cardiac muscle pathologies (Puckelwartz *et al.*, 2009; Zhang *et al.*, 2009; Zhang *et al.*, 2010). Although these findings indicate that Nesprin-1 controls several functions, how Nesprin-1 masters all these multiple functions is poorly understood. It will be of great interest to determine the specific roles of Nesprin-1 on nuclear structure, centrosome, cytoskeleton organization, cellular aging, tumorigenesis and genome stability.

The mechanisms establishing nuclear architecture are not sufficiently known nor are the consequences of a deformed nuclear structure for normal cell function unraveled. Nuclei of most normal cells have a smooth and ovoid shape, whereas in many cancer cells severe nuclear distortions are observed. We studied liver cancer cells and found several alterations which we could reproduce by reducing levels of Nesprin-1 by knock down in several cells. Most remarkable were the loss of Emerin, an upregulation of SUN proteins and changes in the centrosome number and in the DDR. Similarly, Zhang et al. reported that Nesprin-1 siRNA knock down in fibroblasts affected Emerin localization which correlated with deformed nuclei (Zhang *et al.*, 2007). From our data we propose that loss of Nesprin-1 is a casual event in tumorigenesis in analogy to a recent report showing that Emerin reduction was the basis of nuclear morphological deformation and subsequently the cause of aneuploidy in ovarian cancer cells (Capo-chichi *et al.*, 2009).

Deformed nuclear shape and increased size are also SUN1 dependent. Although the function of SUN1 and SUN2 in cancer biology is undefined, the finding that SUN1 accumulation leads to misshapen and enlarged nuclei of HPGS cells is of great

significance (Chen *et al.*, 2012). We also noted that brighter SUN1 staining was associated with misshapen and enlarged nuclei in Nesprin-1 KD, Hep3B and Huh7 cells. Furthermore, Zhang and coworkers found an upregulation of SUN1 and SUN2 in neonatal Nesprin-1$^{-/-}$ cardiac and skeletal muscle, respectively (Zhang *et al.*, 2010).

Earlier reports indicated that LINC complex components link the centrosome to the nucleus (Salpingidou *et al.*, 2007; Schneider *et al.*, 2011a). In order to elucidate the mechanisms behind the centrosome alterations in cancer cells, the effect of a loss of Nesprin-1 on centrosome-nucleus distance and centrosome number was determined. The centrosome was positioned next to the nucleus in C-HF and C- CH310T1/2 cells. In contrast, the centrosome dislodged from the NE in the Nesprin-1 KD-HF, KD-CH310T1/2, Hep3B and Huh7 cells, raising the possibility that the Nesprin-1 deficiency might cause detachment of the centrosome from the NE. Therefore it appears that Nesprin-1 plays a significant role in centrosome positioning and number. Proteins of the Nesprin family connect the nucleus through their N-termini to the actin network (Nesprin-1 and Nesprin-2), the intermediate filament system (Nesprin-3) and the microtubule network (Nesprin-2 and Nesprin-4) (Zhen *et al.*, 2002; Padmakumar *et al.*, 2004; Wilhelmsen *et al.*, 2005; Roux *et al.*, 2009; Schneider *et al.*, 2011a). Extensive F-actin filaments were observed around the nucleus in C-HF and C-CH310T1/2 cells whereas the filaments were reduced in KD-HF and KD- CH310T1/2. The actin staining was reduced in Hep3B and Huh7 cells possibly due to a decrease in Nesprin-1 linkage to F-actin. The microtubule system of Hep3B and Huh7 cells was also disorganized. We noted that KD-HF and KD- CH310T1/2 cells displayed similar microtubule disorganization. This may also support the previously proposed idea that force transmission to the nucleus regulates gene expression by causing conformational changes in the DNA structure and by regulating nuclear transport

(Wang *et al.*, 2009). As stated earlier, Nesprin-1 mislocalization in HeLa and Swiss 3T3 cells results in a softer cytoplasm and a damaged connection between the nucleus and the cytoskeleton. Therefore, F-actin may cause abnormal cellular functions, cytoskeleton network and cancer pathogenesis (Stewart-Hutchinson *et al.*, 2008).

The cytoskeleton organization is important for cell migration. Contrary to earlier reports and our expectations, cell migration in the Nesprin-1 KD-HF and KD-CH310T1/2 cells increased significantly compared to C-HF and C-CH310T1/2 cells. This is consistent with results obtained for cancer cells like Hep3B, and Huh7 cells, where cell velocity was as high as in Nesprin-1 KD-HF and KD- CH310T1/2 cells. Earlier studies have suggested that defective nucleo-cytoskeletal connections impair the activation of mechanosensitive gene Egr-1 (early growth response factor 1) and anti-apoptotic gene iex-1 which are transcription factors (Lammerding *et al.*, 2004; Lammerding *et al.*, 2005). Our data demonstrate that in addition to the impaired cytoskeleton network, loss of Nesprin-1 also leads to tumorigenesis, indicating that Nesprin-1 may suppress several steps in tumorigenesis.

Cellular senescence has gained significant attention in cancer therapeutic strategies. Interestingly, La Porta et al. formulated cancer growth in mathematical terms and made predictions for the progress of cellular senescence (La Porta *et al.*, 2012). In a related report Collado et al. speculated that senescence markers increase during tumor progression (Collado and Serrano, 2010). Cancer stem cells divide forever, by contrast, other tumor cells can go into senescence. Senescent cancer cells are not only growth arrested but can be also cleared by immune cells (Ventura *et al.*, 2007). We have shown here that Nesprin-1 loss also leads to cellular senescence and points to the importance of Nesprin-1 in cellular aging.

Defects in the DDR network can predispose to cancer and foster cancer progression (Clifford *et al.*, 2003; Sherr, 2004). So far, an effect of Nesprin-1 on DNA repair mechanisms has not been addressed. Lei et al. reported a reduction of γH2AX and phosphorylated Chk1 in SUN1$^{-/-}$SUN2$^{-/-}$ mouse embryonic fibroblasts and proposed an impairment of specific repair pathways (Lei *et al.*, 2012). Our results indicated elevated levels of γH2AX, phosphorylated Chk1 and Chk2 in Nesprin-1 KD-HF, Hep3B, and Huh7 cells pointing towards overactive pathways which can cause chromosomal instability. An integration of Nesprin-1 into the DDR, NER and MMR pathways is further supported by its interaction with components of these pathways as demonstrated in pull down assays. We identified proteins of the NER (DDB1) and MMR (MSH2, MSH6) in pull down experiments using the ABD of Nesprin-1 assigning a role to Nesprin-1 isoforms in the NER, and MMR pathway that harbor this domain. Furthermore, bioinformatic analysis by Mascia and Karchin led to the proposal of an interaction network around Nesprin-1 which contained MSH2 and MSH6 (Masica and Karchin, 2011).

In this study, we focused on the role of Nesprin-1 on the MMR pathway. We found that Nesprin-1 interacts not only with MMR proteins MSH2 and MSH6, but also with DNA polymerase delta subunit 3 which belongs to the DNA polymerase type-B family. Notably, DNA polymerase is required for DNA synthesis and repair. The MMR network serves to maintain genome stability (Modrich and Lahue, 1996; Lingle and Salisbury, 2001). Its importance is highlighted by participating in a cell-cycle checkpoint control system which leads to correction of DNA damage and promotes cell-cycle arrest or triggers apoptosis pathways (Kolodner, 1996). Defects in MSH2 resulted in a greatly increased likelihood of developing certain types of tumors (Schofield and Hsieh, 2003). Depending on the type of DNA damage, loss of MMR might therefore cause increased mutagenesis, loss of cell-cycle control and

resistance to apoptosis (Peters *et al.*, 2003). Based on our results, we speculate that Nesprin-1 provides a platform for the association of DNA damage response proteins and contributes to the role of the nuclear envelope to generate specific subcompartments where damaged DNA is sequestered and comes in contact with DNA repair proteins and can be repaired as described for yeast (Figure 38, (Oza *et al.*, 2009).
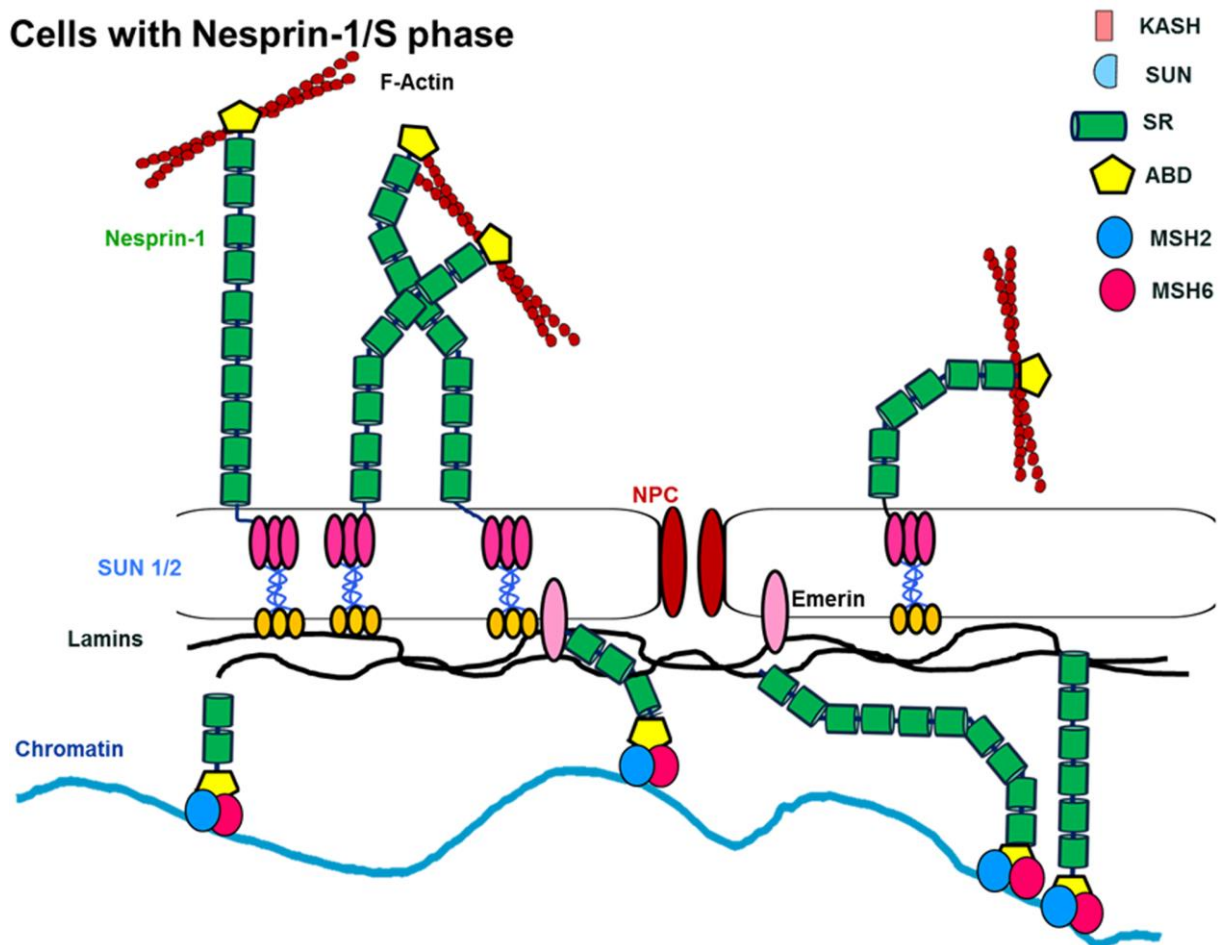
Figure 38: Model illustrating Nesprin-1 and MMR interaction. The Nesprin-1 interaction with the MutSα complex is a constitutive cellular event required for proper DNA repair. Therefore, a defect in this interaction chain leads to genome instability.

Functional deficiency of the DDR and the MMR pathway leads to increased genomic instability. Based on an altered DDR network in Nesprin-1 deficient cancer cells, adequate DDR inhibitors might provide promising methods for selective killing of

cancerous cells and improve the efficiency of radiotherapy and chemotherapy. Thus, during therapy, cancer cells can be killed by DDR inhibitors whereas the surrounding healthy cells can be saved due to their diminished DDR levels. These results can open many doors for the development of DDR inhibitors in therapy.

Since different DNA repair mechanisms exist for certain type of lesions in the genome sequence, special proteins are required to initiate repair signaling networks for maintaining genome stability. DDB1 functions in the NER machinery by participating in the initial steps of DNA repair (Chu et al., 1998; Abbas et al., 2008). Our findings suggest that Nesprin-1 interacts with DDB1 in vitro and in vivo. Future experiments are needed to elucidate the role of Nesprin-1 in NER signaling. We will try to answer these questions: How does Nesprin-1 fit into the picture of NER mechanisms and what might be the consequences of Nesprin-1 loss on the NER pathway?

In conclusion, loss of Nesprin-1 triggers an altered cell fate which could lead to tumorigenesis. This could be achieved by altered gene expression, altered genome stability and an altered nuclear structure. Our data highlight changes in nuclear morphology, centrosome positioning, nuclear membrane structure, cytoskeleton organization, cellular aging and DNA damage responses upon loss of Nesprin-1. Careful evaluation of Nesprin-1 levels may therefore provide novel approaches for early disease diagnosis, intervention, and treatment.

4. Materials and Methods

4.1 Materials

Kits

M-MLV reverse transcriptase RNase H Minus-kit	Promega
NucleoSpin Extraction Kit	Macherey Nagel
pGEM-T easy Cloning Kit	Promega
Pure YieldTM Plasmid System	Promega
Qiagen RNeasy Mini Kit	Qiagen
Cell Line Nucleofector Kit V	Amaxa

Enzymes

Lysozyme	Sigma
Restriction endonucleases	Life technologies, NEB
RNAse	Boehringer
T4 DNA ligase	Boehringer
Taq polymerase	Boehringer
Trypsin	Invitrogen

Inhibitors

Complete mini protease inhibitor cocktail	Sigma

Antibiotics

Ampicillin	Sigma
Kanamycin	Sigma

Penicillin/Streptomycin	Biochrom

Antibodies

<u>Primary Antibodies</u>

Mouse-anti-GFP (K3-184-2)	(Noegel et al., 2004)
Rat-anti-α-tubulin (YL1/2)	(Kilmartin et al., 1982)
Rabbit-anti-pAbK1	(Libotte et al., 2005)
Mouse-anti-LAP2	BD Biosciences
Rabbit-anti-LMNB1	Abcam
Rabbit-anti- LMNA/C	Santa Cruz
Rabbit-anti-Nesprin1 (SpecII)	S.Abraham, Thesis, 2004
Rabbit-anti-pericentrin	Abcam
Mouse-anti-emerin (4G5)	Abcam
Mouse-anti-LAP-2	BD Transduction Laboratories
Rabbit-anti-SUN1	Abcam
Rabbit-anti-SUN2	Abcam
Mouse-anti-NPC	Abcam
Mouse-anti-phospho-Ser139 H2AX	Millipore
Mouse-anti-phospho-Ser317 Chk1	Cell Signalling
Mouse-anti-phospho-Ser345 Chk1	Cell Signalling
Mouse-anti-phospho-Thr68 Chk2	Cell Signalling
Mouse-anti-Ku70+Ku80	Abcam
Rabbit-anti-MSH2	Abcam
Rabbit-anti-MSH6	Abcam
Rabbit-anti-DDB1	Abcam
Mouse-anti-Nesprin-1 (K43-222-2)	(Taranum *et al.*, 2012a)

Mouse-anti-γ-tubulin   Sigma

Secondary Antibodies

Anti-mouse IgG, Alexa488-conjugated	Sigma
Anti-mouse IgG, Alexa568-conjugated	Sigma
Anti-goat IgG, Alexa568-conjugated	Sigma
Anti-mouse IgG Alexa Fluor 488	Invitrogen
Anti-mouse IgG POD	Sigma
Anti-rabbit IgG POD	Sigma
Anti-rat IgG POD	Sigma

Bacterial host strains

E. coli XL1 blue	(Bullock et al., 1987)
E. coli DH5α	(Hanahan, 1983)

Oligonucleotides

Nesprin-1-RT-F	CGAACTTTCACAAAATGGATCA
Nesprin-1-RT-R	TGGTCCACATCAATCCAAGA
MSH2-RT-F	GGAGAGATTGAATTTAGTGGAAGC
MSH2-RT-R	TCATTTCCTGAAACTTGGAGAA
MSH6-RT-F	CATGCGGCGACTGTTCTAT
MSH6-RT-R	TCATTTCCTGAAACTTGGAGAA
DDB1-RT-F	TCCAGATCACTTCAGCATCG
DDB1-RT-R	AGGTGGTCATCAGGATGGAG

Media, Buffers and solutions

10x NCP buffer, pH 8.0

12.1 g TrisHCl, pH 8.0 (100 mM)

87.0 g NaCl (1.5 M)

5.0 ml Tween 20

2.0 g sodium azide, add H_2O to make 1 liter

1x PBS, pH 7.4

0.2 g KCl (10 mM)

8.0 g NaCl (10 mM)

1.15 g Na_2HPO_4 (16 mM)

0.2 g KH_2PO_4 (32 mM) dissolved in 900 ml deionized H_2O, adjust to pH 7.4, add H_2O

to make 1 liter, autoclaved.

Gel drying buffer

EtOH (50%)

Glycerin (5%)

Water (45%)

Destaining solution

EtOH (5%)

Acetic acid (7%)

Water (88%)

10 x SDS-PAGE running buffer

 0.25 M Tris

1.9 M Glycine

1% SDS

4.2 Molecular biological methods

4.2.1 Primer design

Fragments of mouse Nesprin-1-165 (Enaptin-165) were PCR amplified with the following primers: Nesprin-1-165-1-286 (5′-GCGAATTCATGGCAACCTCCAGAGCATC-3′ and 5′-GCGTCGACTTCTGTTGAAACTGGGCCAC-3′), Nesprin-1-165-573-858 (5′-GCGAATTCAAATTCATGAGTAAGCACTG-3′ and 5′-GCGTCGACTTAGAGTGTCAAGGATTTCTTAC-3′), Nesprin-1-165-859-1144 (5′-GCGAATTCATAGAGAAGGGCAGCCAAAG-3′ and 5′-GCGTCGACTAGCCATTCAATGGGCTC-3′), Nesprin-1-1145-1431 (5′-GCGAATTCAACCACGACGAGTTAGATATG-3′, and 5′-GCGTCGACTTAGAAGTGGTGAAGCACATAC-3′) and cloned into the EcoRI/SalI site of pGBKT7 (BD Biosciences Clontech, Palo Alto, CA), into pGEX-4T-2 (Amersham, Piscataway, NJ) or into pEGFP-C vectors (BD Biosciences Clontech).

Fragments of human Nesprin-1 were PCR amplified with the following primers: Nesprin-1-7938-8644 (5′-TCACGTTTTGAAGATTGGCTGAAGTCTTCA-3′ and 5′-GGGTCTGTGAGTCCCACATCAGGAAGGAGCACC-3′), Nesprin-1-8034-8749 (5′-CATTTTATTGGCCAGCGTGAGGAGTTTGAG-3′ and 5′-AGATACACGAATGGCCCTCCTCCACTCTGA-3′ cloned into pEGFP-C vectors (BD Biosciences Clontech).

Nesprin-1 knock down in HF and CH310T1/2 cells was performed by plasmid based shRNA (short hairpin RNA) technique.

74

Oligonucleotides were cloned into pSHAG-1 vector using BseRI and BamHI restriction sites (Paddison *et al.*, 2002). To knock down Nesprin-1 in HF cells, two sets of primers were designed by taking 31 nucleotides from each of exon 6 (5'-GGATGAAGCGAATCCATGCTGTGGCTAACAT-3') and exon 143 (5'-GAAGGAGGTCAGTCGTCATATCAAGGAACTG-3') of human *SYNE1*.

For Nesprin-1 knock down in CH310T1/2 cells, two sets of primers were designed by taking 31 nucleotides from each of exon 5 (5'-GGCTAACATTGGCACCGCACTCAAATTCCTT-3') and exon 32 (5'-AGAAGTGGCAGCAGTTTAATTCTGACCTCAA-3') of murine *SYNE1*. The procedure described in (http://hannonlab.cshl.edu/protocols/BseRI-BamHI_Strategy.pdf) was used for primer design.

4.2.2 Annealing of oligonucleotides

To anneal phosphorylated forward and reverse single-stranded oligonucleotides, 9 µl forward oligonucleotide (100 mM) and 9 µl reverse oligonucleotide (100 mM) were mixed with 9 µl of 10X annealing buffer (100 mM Tris-HCl, pH 8.0, 500 mM NaCl, 70 mM MgCl$_2$). The mixture of oligos was kept in the boiling water for 5 minutes and incubated until the temperature of the water decreased to RT. Annealed oligos were diluted in HPLC water with the ratio of 1:60 and ligated into the pSHAG-1 vector (Paddison *et al.*, 2002).

4.2.3 Digestion of pSHAG-1 vector

1 µg of pSHAG-1 vector were linearized using restriction enzymes (*Bse*RI and *Bam*HI) that generate overhanging ends compatible with the target sequences. The digested product was analyzed by agarose gel electrophoresis.

To prevent religation, the 5´-ends of the linearized plasmid were dephosphorylated by calf intestinal alkaline phosphatase (CIP). For this, 1-5 µg of the vector (89 µl) were incubated with 1 U/µl of CIP (1 µl) adding 10 µl 10XCIP buffer in a 100 µl reaction volume (37°C, 30 min). The dephosphorylated vector was purified by the High Pure PCR Product Purification Kit (Roche).

4.2.4 Ligation and cloning procedure

1 µg of linearized and purified pSHAG-1 vector were used for the ligation with 1 µl (1:60 diluted) double-stranded oligonucleotides. 4 µl of T4 Ligase buffer, 2 µl of T4 DNA Ligase (1 U/ µl), and nuclease free water were added to a total volume of 20 µl. This reaction was incubated at 15°C overnight and 5 µl of the ligation were mixed with competent *E. coli* XL1 blue. Incubation was conducted for 15 min on ice. The cells were shocked by heat exposure at 42°C for 90 s and then incubated 2 min on ice. In the next step, 1 ml medium was added to the transformed bacteria followed by 1 h incubation at 37°C. Finally, 50 µl were spread on LB agar plates containing kanamycin (50 mg/ml). The plates were incubated at 37°C overnight.

Colonies (9-15) were picked and DNA-Mini preparation was performed according to Birnboim and Doly (Birnboim and Doly, 1979). Briefly, an overnight culture of single clones was centrifuged for 5 min at 5.500 rpm at room temperature (RT). Subsequently, the pellet was suspended in 300 µl buffer 1 (50 mM Tris-HCl, pH 8.0, 10 mM EDTA, 100 µg/ml RNAse A). After addition of buffer 2 (200 mM NaOH, 1% SDS), the mixture was incubated for 5 min (RT). The reaction was stopped by adding 300 µl buffer 3 (3 M KAc, pH 5.5, 1% SDS) and the sample was centrifuged at 14.000 rpm for 10 min. The supernatant (650 µl) was mixed with 450 µl isopropanol and centrifuged again at 14.000 rpm for 20 min to precipitate the DNA. After drying

the DNA pellet, it was dissolved with 50 µl Tris-HCl, pH 8.0, and analysed by sequencing.

4.2.5 DNA Midi/Maxi preparation

Correct clones were cultured overnight in 250 ml LB medium containing kanamycin (50 mg/ml). Plasmid DNA was isolated using PureYield™ Plasmid Midiprep System (Promega). Briefly, 250 ml of an overnight E. coli culture were centrifuged (7000 rpm, 10 min) and subsequently the pellet was suspended in 6 ml cell suspension solution. After the addition of 6 ml cell lysis solution, the mixture was carefully mixed and incubated 2 min (RT). For neutralization, 10 ml neutralization solution was incubated for 3 minutes (RT), and subsequently centrifuged (10,000 rpm, 15 min). DNA was bound to the resin of a binding-column, washed with 5 ml endotoxin removal wash followed by a washing step with 20 ml column wash solution and eluted with 300 µl nuclease free water.

4.2.6 RNA isolation and cDNA generation for quantitative RT-PCR analysis

For RT-PCR, total RNA was extracted for gene expression analysis using TRIzol (Invitrogen). Briefly, the cells were trypsinised and centrifuged in ice cold PBS (1200 rpm, 5 min). The pellet was suspended in 1 ml TRIzol (50-100 mg cells) and incubated for 5 min (RT). Subsequently, the chloroform (for each ml of TRIzol 200 µl) was added, mixed and incubated at RT for 2-3 min followed by centrifugation (12,000 g, 15 min). The aqueous phase was precipitated with isopropanol (for each ml of solution 500 µl isopropanol) and incubated for 10 min (RT) and centrifuged (12,000 g, 10 min). The pellet was washed with 75% ethanol. After a centrifugation step, the

pellet was dried and dissolved in RNAse-free water. Finally, the concentration and quality of the RNA was determined with the Agilent Bioanalyser (Agilent Technologies) and stored at -80°C.

cDNA was synthesized by reverse transcription of 5 µg RNA with oligo dT18 using Superscript II reverse transcriptase (Invitrogen) according to the manufacturer's guide. In brief, 1µg of total RNA was mixed with 2 µl of random primers (pdN6 50 µM, Stratagene) and filled up to 15 µl with nuclease free water. After incubation for 5 min at 70°C and cooling for 2 min on ice, 5 µl 5x reaction buffer (Promega), 1.25 µl dNTP's (10 mM, Stratagene), 1 µl RNase inhibitor (Rnasin 40 U/µl, Promega), 1.75 µl nuclease free water and 1 µl M-MLV-RT (200 U/µl) were added. The samples were incubated for 1 h at 37°C and stored at -20°C until use.

Each sample for real-time RT-PCR analysis contained 200 ng of cDNA, SYBR Green Master Mix and 0.4 µM of each primer. The PCR amplification and real-time fluorescence detection were performed with the Opticon III instrument (MJ Research) using the QuantitectTM SYBR1 green PCR kit (Qiagen). As quantification standard defined concentrations of annexinA7 cDNA (Doring *et al.*, 1991) were used for amplification. PCR amplification was carried out according to the manufacturer's instruction and all PCR products were amplified in a linear cycle. GAPDH mRNA was employed as an internal standard, and each gene expression was determined by RT-PCR and normalized against GAPDH mRNA levels. All PCR products were amplified in a linear cycle. Data are the mean +/-SD from three samples per group of three independent experiments.

4.3 Protein chemical and immunological methods

4.3.1 Protein extraction from *E.coli* and mammalian cells

E. coli cells were lysed with prokaryotic lysis buffer (50 mM Tris-HCl, pH 7.5, 150 mM NaCl, 1% Sarcosyl, 1 mM DTT, 1 mM benzamidine, 1 mM PMSF, Proteinase Inhibitor Cocktail (PIC, Sigma), and lysozyme). Following 1 h incubation in lysis buffer, the cells were sonicated and centrifuged (13.000 g, 4°C, 20 min). For incubation with GST-Sepharose 4B, 1% Triton X-100 was added to the lysis buffer.

Mammalian cells were trypsinised and washed with ice cold 1x phosphate buffered saline (PBS) plus protease inhibitor (DTT, Benzamidine and PMSF at 1 mM each). After centrifugation at 15,000 rpm at 4°C the pellet was resuspended in lysis buffer (50 mM Tris-HCl, pH 7.5, 150 mM NaCl, 1% Nonidet P-40, 0.5% Na-desoxycholate, 0.1 mM Na_3VO_4, 0.1% SDS, PIC and protease inhibitors (DTT, Benzamidine and PMSF). The sample was denatured in 5x SDS sample buffer at 95°C for 5 minutes. The samples were used for SDS-PAGE and western blot analyses.

5 x SDS-Sample buffer

5 × SDS loading buffer

2.5 ml 1M Tris-HCl; pH 6.5

4.0 ml 10% SDS

2.0 ml Glycerol

1.0 ml 14.3 M ß-Mercaptoethanol

200 µl 10% Bromophenol blue

4.3.2 Western blotting

For immunoblotting, equal amounts of total cell protein were separated by SDS-PAGE (12%, 3%-12% gradient gel). After the SDS page, sheets of Whatman filter papers and membranes were pre-cut to the gel dimensions. The Whatman papers, sponges, membranes, and gels were also immersed in cold transfer buffer for 5 min. For protein transfer, semi-dry or wet blotting transfer was used. Subsequently, the membrane was blocked with 12.5 ml 1% blocking solution under constant shaking for 1 h. After blocking, the membrane was incubated with primary antibody solution for either overnight (+4°C) or 1 h (RT). The membrane was washed three times with TBS for 15 min. The corresponding appropriate horseradish peroxidase coupled secondary antibodies (1:10.000) were incubated for 1 h, and the membrane was washed three times with TBS. Antigen-antibody complexes were detected by using the ECL western blotting detection solution. The protein bands were visualized using X-ray films. After imaging, the membrane was stripped with 0.2 M NaOH for 15 min. The stripped membrane was washed twice with TBS for 15 min. After washing the membrane, the membrane was blocked with blocking solution for 1 h at room temperature and used for antibody incubation.

Transfer buffer SDS-gels   **TBS-T**

48 mM Tris-HCl, pH 8.3   15 mM NaCl

39 mM glycine   1 mM Tris-HCl, pH 8.0

10% ethanol   0.04% Tween 20 (freshly added)

Ponceau staining solution

2 g Ponceau S

100 ml 3% Trichloroacetic acid

0.04% Tween 20

ECL solution

2 ml 1 M Tris-HCl (pH 8.0)

200 µl Luminol (0.25 M in DMSO) 3-aminonaphthylhydrazide

89 µl (0.1 M in DMSO) p-coumaric acid

18 ml dH$_2$O

6.3 µl 30% H$_2$O$_2$

Blocking solution

4% milk-powder in TBS-T

4.3.3 Recombinant protein purification and pull downs

To identify interaction partners of Nesprin-1, GST-Nesprin-1-286 was used for pull down experiments. It encodes the F-actin binding domain of Nesprin-1 (Taranum et al., 2012). For pull down assays C2F3 cells were lysed in lysis buffer (50 mM Tris-HCl, pH 7.5, 150 mM NaCl, 1% NP40, 0.5% sodium desoxycholate, 1 mM DTT, 1 mM benzamidine, and 1 mM PMSF). For preclearing, lysates of cells were incubated with beads for one hour at 4°C followed by incubation with GST-Nesprin-1-286 and GST for control. Beads were washed three times with PBS (500 g, 4°C, 1 min) and boiled in SDS sample buffer (95°C, 5 min). Samples were separated using 12% SDS polyacrylamide gels and stained with Coomassie Brilliant Blue. Protein bands of

interest were cut out and subjected to LCMS analysis. To confirm the interactions, samples were run using 12% SDS polyacrylamide gels and immunoblotted with a rabbit polyclonal MSH2, MSH6, and DDB1 antibody (Abcam).

Coomassie Blue R 250

0,1% Coomassie brilliant blue R 250

50% Ethanol

10% Acetic acid

4.3.4 Co-immunoprecipitation (Co-IP)

For immunoprecipitation, COS7 cells were transfected with GFP-Nesprin-1-286. The untreated and UV treated cells (20 J/m^2) were immediately suspended in 1 ml hypotonic buffer (10 mM HEPES, pH 7.9, 1.5 mM $MgCl_2$, and 10 mM KCl, PIC) followed by centrifugation (1000 rpm, 20 s, 4°C). Pellets were again resuspended in 1 ml hypotonic buffer. Cell suspensions were lysed through a needle (0.4 mm) for 10 times and incubated on ice for 10 min. Nuclear and cytoplasmic fractions were separated by centrifugation (1000 rpm, 10 min, 4°C). Pellets (nuclear fraction) were washed with 1 ml PBS (1000 rpm, 6x10 min, 4°C). Finally nuclear fractions were pre-cleared with Protein-A-Sepharose CL-4B (Pharmacia Biotech) for 2 h at 4°C. The samples were incubated for 2 h at 4°C with GFP-TRAP beads (ChromoTek). Immunocomplexes were washed three times with PBS supplemented with protease inhibitors. The samples from pull down and immunoprecipitations were boiled in SDS sample buffer (95°C, 5 min) and analyzed by western blot.

4.3.5 Immunofluorescence

Immunofluorescence was done as described (Taranum et al., 2012). The cells were grown on 12 mm coverslips and fixed with 3% paraformaldehyde (5 min, RT), followed by permeabilization with 0.5% Triton X-100 for 3 minutes (RT). In another method for fixation and permeabilization, the cells were incubated with cold methanol (-20°C) for 5 minutes. Subsequently, the fixed cells were washed three times with 1X PBS and incubated for 15 minutes with blocking solution (1x PBG: PBS containing 5% BSA and 0.045% fish gelatine in 1x PBS, pH 7.4). After blocking, primary antibodies were diluted in PBG and incubated 1 h (RT) or overnight (4°C). Antibodies used were specific for Emerin (4G5, Abcam), LAP-2 (BD Transduction Laboratories), Lamin B1 (Abcam), Lamin A/C (StCruz), SUN1 (Abcam), SUN2 (Abcam), mAb414 recognizing NPC (Abcam), anti-phospho-Ser139 H2AX (Millipore), Ku70 (Abcam), MSH2 (Abcam), MSH6 (Abcam), rabbit polyclonal Nesprin-2 pAbK1 (Padmakumar *et al.*, 2005), anti-tubulin YL1/2. Nesprin-1 polyclonal antibodies SpecII and mAb K58-398-2 directed against the C-terminus of human Nesprin-1, affinity-purified rabbit anti-Nesprin-1 ABD and mAb K43-322-2 directed against the N-terminus were also used (Taranum *et al.*, 2012a). The cells were washed three times for 5 minutes each, the samples were incubated for appropriate secondary antibodies conjugated to Alexa 488/568 (1:1.000 diluted in PBG) were added for one hour at room temperature. Nuclear DNA was stained with 4',6-Diamidino-2'-phenylindole (DAPI, Sigma). Finally the coverslips were mounted on glass slides with gelvatol. Imaging was done by confocal laser scanning microscopy (Leica TCS-SP5). Images were processed using TCS-SP5 software.

4.4 Cell culture and transfections

CMT93 (mouse rectum carcinoma), CT26 (murine colorectal carcinoma), WIDR (human colorectal carcinoma), CH310T1/2 cells (embryonic mouse mesenchymal stem cell line), C2F3 (mouse myoblast), HaCaT (human keratinocyte), HeLa (human epithelial carcinoma), Hep3B (human liver cancer) and Huh7 (human hepatocellular cancer), DLD-1 (human colorectal carcinoma (Plaschke *et al.*, 2006)) cell lines were grown in high glucose Dulbecco's Modified Eagle's Medium (DMEM, Sigma) supplemented with 10% FBS, 2 mM glutamine, and 1% penicillin/streptomycin. Primary human dermal fibroblasts (HF) were isolated from foreskin and cultured in high glucose DMEM. All cells were grown in a humidified atmosphere containing 5% CO_2.

To knock down Nesprin-1, CH310T1/2 cells were transfected twice at intervals of 4 d using the Amaxa Nucleofector kit V solution (Lonza). For HF cells, Lipofectamine 2000 transfection reagent (Invitrogen) was utilized.

Gelvatol PBG (pH 7.4)

4.8 g Polyvinyl alcohol (87%-89%, Sigma P 8136)

12 g Glycerol

Add 12 ml de-ionized water, stir (RT, 10h)

24 ml 0.2 M Tris-HCl; pH 8.5; stir (50°C, 20-40 min)

cenrifugation (15 min, 5000 g)

2.5% Diazabicyclooktan (DABCO)

Aliquot-storage: – 20°C

4.5 Cell biological assays

4.5.1 Heat stress experiments

Cells were allowed to attach onto 12 mm glass coverslips for two days before the experiment. For heat stress, cells were transferred for heat treatment to a 45°C incubator for 30 min. After fixation with cold methanol at -20°C for 5 min cells were incubated with monoclonal antibody LAP2 (Abcam) to detect nuclear deformations.

4.5.2 Senescence-associated β-galactosidase

The cells were seeded in 24-well plates. After a 24 h incubation period, they were fixed with 2% formaldehyde, 0.2% glutaraldehye (5 min, RT). Cells were washed three times with PBS and incubated at 37°C with freshly prepared senescence-associated β-Gal (SA-β-Gal) staining solution (1 mg/ml 5-bromo-4-chloro-3-indolyl β-D-galactoside (X-Gal), 40 mM citric acid/sodium phosphate, pH 6.0, 5 mM potassium ferrocyanide $K_4Fe(CN)_6$, 5 mM potassium ferricyanide $K_3Fe(CN)_6$, 150 mM NaCl, 2 mM $MgCl_2$) for 8 h. The cells were imaged using bright field microscopy at 40xmagnification.

4.5.3 Cell migration assay

Cell migration was analyzed according to the manufacturer's instructions using an Ibidi Culture Insert (Ibidi, Munich, Germany). 100 µl of a cell suspension ($4x10^5$ cells/ml) was applied into each well. After 24 h incubation period at 37°C and 5% CO_2, the culture insert was removed and the well was filled with serum-supplemented normal growth medium (300 µl of cell media). Cell migration into the wounded area was monitored using a Leica CTR7000 HS (10x0.3 objective). Images were captured

at various time points and the cell velocity was calculated by Image J. Experiments were repeated at least thrice for each cell type.

4.5.4 DDR assays

To assay for DNA damage response, the cells were grown for 24 h in 500 µM hydroxyurea (HU) or taken after 20 J/m^2 UV (Hajdu *et al.*, 2011). The HU treated cells were processed for immunofluorescence and western blot analysis, UV exposed cells were processed for immunofluorescence.

Cell synchronization was performed according to a recent study (Li *et al.*, 2013). In brief, cells were arrested at G1/S by culturing for 18 h in 2 mM thymidine-containing medium, and then for 10 h in thymidine-free medium. Subsequently, cells were incubated with complete medium containing thymidine for an additional 15 h before release into complete medium. Finally, cells were harvested at 0 h (G1 phase), 1 h (early S), 2.5 h (middle S), 4 h (late S), and 8 h (G2/M). The cell-cycle status was confirmed by flow cytometry. FACS cell sorting was carried out at the central facilities of the CMMC.

5. References

Acharya, S., Wilson, T., Gradia, S., Kane, M. F., Guerrette, S., Marsischky, G. T., Kolodner, R., and Fishel, R. (1996). *hMSH2 forms specific mispair-binding complexes with hMSH3 and hMSH6.* Proc Natl Acad Sci U S A *93*, 13629-13634.

Agudo, D., Gomez-Esquer, F., Martinez-Arribas, F., Nunez-Villar, M. J., Pollan, M., and Schneider, J. (2004). *Nup88 mRNA overexpression is associated with high aggressiveness of breast cancer.* Int J Cancer *109*, 717-720.

Apel, E. D., Lewis, R. M., Grady, R. M., and Sanes, J. R. (2000). *Syne-1, a dystrophin- and Klarsicht-related protein associated with synaptic nuclei at the neuromuscular junction.* J Biol Chem *275*, 31986-31995.

Attali, R., Warwar, N., Israel, A., Gurt, I., McNally, E., Puckelwartz, M., Glick, B., Nevo, Y., Ben-Neriah, Z., and Melki, J. (2009). *Mutation of SYNE-1, encoding an essential component of the nuclear lamina, is responsible for autosomal recessive arthrogryposis.* Hum Mol Genet *18*, 3462-3469.

Bengtsson, L., and Wilson, K. L. (2004). *Multiple and surprising new functions for emerin, a nuclear membrane protein.* Curr Opin Cell Biol *16*, 73-79.

Berger, R., Theodor, L., Shoham, J., Gokkel, E., Brok-Simoni, F., Avraham, K. B., Copeland, N. G., Jenkins, N. A., Rechavi, G., and Simon, A. J. (1996). *The characterization and localization of the mouse thymopoietin/lamina-associated polypeptide 2 gene and its alternatively spliced products.* Genome Res *6*, 361-370.

Bione, S., Maestrini, E., Rivella, S., Mancini, M., Regis, S., Romeo, G., and Toniolo, D. (1994). *Identification of a novel X-linked gene responsible for Emery-Dreifuss muscular dystrophy.* Nat Genet *8*, 323-327.

Birnboim, H. C., and Doly, J. (1979). *A rapid alkaline extraction procedure for screening recombinant plasmid DNA.* Nucleic Acids Res *7*, 1513-1523.

Bohr, V. A., Smith, C. A., Okumoto, D. S., and Hanawalt, P. C. (1985). *DNA repair in an active gene: removal of pyrimidine dimers from the DHFR gene of CHO cells is much more efficient than in the genome overall.* Cell *40*, 359-369.

Broers, J. L., Raymond, Y., Rot, M. K., Kuijpers, H., Wagenaar, S. S., and Ramaekers, F. C. (1993). *Nuclear A-type lamins are differentially expressed in human lung cancer subtypes.* Am J Pathol *143*, 211-220.

Bronner, C. E., Baker, S. M., Morrison, P. T., Warren, G., Smith, L. G., Lescoe, M. K., Kane, M., Earabino, C., Lipford, J., Lindblom, A., and et al. (1994). *Mutation in the DNA mismatch repair gene homologue hMLH1 is associated with hereditary non-polyposis colon cancer.* Nature *368*, 258-261.

Brustmann, H., and Hager, M. (2009). *Nucleoporin 88 expression in normal and neoplastic squamous epithelia of the uterine cervix*. Ann Diagn Pathol *13*, 303-307.

Cann, K. L., and Hicks, G. G. (2007). *Regulation of the cellular DNA double-strand break response*. Biochem Cell Biol *85*, 663-674.

Capo-chichi, C. D., Cai, K. Q., Testa, J. R., Godwin, A. K., and Xu, X. X. (2009). *Loss of GATA6 leads to nuclear deformation and aneuploidy in ovarian cancer*. Mol Cell Biol *29*, 4766-4777.

Cartegni, L., di Barletta, M. R., Barresi, R., Squarzoni, S., Sabatelli, P., Maraldi, N., Mora, M., Di Blasi, C., Cornelio, F., Merlini, L., Villa, A., Cobianchi, F., and Toniolo, D. (1997). *Heart-specific localization of emerin: new insights into Emery-Dreifuss muscular dystrophy*. Hum Mol Genet *6*, 2257-2264.

Chancellor, T. J., Lee, J., Thodeti, C. K., and Lele, T. (2010). *Actomyosin tension exerted on the nucleus through nesprin-1 connections influences endothelial cell adhesion, migration, and cyclic strain-induced reorientation*. Biophys J *99*, 115-123.

Chen, C. Y., Chi, Y. H., Mutalif, R. A., Starost, M. F., Myers, T. G., Anderson, S. A., Stewart, C. L., and Jeang, K. T. (2012). *Accumulation of the inner nuclear envelope protein Sun1 is pathogenic in progeric and dystrophic laminopathies*. Cell *149*, 565-577.

Chow, K. H., Factor, R. E., and Ullman, K. S. (2012). *The nuclear envelope environment and its cancer connections*. Nat Rev Cancer *12*, 196-209.

Chowdhury, D., Choi, Y. E., and Brault, M. E. (2013). *Charity begins at home: non-coding RNA functions in DNA repair*. Nat Rev Mol Cell Biol *14*, 181-189.

Christmann, M., Tomicic, M. T., Roos, W. P., and Kaina, B. (2003). *Mechanisms of human DNA repair: an update*. Toxicology *193*, 3-34.

Clifford, B., Beljin, M., Stark, G. R., and Taylor, W. R. (2003). *G2 arrest in response to topoisomerase II inhibitors: the role of p53*. Cancer Res *63*, 4074-4081.

Collado, M., and Serrano, M. (2010). *Senescence in tumours: evidence from mice and humans*. Nat Rev Cancer *10*, 51-57.

Cottrell, J. R., Borok, E., Horvath, T. L., and Nedivi, E. (2004). *CPG2: a brain- and synapse-specific protein that regulates the endocytosis of glutamate receptors*. Neuron *44*, 677-690.

Crisp, M., Liu, Q., Roux, K., Rattner, J. B., Shanahan, C., Burke, B., Stahl, P. D., and Hodzic, D. (2006). *Coupling of the nucleus and cytoplasm: role of the LINC complex*. J Cell Biol *172*, 41-53.

de Boer, J., and Hoeijmakers, J. H. (2000). *Nucleotide excision repair and human syndromes*. Carcinogenesis *21*, 453-460.

Di Micco, R., Fumagalli, M., Cicalese, A., Piccinin, S., Gasparini, P., Luise, C., Schurra, C., Garre, M., Nuciforo, P. G., Bensimon, A., Maestro, R., Pelicci, P. G., and d'Adda di Fagagna, F. (2006). *Oncogene-induced senescence is a DNA damage response triggered by DNA hyper-replication*. Nature *444*, 638-642.

Difilippantonio, M. J., Zhu, J., Chen, H. T., Meffre, E., Nussenzweig, M. C., Max, E. E., Ried, T., and Nussenzweig, A. (2000). *DNA repair protein Ku80 suppresses chromosomal aberrations and malignant transformation*. Nature *404*, 510-514.

Djinovic-Carugo, K., Gautel, M., Ylanne, J., and Young, P. (2002). *The spectrin repeat: a structural platform for cytoskeletal protein assemblies*. FEBS Lett *513*, 119-123.

Doherty, J. A., Rossing, M. A., Cushing-Haugen, K. L., Chen, C., Van Den Berg, D. J., Wu, A. H., Pike, M. C., Ness, R. B., Moysich, K., Chenevix-Trench, G., Beesley, J., Webb, P. M., Chang-Claude, J., Wang-Gohrke, S., Goodman, M. T., Lurie, G., Thompson, P. J., Carney, M. E., Hogdall, E., Kjaer, S. K., Hogdall, C., Goode, E. L., Cunningham, J. M., Fridley, B. L., Vierkant, R. A., Berchuck, A., Moorman, P. G., Schildkraut, J. M., Palmieri, R. T., Cramer, D. W., Terry, K. L., Yang, H. P., Garcia-Closas, M., Chanock, S., Lissowska, J., Song, H., Pharoah, P. D., Shah, M., Perkins, B., McGuire, V., Whittemore, A. S., Di Cioccio, R. A., Gentry-Maharaj, A., Menon, U., Gayther, S. A., Ramus, S. J., Ziogas, A., Brewster, W., Anton-Culver, H., Australian Ovarian Cancer Study Management, G., Australian Cancer, S., Pearce, C. L., and Ovarian Cancer Association, C. (2010). *ESR1/SYNE1 polymorphism and invasive epithelial ovarian cancer risk: an Ovarian Cancer Association Consortium study*. Cancer Epidemiol Biomarkers Prev *19*, 245-250.

Doring, T., Greuer, B., and Brimacombe, R. (1991). *The three-dimensional folding of ribosomal RNA; localization of a series of intra-RNA cross-links in 23S RNA induced by treatment of Escherichia coli 50S ribosomal subunits with bis-(2-chloroethyl)-methylamine*. Nucleic Acids Res *19*, 3517-3524.

Dou, Y., Milne, T. A., Tackett, A. J., Smith, E. R., Fukuda, A., Wysocka, J., Allis, C. D., Chait, B. T., Hess, J. L., and Roeder, R. G. (2005). *Physical association and coordinate function of the H3 K4 methyltransferase MLL1 and the H4 K16 acetyltransferase MOF*. Cell *121*, 873-885.

Downs, J. A., and Jackson, S. P. (2004). *A means to a DNA end: the many roles of Ku*. Nat Rev Mol Cell Biol *5*, 367-378.

Fukasawa, K. (2005). *Centrosome amplification, chromosome instability and cancer development*. Cancer Lett *230*, 6-19.

Furukawa, K., and Hotta, Y. (1993). *cDNA cloning of a germ cell specific lamin B3 from mouse spermatocytes and analysis of its function by ectopic expression in somatic cells*. EMBO J *12*, 97-106.

Gazzoli, I., Loda, M., Garber, J., Syngal, S., and Kolodner, R. D. (2002). *A hereditary nonpolyposis colorectal carcinoma case associated with hypermethylation of the MLH1 gene in normal tissue and loss of heterozygosity of the unmethylated*

allele in the resulting microsatellite instability-high tumor. Cancer Res *62*, 3925-3928.

Gerace, L., Blum, A., and Blobel, G. (1978). *Immunocytochemical localization of the major polypeptides of the nuclear pore complex-lamina fraction. Interphase and mitotic distribution*. J Cell Biol *79*, 546-566.

Gillet, L. C., and Scharer, O. D. (2006). *Molecular mechanisms of mammalian global genome nucleotide excision repair*. Chem Rev *106*, 253-276.

Gough, L. L., and Beck, K. A. (2004). *The spectrin family member Syne-1 functions in retrograde transport from Golgi to ER*. Biochim Biophys Acta *1693*, 29-36.

Gough, L. L., Fan, J., Chu, S., Winnick, S., and Beck, K. A. (2003). *Golgi localization of Syne-1*. Mol Biol Cell *14*, 2410-2424.

Gould, V. E., Orucevic, A., Zentgraf, H., Gattuso, P., Martinez, N., and Alonso, A. (2002). *Nup88 (karyoporin) in human malignant neoplasms and dysplasias: correlations of immunostaining of tissue sections, cytologic smears, and immunoblot analysis*. Hum Pathol *33*, 536-544.

Grady, R. M., Starr, D. A., Ackerman, G. L., Sanes, J. R., and Han, M. (2005). *Syne proteins anchor muscle nuclei at the neuromuscular junction*. Proc Natl Acad Sci U S A *102*, 4359-4364.

Graumann, K., and Evans, D. E. (2010). *Plant SUN domain proteins: components of putative plant LINC complexes?* Plant Signal Behav *5*, 154-156.

Gros-Louis, F., Dupre, N., Dion, P., Fox, M. A., Laurent, S., Verreault, S., Sanes, J. R., Bouchard, J. P., and Rouleau, G. A. (2007). *Mutations in SYNE1 lead to a newly discovered form of autosomal recessive cerebellar ataxia*. Nat Genet *39*, 80-85.

Guidos, C. J., Williams, C. J., Grandal, I., Knowles, G., Huang, M. T., and Danska, J. S. (1996). *V(D)J recombination activates a p53-dependent DNA damage checkpoint in scid lymphocyte precursors*. Genes Dev *10*, 2038-2054.

Habraken, Y., Sung, P., Prakash, L., and Prakash, S. (1996). *Binding of insertion/deletion DNA mismatches by the heterodimer of yeast mismatch repair proteins MSH2 and MSH3*. Curr Biol *6*, 1185-1187.

Hajdu, I., Ciccia, A., Lewis, S. M., and Elledge, S. J. (2011). *Wolf-Hirschhorn syndrome candidate 1 is involved in the cellular response to DNA damage*. Proc Natl Acad Sci U S A *108*, 13130-13134.

Hanawalt, P. C. (2002). *Subpathways of nucleotide excision repair and their regulation*. Oncogene *21*, 8949-8956.

Haque, F., Lloyd, D. J., Smallwood, D. T., Dent, C. L., Shanahan, C. M., Fry, A. M., Trembath, R. C., and Shackleton, S. (2006). *SUN1 interacts with nuclear lamin A and cytoplasmic nesprins to provide a physical connection between the nuclear lamina and the cytoskeleton*. Mol Cell Biol *26*, 3738-3751.

Hartlerode, A. J., and Scully, R. (2009). *Mechanisms of double-strand break repair in somatic mammalian cells*. Biochem J *423*, 157-168.

Hassold, T., Hall, H., and Hunt, P. (2007). *The origin of human aneuploidy: where we have been, where we are going*. Hum Mol Genet *16 Spec No. 2*, R203-208.

Hayflick, L. (1965). *The Limited in Vitro Lifetime of Human Diploid Cell Strains*. Exp Cell Res *37*, 614-636.

Hetzer, M. W., Walther, T. C., and Mattaj, I. W. (2005). *Pushing the envelope: structure, function, and dynamics of the nuclear periphery*. Annu Rev Cell Dev Biol *21*, 347-380.

Holaska, J. M., Kowalski, A. K., and Wilson, K. L. (2004). *Emerin caps the pointed end of actin filaments: evidence for an actin cortical network at the nuclear inner membrane*. PLoS Biol *2*, E231.

Horn, H. F., Brownstein, Z., Lenz, D. R., Shivatzki, S., Dror, A. A., Dagan-Rosenfeld, O., Friedman, L. M., Roux, K. J., Kozlov, S., Jeang, K. T., Frydman, M., Burke, B., Stewart, C. L., and Avraham, K. B. (2013). *The LINC complex is essential for hearing*. J Clin Invest *123*, 740-750.

Iaccarino, I., Palombo, F., Drummond, J., Totty, N. F., Hsuan, J. J., Modrich, P., and Jiricny, J. (1996). *MSH6, a Saccharomyces cerevisiae protein that binds to mismatches as a heterodimer with MSH2*. Curr Biol *6*, 484-486.

Jacob, S., and Praz, F. (2002). *DNA mismatch repair defects: role in colorectal carcinogenesis*. Biochimie *84*, 27-47.

Kandert, S., Luke, Y., Kleinhenz, T., Neumann, S., Lu, W., Jaeger, V. M., Munck, M., Wehnert, M., Muller, C. R., Zhou, Z., Noegel, A. A., Dabauvalle, M. C., and Karakesisoglou, I. (2007). *Nesprin-2 giant safeguards nuclear envelope architecture in LMNA S143F progeria cells*. Hum Mol Genet *16*, 2944-2959.

Kastan, M. B., and Lim, D. S. (2000). *The many substrates and functions of ATM*. Nat Rev Mol Cell Biol *1*, 179-186.

Khatau, S. B., Bloom, R. J., Bajpai, S., Razafsky, D., Zang, S., Giri, A., Wu, P. H., Marchand, J., Celedon, A., Hale, C. M., Sun, S. X., Hodzic, D., and Wirtz, D. (2012). *The distinct roles of the nucleus and nucleus-cytoskeleton connections in three-dimensional cell migration*. Sci Rep *2*, 488.

Khatau, S. B., Hale, C. M., Stewart-Hutchinson, P. J., Patel, M. S., Stewart, C. L., Searson, P. C., Hodzic, D., and Wirtz, D. (2009). *A perinuclear actin cap regulates nuclear shape*. Proc Natl Acad Sci U S A *106*, 19017-19022.

Kilmartin, J. V., Wright, B., and Milstein, C. (1982). *Rat monoclonal antitubulin antibodies derived by using a new nonsecreting rat cell line*. J Cell Biol *93*, 576-582.

Knoess, M., Kurz, A. K., Goreva, O., Bektas, N., Breuhahn, K., Odenthal, M., Schirmacher, P., Dienes, H. P., Bock, C. T., Zentgraf, H., and zur Hausen, A.

(2006). *Nucleoporin 88 expression in hepatitis B and C virus-related liver diseases*. World J Gastroenterol *12*, 5870-5874.

Kobayashi, Y., Katanosaka, Y., Iwata, Y., Matsuoka, M., Shigekawa, M., and Wakabayashi, S. (2006). *Identification and characterization of GSRP-56, a novel Golgi-localized spectrin repeat-containing protein*. Exp Cell Res *312*, 3152-3164.

Kolodner, R. (1996). *Biochemistry and genetics of eukaryotic mismatch repair*. Genes Dev *10*, 1433-1442.

Kulaksiz, G., Reardon, J. T., and Sancar, A. (2005). *Xeroderma pigmentosum complementation group E protein (XPE/DDB2): purification of various complexes of XPE and analyses of their damaged DNA binding and putative DNA repair properties*. Mol Cell Biol *25*, 9784-9792.

Kumaran, R. I., Muralikrishna, B., and Parnaik, V. K. (2002). *Lamin A/C speckles mediate spatial organization of splicing factor compartments and RNA polymerase II transcription*. J Cell Biol *159*, 783-793.

Kunkel, T. A., and Erie, D. A. (2005). *DNA mismatch repair*. Annu Rev Biochem *74*, 681-710.

La Porta, C. A., Zapperi, S., and Sethna, J. P. (2012). *Senescent cells in growing tumors: population dynamics and cancer stem cells*. PLoS Comput Biol *8*, e1002316.

Laguri, C., Gilquin, B., Wolff, N., Romi-Lebrun, R., Courchay, K., Callebaut, I., Worman, H. J., and Zinn-Justin, S. (2001). *Structural characterization of the LEM motif common to three human inner nuclear membrane proteins*. Structure *9*, 503-511.

Lamers, M. H., Perrakis, A., Enzlin, J. H., Winterwerp, H. H., de Wind, N., and Sixma, T. K. (2000). *The crystal structure of DNA mismatch repair protein MutS binding to a G x T mismatch*. Nature *407*, 711-717.

Lammerding, J., Hsiao, J., Schulze, P. C., Kozlov, S., Stewart, C. L., and Lee, R. T. (2005). *Abnormal nuclear shape and impaired mechanotransduction in emerin-deficient cells*. J Cell Biol *170*, 781-791.

Lammerding, J., Schulze, P. C., Takahashi, T., Kozlov, S., Sullivan, T., Kamm, R. D., Stewart, C. L., and Lee, R. T. (2004). *Lamin A/C deficiency causes defective nuclear mechanics and mechanotransduction*. J Clin Invest *113*, 370-378.

Lavin, M. F., and Kozlov, S. (2007). *ATM activation and DNA damage response*. Cell Cycle *6*, 931-942.

Le Dour, C., Schneebeli, S., Bakiri, F., Darcel, F., Jacquemont, M. L., Maubert, M. A., Auclair, M., Jeziorowska, D., Reznik, Y., Bereziat, V., Capeau, J., Lascols, O., and Vigouroux, C. (2011). *A homozygous mutation of prelamin-A preventing its farnesylation and maturation leads to a severe lipodystrophic phenotype: new insights into the pathogenicity of nonfarnesylated prelamin-A*. J Clin Endocrinol Metab *96*, E856-862.

Lei, K., Zhu, X., Xu, R., Shao, C., Xu, T., Zhuang, Y., and Han, M. (2012). *Inner nuclear envelope proteins SUN1 and SUN2 play a prominent role in the DNA damage response*. Curr Biol *22*, 1609-1615.

Li, F., Mao, G., Tong, D., Huang, J., Gu, L., Yang, W., and Li, G. M. (2013). *The histone mark H3K36me3 regulates human DNA mismatch repair through its interaction with MutSalpha*. Cell *153*, 590-600.

Liang, F., and Jasin, M. (1996). *Ku80-deficient cells exhibit excess degradation of extrachromosomal DNA*. J Biol Chem *271*, 14405-14411.

Libotte, T., Zaim, H., Abraham, S., Padmakumar, V. C., Schneider, M., Lu, W., Munck, M., Hutchison, C., Wehnert, M., Fahrenkrog, B., Sauder, U., Aebi, U., Noegel, A. A., and Karakesisoglou, I. (2005). *Lamin A/C-dependent localization of Nesprin-2, a giant scaffolder at the nuclear envelope*. Mol Biol Cell *16*, 3411-3424.

Lim, D. S., Vogel, H., Willerford, D. M., Sands, A. T., Platt, K. A., and Hasty, P. (2000). *Analysis of ku80-mutant mice and cells with deficient levels of p53*. Mol Cell Biol *20*, 3772-3780.

Lim, S. O., Park, S. J., Kim, W., Park, S. G., Kim, H. J., Kim, Y. I., Sohn, T. S., Noh, J. H., and Jung, G. (2002). *Proteome analysis of hepatocellular carcinoma*. Biochem Biophys Res Commun *291*, 1031-1037.

Lin, F., Blake, D. L., Callebaut, I., Skerjanc, I. S., Holmer, L., McBurney, M. W., Paulin-Levasseur, M., and Worman, H. J. (2000). *MAN1, an inner nuclear membrane protein that shares the LEM domain with lamina-associated polypeptide 2 and emerin*. J Biol Chem *275*, 4840-4847.

Lingle, W. L., and Salisbury, J. L. (2001). *Methods for the analysis of centrosome reproduction in cancer cells*. Methods Cell Biol *67*, 325-336.

Lipkin, S. M., Wang, V., Jacoby, R., Banerjee-Basu, S., Baxevanis, A. D., Lynch, H. T., Elliott, R. M., and Collins, F. S. (2000). *MLH3: a DNA mismatch repair gene associated with mammalian microsatellite instability*. Nat Genet *24*, 27-35.

Liu, J., Lee, K. K., Segura-Totten, M., Neufeld, E., Wilson, K. L., and Gruenbaum, Y. (2003). *MAN1 and emerin have overlapping function(s) essential for chromosome segregation and cell division in Caenorhabditis elegans*. Proc Natl Acad Sci U S A *100*, 4598-4603.

Liu, Q., Guntuku, S., Cui, X. S., Matsuoka, S., Cortez, D., Tamai, K., Luo, G., Carattini-Rivera, S., DeMayo, F., Bradley, A., Donehower, L. A., and Elledge, S. J. (2000). *Chk1 is an essential kinase that is regulated by Atr and required for the G(2)/M DNA damage checkpoint*. Genes Dev *14*, 1448-1459.

Lu, W., Schneider, M., Neumann, S., Jaeger, V. M., Taranum, S., Munck, M., Cartwright, S., Richardson, C., Carthew, J., Noh, K., Goldberg, M., Noegel, A. A., and Karakesisoglou, I. (2012). *Nesprin interchain associations control nuclear size*. Cell Mol Life Sci *69*, 3493-3509.

Luke, Y., Zaim, H., Karakesisoglou, I., Jaeger, V. M., Sellin, L., Lu, W., Schneider, M., Neumann, S., Beijer, A., Munck, M., Padmakumar, V. C., Gloy, J., Walz, G., and Noegel, A. A. (2008). *Nesprin-2 Giant (NUANCE) maintains nuclear envelope architecture and composition in skin*. J Cell Sci *121*, 1887-1898.

Mahaney, B. L., Meek, K., and Lees-Miller, S. P. (2009). *Repair of ionizing radiation-induced DNA double-strand breaks by non-homologous end-joining*. Biochem J *417*, 639-650.

Maraldi, N. M., Lattanzi, G., Cenni, V., Bavelloni, A., Marmiroli, S., and Manzoli, F. A. (2010). *Laminopathies and A-type lamin-associated signalling pathways*. Adv Enzyme Regul *50*, 248-261.

Markiewicz, E., Tilgner, K., Barker, N., van de Wetering, M., Clevers, H., Dorobek, M., Hausmanowa-Petrusewicz, I., Ramaekers, F. C., Broers, J. L., Blankesteijn, W. M., Salpingidou, G., Wilson, R. G., Ellis, J. A., and Hutchison, C. J. (2006). *The inner nuclear membrane protein emerin regulates beta-catenin activity by restricting its accumulation in the nucleus*. EMBO J *25*, 3275-3285.

Marme, A., Zimmermann, H. P., Moldenhauer, G., Schorpp-Kistner, M., Muller, C., Keberlein, O., Giersch, A., Kretschmer, J., Seib, B., Spiess, E., Hunziker, A., Merchan, F., Moller, P., Hahn, U., Kurek, R., Marme, F., Bastert, G., Wallwiener, D., and Ponstingl, H. (2008). *Loss of Drop1 expression already at early tumor stages in a wide range of human carcinomas*. Int J Cancer *123*, 2048-2056.

Marsischky, G. T., Filosi, N., Kane, M. F., and Kolodner, R. (1996). *Redundancy of Saccharomyces cerevisiae MSH3 and MSH6 in MSH2-dependent mismatch repair*. Genes Dev *10*, 407-420.

Marti, T. M., Hefner, E., Feeney, L., Natale, V., and Cleaver, J. E. (2006). *H2AX phosphorylation within the G1 phase after UV irradiation depends on nucleotide excision repair and not DNA double-strand breaks*. Proc Natl Acad Sci U S A *103*, 9891-9896.

Martin, A., and Scharff, M. D. (2002). *AID and mismatch repair in antibody diversification*. Nat Rev Immunol *2*, 605-614.

Martinez, N., Alonso, A., Moragues, M. D., Ponton, J., and Schneider, J. (1999). *The nuclear pore complex protein Nup88 is overexpressed in tumor cells*. Cancer Res *59*, 5408-5411.

Masica, D. L., and Karchin, R. (2011). *Correlation of somatic mutation and expression identifies genes important in human glioblastoma progression and survival*. Cancer Res *71*, 4550-4561.

McKeon, F. D., Kirschner, M. W., and Caput, D. (1986). *Homologies in both primary and secondary structure between nuclear envelope and intermediate filament proteins*. Nature *319*, 463-468.

Mejat, A., and Misteli, T. (2010). *LINC complexes in health and disease*. Nucleus *1*, 40-52.

Melis, J. P., Luijten, M., Mullenders, L. H., and van Steeg, H. (2011). *The role of XPC: implications in cancer and oxidative DNA damage*. Mutat Res *728*, 107-117.

Mellad, J. A., Warren, D. T., and Shanahan, C. M. (2011). *Nesprins LINC the nucleus and cytoskeleton*. Curr Opin Cell Biol *23*, 47-54.

Mellon, I., Spivak, G., and Hanawalt, P. C. (1987). *Selective removal of transcription-blocking DNA damage from the transcribed strand of the mammalian DHFR gene*. Cell *51*, 241-249.

Mislow, J. M., Holaska, J. M., Kim, M. S., Lee, K. K., Segura-Totten, M., Wilson, K. L., and McNally, E. M. (2002a). *Nesprin-1alpha self-associates and binds directly to emerin and lamin A in vitro*. FEBS Lett *525*, 135-140.

Mislow, J. M., Kim, M. S., Davis, D. B., and McNally, E. M. (2002b). *Myne-1, a spectrin repeat transmembrane protein of the myocyte inner nuclear membrane, interacts with lamin A/C*. J Cell Sci *115*, 61-70.

Modrich, P., and Lahue, R. (1996). *Mismatch repair in replication fidelity, genetic recombination, and cancer biology*. Annu Rev Biochem *65*, 101-133.

Moir, R. D., Spann, T. P., Herrmann, H., and Goldman, R. D. (2000). *Disruption of nuclear lamin organization blocks the elongation phase of DNA replication*. J Cell Biol *149*, 1179-1192.

Morgan, J. T., Pfeiffer, E. R., Thirkill, T. L., Kumar, P., Peng, G., Fridolfsson, H. N., Douglas, G. C., Starr, D. A., and Barakat, A. I. (2011). *Nesprin-3 regulates endothelial cell morphology, perinuclear cytoskeletal architecture, and flow-induced polarization*. Mol Biol Cell *22*, 4324-4334.

Moss, S. F., Krivosheyev, V., de Souza, A., Chin, K., Gaetz, H. P., Chaudhary, N., Worman, H. J., and Holt, P. R. (1999). *Decreased and aberrant nuclear lamin expression in gastrointestinal tract neoplasms*. Gut *45*, 723-729.

Nacht, M., Strasser, A., Chan, Y. R., Harris, A. W., Schlissel, M., Bronson, R. T., and Jacks, T. (1996). *Mutations in the p53 and SCID genes cooperate in tumorigenesis*. Genes Dev *10*, 2055-2066.

Nedivi, E., Fieldust, S., Theill, L. E., and Hevron, D. (1996). *A set of genes expressed in response to light in the adult cerebral cortex and regulated during development*. Proc Natl Acad Sci U S A *93*, 2048-2053.

Nicolaides, N. C., Papadopoulos, N., Liu, B., Wei, Y. F., Carter, K. C., Ruben, S. M., Rosen, C. A., Haseltine, W. A., Fleischmann, R. D., Fraser, C. M., and et al. (1994). *Mutations of two PMS homologues in hereditary nonpolyposis colon cancer*. Nature *371*, 75-80.

Nigg, E. A. (2006). *Origins and consequences of centrosome aberrations in human cancers*. Int J Cancer *119*, 2717-2723.

Nili, E., Cojocaru, G. S., Kalma, Y., Ginsberg, D., Copeland, N. G., Gilbert, D. J., Jenkins, N. A., Berger, R., Shaklai, S., Amariglio, N., Brok-Simoni, F., Simon, A.

J., and Rechavi, G. (2001). *Nuclear membrane protein LAP2beta mediates transcriptional repression alone and together with its binding partner GCL (germ-cell-less).* J Cell Sci *114*, 3297-3307.

Noegel, A., Witke, W., and Schleicher, M. (1987). *Calcium-sensitive non-muscle alpha-actinin contains EF-hand structures and highly conserved regions.* FEBS Lett *221*, 391-396.

Noegel, A. A., Blau-Wasser, R., Sultana, H., Muller, R., Israel, L., Schleicher, M., Patel, H., and Weijer, C. J. (2004). *The cyclase-associated protein CAP as regulator of cell polarity and cAMP signaling in Dictyostelium.* Mol Biol Cell *15*, 934-945.

Obmolova, G., Ban, C., Hsieh, P., and Yang, W. (2000). *Crystal structures of mismatch repair protein MutS and its complex with a substrate DNA.* Nature *407*, 703-710.

Oza, P., Jaspersen, S. L., Miele, A., Dekker, J., and Peterson, C. L. (2009). *Mechanisms that regulate localization of a DNA double-strand break to the nuclear periphery.* Genes Dev *23*, 912-927.

Paddison, P. J., Caudy, A. A., Bernstein, E., Hannon, G. J., and Conklin, D. S. (2002). *Short hairpin RNAs (shRNAs) induce sequence-specific silencing in mammalian cells.* Genes Dev *16*, 948-958.

Padmakumar, V. C., Abraham, S., Braune, S., Noegel, A. A., Tunggal, B., Karakesisoglou, I., and Korenbaum, E. (2004). *Enaptin, a giant actin-binding protein, is an element of the nuclear membrane and the actin cytoskeleton.* Exp Cell Res *295*, 330-339.

Padmakumar, V. C., Libotte, T., Lu, W., Zaim, H., Abraham, S., Noegel, A. A., Gotzmann, J., Foisner, R., and Karakesisoglou, I. (2005). *The inner nuclear membrane protein Sun1 mediates the anchorage of Nesprin-2 to the nuclear envelope.* J Cell Sci *118*, 3419-3430.

Palombo, F., Iaccarino, I., Nakajima, E., Ikejima, M., Shimada, T., and Jiricny, J. (1996). *hMutSbeta, a heterodimer of hMSH2 and hMSH3, binds to insertion/deletion loops in DNA.* Curr Biol *6*, 1181-1184.

Pan, D., Estevez-Salmeron, L. D., Stroschein, S. L., Zhu, X., He, J., Zhou, S., and Luo, K. (2005). *The integral inner nuclear membrane protein MAN1 physically interacts with the R-Smad proteins to repress signaling by the transforming growth factor-{beta} superfamily of cytokines.* J Biol Chem *280*, 15992-16001.

Pang, Q., Prolla, T. A., and Liskay, R. M. (1997). *Functional domains of the Saccharomyces cerevisiae Mlh1p and Pms1p DNA mismatch repair proteins and their relevance to human hereditary nonpolyposis colorectal cancer-associated mutations.* Mol Cell Biol *17*, 4465-4473.

Papadopoulos, N., Nicolaides, N. C., Wei, Y. F., Ruben, S. M., Carter, K. C., Rosen, C. A., Haseltine, W. A., Fleischmann, R. D., Fraser, C. M., Adams, M. D., and et al. (1994). *Mutation of a mutL homolog in hereditary colon cancer.* Science *263*, 1625-1629.

Peters, A. C., Young, L. C., Maeda, T., Tron, V. A., and Andrew, S. E. (2003). *Mammalian DNA mismatch repair protects cells from UVB-induced DNA damage by facilitating apoptosis and p53 activation*. DNA Repair (Amst) *2*, 427-435.

Plaschke, J., Linnebacher, M., Kloor, M., Gebert, J., Cremer, F. W., Tinschert, S., Aust, D. E., von Knebel Doeberitz, M., and Schackert, H. K. (2006). *Compound heterozygosity for two MSH6 mutations in a patient with early onset of HNPCC-associated cancers, but without hematological malignancy and brain tumor*. Eur J Hum Genet *14*, 561-566.

Postel, R., Ketema, M., Kuikman, I., de Pereda, J. M., and Sonnenberg, A. (2011). *Nesprin-3 augments peripheral nuclear localization of intermediate filaments in zebrafish*. J Cell Sci *124*, 755-764.

Prolla, T. A., Pang, Q., Alani, E., Kolodner, R. D., and Liskay, R. M. (1994). *MLH1, PMS1, and MSH2 interactions during the initiation of DNA mismatch repair in yeast*. Science *265*, 1091-1093.

Puckelwartz, M. J., Kessler, E., Zhang, Y., Hodzic, D., Randles, K. N., Morris, G., Earley, J. U., Hadhazy, M., Holaska, J. M., Mewborn, S. K., Pytel, P., and McNally, E. M. (2009). *Disruption of nesprin-1 produces an Emery Dreifuss muscular dystrophy-like phenotype in mice*. Hum Mol Genet *18*, 607-620.

Raffaele Di Barletta, M., Ricci, E., Galluzzi, G., Tonali, P., Mora, M., Morandi, L., Romorini, A., Voit, T., Orstavik, K. H., Merlini, L., Trevisan, C., Biancalana, V., Housmanowa-Petrusewicz, I., Bione, S., Ricotti, R., Schwartz, K., Bonne, G., and Toniolo, D. (2000). *Different mutations in the LMNA gene cause autosomal dominant and autosomal recessive Emery-Dreifuss muscular dystrophy*. Am J Hum Genet *66*, 1407-1412.

Rajgor, D., Mellad, J. A., Autore, F., Zhang, Q., and Shanahan, C. M. (2012). *Multiple novel nesprin-1 and nesprin-2 variants act as versatile tissue-specific intracellular scaffolds*. PLoS One *7*, e40098.

Riches, L. C., Lynch, A. M., and Gooderham, N. J. (2008). *Early events in the mammalian response to DNA double-strand breaks*. Mutagenesis *23*, 331-339.

Riha, K., Heacock, M. L., and Shippen, D. E. (2006). *The role of the nonhomologous end-joining DNA double-strand break repair pathway in telomere biology*. Annu Rev Genet *40*, 237-277.

Rodier, F., and Campisi, J. (2011). *Four faces of cellular senescence*. J Cell Biol *192*, 547-556.

Rosenberg-Hasson, Y., Renert-Pasca, M., and Volk, T. (1996). *A Drosophila dystrophin-related protein, MSP-300, is required for embryonic muscle morphogenesis*. Mech Dev *60*, 83-94.

Rothballer, A., Schwartz, T. U., and Kutay, U. (2013). *LINCing complex functions at the nuclear envelope: what the molecular architecture of the LINC complex can reveal about its function*. Nucleus *4*, 29-36.

Roux, K. J., Crisp, M. L., Liu, Q., Kim, D., Kozlov, S., Stewart, C. L., and Burke, B. (2009). *Nesprin 4 is an outer nuclear membrane protein that can induce kinesin-mediated cell polarization*. Proc Natl Acad Sci U S A *106*, 2194-2199.

Sahai, E., Garcia-Medina, R., Pouyssegur, J., and Vial, E. (2007). *Smurf1 regulates tumor cell plasticity and motility through degradation of RhoA leading to localized inhibition of contractility*. J Cell Biol *176*, 35-42.

Salisbury, J. L. (2005). *On the origin of centrosome amplification and chromosomal instability in cancer*. Microsc Microanal *11 Suppl 2*, 1002-1003.

Salpingidou, G., Smertenko, A., Hausmanowa-Petrucewicz, I., Hussey, P. J., and Hutchison, C. J. (2007). *A novel role for the nuclear membrane protein emerin in association of the centrosome to the outer nuclear membrane*. J Cell Biol *178*, 897-904.

Schirmer, E. C., Florens, L., Guan, T., Yates, J. R., 3rd, and Gerace, L. (2003). *Nuclear membrane proteins with potential disease links found by subtractive proteomics*. Science *301*, 1380-1382.

Schirmer, E. C., Guan, T., and Gerace, L. (2001). *Involvement of the lamin rod domain in heterotypic lamin interactions important for nuclear organization*. J Cell Biol *153*, 479-489.

Schneider, J., Martinez-Arribas, F., and Torrejon, R. (2010). *Nup88 expression is associated with myometrial invasion in endometrial carcinoma*. Int J Gynecol Cancer *20*, 804-808.

Schneider, M., Lu, W., Neumann, S., Brachner, A., Gotzmann, J., Noegel, A. A., and Karakesisoglou, I. (2011a). *Molecular mechanisms of centrosome and cytoskeleton anchorage at the nuclear envelope*. Cell Mol Life Sci *68*, 1593-1610.

Schneider, M., Noegel, A. A., and Karakesisoglou, I. (2008). *KASH-domain proteins and the cytoskeletal landscapes of the nuclear envelope*. Biochem Soc Trans *36*, 1368-1372.

Schneider, M. A., Spoden, G. A., Florin, L., and Lambert, C. (2011b). *Identification of the dynein light chains required for human papillomavirus infection*. Cell Microbiol *13*, 32-46.

Schofield, M. J., and Hsieh, P. (2003). *DNA mismatch repair: molecular mechanisms and biological function*. Annu Rev Microbiol *57*, 579-608.

Schreiber, K. H., and Kennedy, B. K. (2013). *When lamins go bad: nuclear structure and disease*. Cell *152*, 1365-1375.

Schuebel, K. E., Chen, W., Cope, L., Glockner, S. C., Suzuki, H., Yi, J. M., Chan, T. A., Van Neste, L., Van Criekinge, W., van den Bosch, S., van Engeland, M., Ting, A. H., Jair, K., Yu, W., Toyota, M., Imai, K., Ahuja, N., Herman, J. G., and Baylin, S. B. (2007). *Comparing the DNA hypermethylome with gene mutations in human colorectal cancer*. PLoS Genet *3*, 1709-1723.

Schulz, I., Baumann, O., Samereier, M., Zoglmeier, C., and Graf, R. (2009). *Dictyostelium Sun1 is a dynamic membrane protein of both nuclear membranes and required for centrosomal association with clustered centromeres*. Eur J Cell Biol *88*, 621-638.

Shahi, A., Lee, J. H., Kang, Y., Lee, S. H., Hyun, J. W., Chang, I. Y., Jun, J. Y., and You, H. J. (2011). *Mismatch-repair protein MSH6 is associated with Ku70 and regulates DNA double-strand break repair*. Nucleic Acids Res *39*, 2130-2143.

Sharpless, N. E., Ferguson, D. O., O'Hagan, R. C., Castrillon, D. H., Lee, C., Farazi, P. A., Alson, S., Fleming, J., Morton, C. C., Frank, K., Chin, L., Alt, F. W., and DePinho, R. A. (2001). *Impaired nonhomologous end-joining provokes soft tissue sarcomas harboring chromosomal translocations, amplifications, and deletions*. Mol Cell *8*, 1187-1196.

Sherr, C. J. (2004). *Principles of tumor suppression*. Cell *116*, 235-246.

Shimi, T., Butin-Israeli, V., and Goldman, R. D. (2012). *The functions of the nuclear envelope in mediating the molecular crosstalk between the nucleus and the cytoplasm*. Curr Opin Cell Biol *24*, 71-78.

Shumaker, D. K., Lee, K. K., Tanhehco, Y. C., Craigie, R., and Wilson, K. L. (2001). *LAP2 binds to BAF.DNA complexes: requirement for the LEM domain and modulation by variable regions*. EMBO J *20*, 1754-1764.

Sjoblom, T., Jones, S., Wood, L. D., Parsons, D. W., Lin, J., Barber, T. D., Mandelker, D., Leary, R. J., Ptak, J., Silliman, N., Szabo, S., Buckhaults, P., Farrell, C., Meeh, P., Markowitz, S. D., Willis, J., Dawson, D., Willson, J. K., Gazdar, A. F., Hartigan, J., Wu, L., Liu, C., Parmigiani, G., Park, B. H., Bachman, K. E., Papadopoulos, N., Vogelstein, B., Kinzler, K. W., and Velculescu, V. E. (2006). *The consensus coding sequences of human breast and colorectal cancers*. Science *314*, 268-274.

Somech, R., Gal-Yam, E. N., Shaklai, S., Geller, O., Amariglio, N., Rechavi, G., and Simon, A. J. (2007). *Enhanced expression of the nuclear envelope LAP2 transcriptional repressors in normal and malignant activated lymphocytes*. Ann Hematol *86*, 393-401.

Sosa, B. A., Rothballer, A., Kutay, U., and Schwartz, T. U. (2012). *LINC complexes form by binding of three KASH peptides to domain interfaces of trimeric SUN proteins*. Cell *149*, 1035-1047.

Squarzoni, S., Sabatelli, P., Ognibene, A., Toniolo, D., Cartegni, L., Cobianchi, F., Petrini, S., Merlini, L., and Maraldi, N. M. (1998). *Immunocytochemical detection of emerin within the nuclear matrix*. Neuromuscul Disord *8*, 338-344.

Starr, D. A., and Fridolfsson, H. N. (2010). *Interactions between nuclei and the cytoskeleton are mediated by SUN-KASH nuclear-envelope bridges*. Annu Rev Cell Dev Biol *26*, 421-444.

Starr, D. A., and Han, M. (2002). *Role of ANC-1 in tethering nuclei to the actin cytoskeleton*. Science *298*, 406-409.

Stewart-Hutchinson, P. J., Hale, C. M., Wirtz, D., and Hodzic, D. (2008). *Structural requirements for the assembly of LINC complexes and their function in cellular mechanical stiffness*. Exp Cell Res *314*, 1892-1905.

Sun, J., Lee, K. J., Davis, A. J., and Chen, D. J. (2012). *Human Ku70/80 protein blocks exonuclease 1-mediated DNA resection in the presence of human Mre11 or Mre11/Rad50 protein complex*. J Biol Chem *287*, 4936-4945.

Sun, S., Xu, M. Z., Poon, R. T., Day, P. J., and Luk, J. M. (2010). *Circulating Lamin B1 (LMNB1) biomarker detects early stages of liver cancer in patients*. J Proteome Res *9*, 70-78.

Taranum, S., Sur, I., Muller, R., Lu, W., Rashmi, R. N., Munck, M., Neumann, S., Karakesisoglou, I., and Noegel, A. A. (2012a). *Cytoskeletal interactions at the nuclear envelope mediated by nesprins*. Int J Cell Biol *2012*, 736524.

Taranum, S., Vaylann, E., Meinke, P., Abraham, S., Yang, L., Neumann, S., Karakesisoglou, I., Wehnert, M., and Noegel, A. A. (2012b). *LINC complex alterations in DMD and EDMD/CMT fibroblasts*. Eur J Cell Biol *91*, 614-628.

Tessema, M., Willink, R., Do, K., Yu, Y. Y., Yu, W., Machida, E. O., Brock, M., Van Neste, L., Stidley, C. A., Baylin, S. B., and Belinsky, S. A. (2008). *Promoter methylation of genes in and around the candidate lung cancer susceptibility locus 6q23-25*. Cancer Res *68*, 1707-1714.

Therizols, P., Fairhead, C., Cabal, G. G., Genovesio, A., Olivo-Marin, J. C., Dujon, B., and Fabre, E. (2006). *Telomere tethering at the nuclear periphery is essential for efficient DNA double strand break repair in subtelomeric region*. J Cell Biol *172*, 189-199.

Trego, K. S., and Turchi, J. J. (2006). *Pre-steady-state binding of damaged DNA by XPC-hHR23B reveals a kinetic mechanism for damage discrimination*. Biochemistry *45*, 1961-1969.

Valerie, K., and Povirk, L. F. (2003). *Regulation and mechanisms of mammalian double-strand break repair*. Oncogene *22*, 5792-5812.

Ventura, A., Kirsch, D. G., McLaughlin, M. E., Tuveson, D. A., Grimm, J., Lintault, L., Newman, J., Reczek, E. E., Weissleder, R., and Jacks, T. (2007). *Restoration of p53 function leads to tumour regression in vivo*. Nature *445*, 661-665.

Vigouroux, C., Auclair, M., Dubosclard, E., Pouchelet, M., Capeau, J., Courvalin, J. C., and Buendia, B. (2001). *Nuclear envelope disorganization in fibroblasts from lipodystrophic patients with heterozygous R482Q/W mutations in the lamin A/C gene*. J Cell Sci *114*, 4459-4468.

Villemure, J. F., Abaji, C., Cousineau, I., and Belmaaza, A. (2003). *MSH2-deficient human cells exhibit a defect in the accurate termination of homology-directed repair of DNA double-strand breaks*. Cancer Res *63*, 3334-3339.

Volker, M., Mone, M. J., Karmakar, P., van Hoffen, A., Schul, W., Vermeulen, W., Hoeijmakers, J. H. J., van Driel, R., van Zeeland, A. A., and Mullenders, L. H. F.

(2001). *Sequential assembly of the nucleotide excision repair factors in vivo.* Molecular Cell *8*, 213-224.

Wang, N., Tytell, J. D., and Ingber, D. E. (2009). *Mechanotransduction at a distance: mechanically coupling the extracellular matrix with the nucleus.* Nat Rev Mol Cell Biol *10*, 75-82.

Wang, W., Shi, Z., Jiao, S., Chen, C., Wang, H., Liu, G., Wang, Q., Zhao, Y., Greene, M. I., and Zhou, Z. (2012). *Structural insights into SUN-KASH complexes across the nuclear envelope.* Cell Res *22*, 1440-1452.

Warren, J. J., Pohlhaus, T. J., Changela, A., Iyer, R. R., Modrich, P. L., and Beese, L. S. (2007). *Structure of the human MutSalpha DNA lesion recognition complex.* Mol Cell *26*, 579-592.

Wilhelmsen, K., Litjens, S. H., Kuikman, I., Tshimbalanga, N., Janssen, H., van den Bout, I., Raymond, K., and Sonnenberg, A. (2005). *Nesprin-3, a novel outer nuclear membrane protein, associates with the cytoskeletal linker protein plectin.* J Cell Biol *171*, 799-810.

Worman, H. J., and Bonne, G. (2007). *"Laminopathies": a wide spectrum of human diseases.* Exp Cell Res *313*, 2121-2133.

Yamaguchi, H., Pixley, F., and Condeelis, J. (2006). *Invadopodia and podosomes in tumor invasion.* Eur J Cell Biol *85*, 213-218.

Yasuda, G., Nishi, R., Watanabe, E., Mori, T., Iwai, S., Orioli, D., Stefanini, M., Hanaoka, F., and Sugasawa, K. (2007). *In vivo destabilization and functional defects of the xeroderma pigmentosum C protein caused by a pathogenic missense mutation.* Mol Cell Biol *27*, 6606-6614.

Yu, J., Lei, K., Zhou, M., Craft, C. M., Xu, G., Xu, T., Zhuang, Y., Xu, R., and Han, M. (2011). *KASH protein Syne-2/Nesprin-2 and SUN proteins SUN1/2 mediate nuclear migration during mammalian retinal development.* Hum Mol Genet *20*, 1061-1073.

Zaremba-Czogalla, M., Dubinska-Magiera, M., and Rzepecki, R. (2011). *Laminopathies: the molecular background of the disease and the prospects for its treatment.* Cell Mol Biol Lett *16*, 114-148.

Zhang, J., Felder, A., Liu, Y., Guo, L. T., Lange, S., Dalton, N. D., Gu, Y., Peterson, K. L., Mizisin, A. P., Shelton, G. D., Lieber, R. L., and Chen, J. (2010). *Nesprin 1 is critical for nuclear positioning and anchorage.* Hum Mol Genet *19*, 329-341.

Zhang, Q., Bethmann, C., Worth, N. F., Davies, J. D., Wasner, C., Feuer, A., Ragnauth, C. D., Yi, Q., Mellad, J. A., Warren, D. T., Wheeler, M. A., Ellis, J. A., Skepper, J. N., Vorgerd, M., Schlotter-Weigel, B., Weissberg, P. L., Roberts, R. G., Wehnert, M., and Shanahan, C. M. (2007). *Nesprin-1 and -2 are involved in the pathogenesis of Emery Dreifuss muscular dystrophy and are critical for nuclear envelope integrity.* Hum Mol Genet *16*, 2816-2833.

Zhang, Q., Ragnauth, C., Greener, M. J., Shanahan, C. M., and Roberts, R. G. (2002). *The nesprins are giant actin-binding proteins, orthologous to Drosophila melanogaster muscle protein MSP-300*. Genomics *80*, 473-481.

Zhang, Q., Ragnauth, C. D., Skepper, J. N., Worth, N. F., Warren, D. T., Roberts, R. G., Weissberg, P. L., Ellis, J. A., and Shanahan, C. M. (2005). *Nesprin-2 is a multi-isomeric protein that binds lamin and emerin at the nuclear envelope and forms a subcellular network in skeletal muscle*. J Cell Sci *118*, 673-687.

Zhang, X., Lei, K., Yuan, X., Wu, X., Zhuang, Y., Xu, T., Xu, R., and Han, M. (2009). *SUN1/2 and Syne/Nesprin-1/2 complexes connect centrosome to the nucleus during neurogenesis and neuronal migration in mice*. Neuron *64*, 173-187.

Zhen, Y. Y., Libotte, T., Munck, M., Noegel, A. A., and Korenbaum, E. (2002). *NUANCE, a giant protein connecting the nucleus and actin cytoskeleton*. J Cell Sci *115*, 3207-3222.

Zhong, Z., Chang, S. A., Kalinowski, A., Wilson, K. L., and Dahl, K. N. (2010). *Stabilization of the spectrin-like domains of nesprin-1alpha by the evolutionarily conserved "adaptive" domain*. Cell Mol Bioeng *3*, 139-150.

6. Erklärung

Ich versichere, dass ich die von mir vorgelegte Dissertation selbständig angefertigt, die benutzten Quellen und Hilfsmittel vollständig angegeben und die Stellen der Arbeit- einschließlich Tabellen und Abbildungen-, die anderen Werken im Wortlaut oder dem Sinn nach entnommen sind, in jedem Einzelfall als Entlehnung kenntlich gemacht habe; dass diese Dissertation noch keiner anderen Fakultät oder Universität zur Prüfung vorgelegen hat; dass sie - abgesehen von unten angegebenen Teilpublikationen noch nicht veröffentlicht ist, sowie, dass ich eine Veröffentlichung vor Abschluss des Promotionsverfahrens nicht vornehmen werde.

Die Bestimmungen dieser Promotionsordnung sind mir bekannt. Die von mir vorgelegte Dissertation ist von Prof. Dr. Angelika A. Noegel betreut worden.

Köln, November 2013

Ilknur Sur

Teilpublicationen:

Taranum S, **Sur I**, Müller R, Lu W, Rashmi RN, Munck M, Neumann S, Karakesisoglou I, Noegel A A. Cytoskeletal interactions at the nuclear envelope mediated by Nesprins. Int J Cell Biol. 2012; 2012:736524.

Sur I, Neumann S, Noegel A A. Nesprin-1 role in DNA damage response. Nucleus 2014, 5 (2), doi:10.4161/nucl.29023.

Curriculum Vitae

Name: Ilknur Sur

Date of Birth: 10.01.1984

Place of Birth: Turhal, Turkey

Nationality: Turkish

E-mail: ilknursur@gmail.com

Doctoral studies

2010-2013   Faculty of Mathematics and Natural Science,

                   Institute for Biochemistry I, Medical Faculty,

                   University of Cologne, Cologne, Germany

                   Supervisor: Prof. Dr. Angelika A. Noegel

University Studies

2008-2010   Master of Science (Biotechnology), Department of Genetics and

                   Bioengineering Yeditepe University, Istanbul, Turkey

2008-2010   **Teaching experience:** Cell Biology Laboratory Assistant,

                   Department of Genetics and Bioengineering, Yeditepe University,

                   Istanbul, Turkey

2003-2008   Bachelor of Education (Biology), Gazi University, Turkey

2006-2007   Department of Biology, Hamburg University, Germany

School studies

1998-2002   Pendik Foreign Language Intensive High School, Istanbul,

                   Turkey

Lebenslauf

Name:	Ilknur Sur
Geburtsdatum:	10.01.1984
Geburtsort:	Turhal, Türkei
Staatsangehörigkeit:	Turkish
E-mail:	ilknursur@gmail.com

Promotions Studium

2010-2013   Mathematisch-Naturwissenschaftliche Fakultat,

Institut für Biochemie I, Medizinische Fakultät,

Universität zu Köln, Köln, Deutschland,

Betreuerin: Prof. Dr. Angelika A. Noegel

Universität Studium

2008-2010   Master of Science (Biotechnologie), Department of Genetics and

Bioengineering, Yeditepe University, Istanbul, Türkei

20008-2010   **Lehrerfahrung:** Zellbiologie Laboratory Assistant, Department

of Genetics and Bioengineering, Yeditepe University, Istanbul,

Türkei

2003-2008   Bachelor of Education (Biologie), Gazi Universität, Türkei

2006-2007   Department of Biology, Universität Hamburg, Deutschland

Schulausbildung

1998-2002   Pendik Foreign Language Intensive High School, Istanbul,

Türkei